

*Seasonal and interannual variability of oceanographic
conditions in a Northeast Greenland Fjord*

by

Wieter Boone

A thesis submitted to the Faculty of Graduate Studies of
The University of Manitoba
in partial fulfilment of the degree of

Doctor of Philosophy

Department of Environment and Geography
University of Manitoba
Winnipeg, MB, Canada

Copyright © 2018 by Wieter Boone

Abstract

The Arctic is undergoing rapid changes due to climatic changes. Studies show that the Arctic is not only warming, but also freshening, which can induce changes to the distribution and spreading pathways of freshwater and impact ecosystems. Here, we focus on the coast of Northeast Greenland, which lies along the primary outflow shelf of the Arctic Ocean. Long term mooring-arrays monitor the gateways of the East Greenland Current at Fram Strait and Denmark Strait, but seasonal and interannual variability of oceanographic conditions along the coast of Northeast Greenland and its impact on fjord hydrography are not well known. This is mainly due to costs and logistical constraints encountered when operating in such a harsh and remote environment, where sea ice hampers coastal navigation. For this thesis, we analyzed in-situ observations, including moorings, from Young Sound-Tyrolerfjord (74° N), to gain more knowledge on the seasonal and long-term response of the fjord system to local and regional processes inducing changes in oceanographic conditions in the fjord and in the coastal domain. Our results include a description of the variability in hydrography and circulation during the ice-covered period, an impact analysis of coastal freshening on the renewal of the fjord basin water, and a process study of the drivers of freshwater variability along the coast of Northeast Greenland. The results suggest that sea ice melt along the coast is a prominent driver of freshwater variability in the coastal domain, and that sea ice melt might be impacted by the recirculation of warm Atlantic Water. An increase of temperatures in the North Atlantic could induce more sea ice might melt at higher latitude and freshen the coastal waters of Northeast Greenland. This is important, as our data already shows that

after strong coastal freshening in the periods since 2005, fjord bottom renewal of Young Sound-Tyrolerfjord was prevented, which may affect the fjord's ecosystem functions. This study was enabled by the extensive dataset from the Marine Basis Monitoring Program under the Greenland Ecosystem Monitoring Program, and underlines the importance to maintain strong monitoring capacity in Northeast Greenland, to assess recent and future changes to the marine system due to climate change.

Acknowledgements

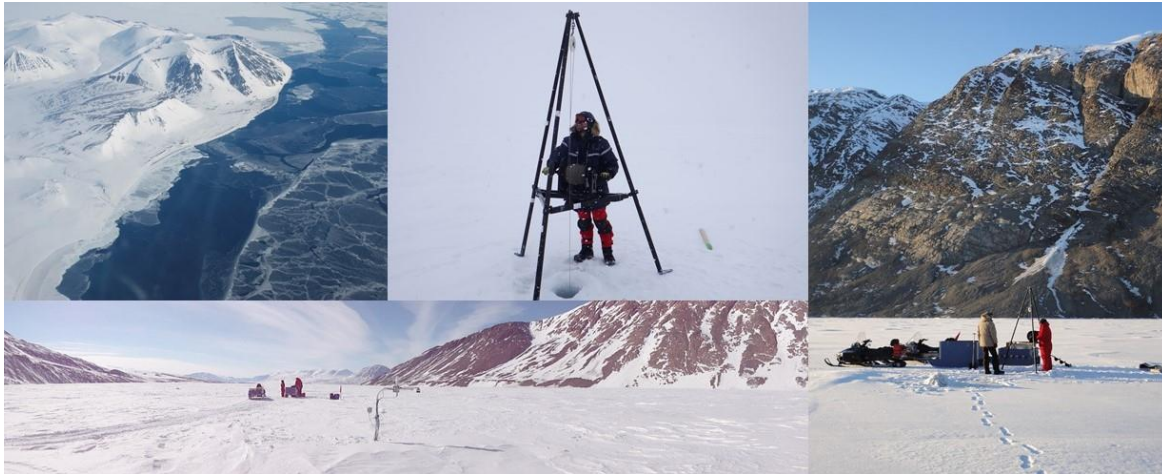
A sincere thanks to my supervisors Dr. Søren Rysgaard and Dr. Igor Dmitrenko for their leadership and enthusiasm. I extend my thanks to my committee members Drs. Zou Zou Kuzyk, Jens Ehn, Jørgen Bentsen and Dirk Notz, and CEOS Director Tim Papakyriakou for their support and guidance during this research project. Furthermore, I would like to thank all colleagues at CEOS and within the Arctic Science Partnership for their part in this research project.

Financial support for this research was provided by the Canada Excellence Research Chair (CERC) unit at the University of Manitoba's Centre for Earth Observation and Science (CEOS), the Canada Research Chair (CRC) program, the Canada Foundation of Innovation (CFI), the Natural Sciences and Engineering Research Council of Canada, Research Manitoba, and the University of Manitoba, Aarhus University and the Greenland Institute of Natural Resources.

I have personally received support via the University of Manitoba's International Graduate Student Scholarship and the University of Manitoba Graduate Scholarship.

This research contributes to the research programs of the Arctic Science Partnership (ASP), the Canada Excellence Research Chair of Dr. Søren Rysgaard and ArcticNet.

The possibility to do research in the Arctic with challenging fieldwork was the incentive of my move to Canada. A great journey, which I tried to live to the fullest together with my wife Isabeau. It was a success. Big thanks to Odile, Masayo, Sergey, Lorenz, Leendert, John, Annie, Tim, Jens, Heather, Yubin, Michelle, Satwant, Nathalie, Søren, Igor, Denise, David, Lucette and Linda for their part in this undertaking. Thanks to my mom, dad, sisters and friends for the support and love we received via dozens of postcards and visits. Thanks to Lio, just for being there.



Memories from the expedition to Young Sound-Tyrolerfjord in 2013 : coastal Northeast Greenland as seen from Twinotter-plane, myself casting a CTD on sea ice, my supervisors (Igor and Søren) casting a CTD, Ice mass balance buoy on the foreground with researchers casting a CTD in the background (photo credit: Wieter Boone and Sergei Kirillov)

Contents

Abstract.....	i
Acknowledgements	iii
Contents.....	v
List of Tables	ix
List of Figures	x
Use of Copyrighted Material.....	xvii
Chapter 1 Introduction.....	1
1.1 Motivation	1
1.2 Thesis Objectives	3
1.3 Thesis Outline	3
Chapter 2 Background.....	7
2.1 Hydrography of the Arctic Marine System	7
2.1.1 Regions, domains and general circulations.....	7
2.1.2 Primary freshwater sources of the Arctic Ocean	10
2.1.3 Fate of freshwater in the Arctic Ocean	12
2.2 Hydrography of the Greenland Sea	14
2.2.1 General circulation and water mass transformation in the Nordic Seas	14
2.2.2 East Greenland Current	17
2.3 Summary.....	25
References	26
Chapter 3	33

Circulation and fjord-shelf exchange during the ice-covered period in Young Sound-Tyrolerfjord, Northeast Greenland (74°N).....	33
3.1 Introduction	34
3.2 Physical setting	37
3.2.1 Young Sound-Tyrolerfjord system.....	37
3.2.2 Coastal water masses	38
3.2.3 Sea ice cover in winter 2013-2014.....	39
3.3 Data and methods	40
3.3.1 Ice-tethered mooring data	40
3.3.2 Hydrographic and meteorological data.....	43
3.4 Results.....	44
3.4.1 Seasonal thermohaline variability	44
3.4.2 Seasonal circulation.....	45
3.4.3 Tidal analysis.....	50
3.4.4 Cross sill exchange.....	53
3.5 Discussion	57
3.5.1 Circulation dynamics and environmental factors	57
3.5.2 Temporal changes in fjord circulation pattern.....	59
3.5.3 Link between sea ice cover and circulation.....	60
3.5.4 Cross-sill salt fluxes.....	61
3.6 Conclusions	69
Acknowledgments	70
References	71
Chapter 4	79

Coastal freshening prevents fjord bottom water renewal in a Northeast Greenland fjord – a mooring study from 2003-2015	79
4.1 Introduction	80
4.2 Data and Methods	82
4.2.1 Study Area.....	82
4.2.2 Mooring and CTD data	84
4.3 Results and Discussion	85
4.3.1 Temperature and salinity of the upper basin layer in 2003-2015.....	85
4.3.2 Temperature and Salinity of Lower Basin Layer in 2004-2014.....	91
3.3 Outlook	93
4.4 Conclusions	95
Acknowledgments	97
References	98
Supporting information	105
Chapter 5	109
5.1 Introduction	110
5.2 Data & Methods.....	113
5.2.1 Study Area.....	113
5.2.2 Mooring data and hydrographic data.....	114
5.2.3 Freshwater export variability through Fram Strait.....	116
5.2.4 NorESM Climate Model	117
5.3 Results and discussion	118
5.3.1 Freshening in Young-Sound	118
5.3.2 Sources of freshwater variability along the coast	120
5.3.3 Interannual variability of sea Ice export through the Fram Strait.....	124

5.3.4 Melt of sea-ice in the coastal domain	125
5.3.5 Atlantic Water Temperatures linked with freshwater variability along the coast	129
5.4 Conclusions	134
Acknowledgments	135
References	136
Chapter 6 Summary & Conclusions.....	148
6.1 Summary of major findings.....	148
Major Finding 1: Analysis and description of seasonal circulation patterns and drivers of circulation in an ice-covered Northeast Greenland Fjord	148
Major Finding 2: Young Sound- Tyrolerfjord, a fjord along the coast of Northeast Greenland is vulnerable to the effects of freshening	149
Major Finding 3: Fjord freshening rates might be impacted by sea ice melt along the Northeast Greenland Coast.....	150
6.2 Limitations and future work	151
6.3 Summary & Conclusions	155
References	157
Appendix A: Contribution of Authors to Thesis Chapters.	159
Appendix B: Additional Contributions to Peer Reviewed Literature	161

List of Tables

Table 2-1: Dominant Water Masses along the Northeast Greenland coast and in the Greenland Sea (after Buch, 2007; Swift and Aagaard, 1981).....	19
Table 3-1: Instrumental details of oceanographic moorings.	42
Table 3-2: Primary diurnal and semidiurnal components based on the measured tidal currents at 20 m depth at the three locations close to the outer sill (YS05, YS06, and YS07) and long-term mooring locations (YS02, YS03, YS04).	52
Table 4-1: Linear trends of deseasonalized monthly anomalies of salinity at mooring mZERO (Aug-July), with the coefficient of determination (R^2) and root mean squared error (RMSE).	88

List of Figures

Figure 2-1: ‘Maps showing (a) bathymetry of the Arctic Ocean from the International Bathymetric Chart of the Arctic Ocean (Jakobsson et al., 2012) and (b) place names of the major basins, ridges, shelf seas, and gateway straits’ (from Carmack et al., 2016).	9
Figure 2-2: ‘Schematic maps of (a) the major ocean currents (long arrows), the four Arctic Ocean gateways in Fram Strait, the Barents Sea Opening, Davis Strait, and Bering Strait (thick bars with red denoting inflow and blue denoting outflow), the gyral circulation patterns (circular arrows), the salt-stratified ocean domains are shown in light blue, and the All Arctic Regions definition of the terrestrial contributing areas shown in white, and (b) summary of components of the high-latitude freshwater system as introduced in Prowse et al. (2015a, 2015b).’ (Carmack et al. (2016))	10
Figure 2-3: ‘Liquid freshwater content (m) from the PHC (Polar Science Center Hydrographic Climatology) 3.0 climatology (Steele et al., 2001) and trajectories of sea ice computed using 2000–2010 satellite ice velocities from the Polar Pathfinder Sea Ice Motion data (Fowler et al., 2013). The small red dots indicate the starting points of the trajectories, which last 2 years’ (Carmack et al., 2016).	13
Figure 2-4: ‘Schematic circulation in the Nordic Seas. The transformation of warm Atlantic Water to colder, fresher, and denser Atlantic-origin Water in the rim current of the Nordic Seas and Arctic Ocean is illustrated with a transition from red to green colours. The fresh Polar surface water (PSW) in the East Greenland Current is indicated in blue. The green circles in the Greenland and Iceland Seas indicate cyclonic gyres. The acronyms are: NwASC = Norwegian Atlantic Slope Current; NwAFC = Norwegian Atlantic Frontal Current; WSC = West Spitsbergen Current; RAC = Return Atlantic Current; JMC = Jan Mayen Current; JMFZ = Jan Mayen Fracture Zone; NIJ = North Icelandic Jet; EIC = East Icelandic Current; and NIIC = North Icelandic Irminger Current; PSW Jet= Polar Surface Water Jet; EGC= East Greenland Current’ (Håvik et al., 2017).	16
Figure 2-5: ‘Vertical sections of (a) potential temperature, (b) salinity, and (c) absolute geostrophic velocity with contours of potential density (kg/m^3), for a section perpendicular	

with the coast near the Jan Mayen Fracture Zone. The location of the section is shown in the inset in (a). Positive velocities are towards the south. The black inverted triangles along the top of each panel indicate the station locations. The white contours in (a) represent the 0 °C isotherm. The black vertical lines in (c) enclose the shelfbreak branch of the East Greenland Current. The blue contour in (c) is the 27.7 kg/m³ isopycnal which separates the surface layer from the intermediate layer. The lower limit for the Atlantic-origin Water in the shelfbreak EGC is marked by the thick black contour line. The different kinematic features present in the section are identified along the top of panel (c).’ (Håvik et al., 2017).

..... 21

Figure 2-6: Vertical sections of hydrography and velocity for section 8 near Daneborg (~75 km from coast), otherwise as Fig. 2-5 (unpublished data, Håvik, 2017, personal communication)..... 23

Figure 2-7: Satellite image (NASA Worldview, EOSDIS March 20, 2016) of the Northeast Greenland coast near Daneborg and Young Sound - Tyrolerfjord (74°N) with identification of different sea ice types in a cross-section perpendicular to the coast; (a) landfast ice, (b) transition zone, (c) pack ice, and (d) marginal ice zone. 24

Figure 3-1: Study area, station map with bathymetry (Rysgaard et al., 2003) of the Young Sound - Tyrolerfjord system in Greenland. Red crosses depict the location of the CTD stations of the May transects, yellow stars mark the August transect. Black circles mark the location of the landfast ice-tethered oceanographic moorings (a: YS02, b: YS03, c: YS04, d: YS05, e: YS06, f: YS07). Blue line near the outer sill marks the landfast-ice edge after opening of the coastal polynya in December 2013. Inset shows the cross-section of the outer sill and the placement of the ADCP and ITP (mooring YS05). 38

Figure 3-2: Along-fjord transect of temperature (left column) and salinity (right column) taken on (a-b) 18 August 2013, (c-d) 10-12 May, (e-f) 16-19 May and (g-h) 26-28 May 2014. Black triangles on the top identify positions of the CTD stations, distance marked from outermost offshore station. 47

Figure 3-3: Depth time plot and zero contour line of the residual current (m s⁻¹) along the fjord axis and positive toward the inner fjord as calculated with low-pass filter pl66 (Limeburner et al., 1985) from ADCP data at mooring (a) YS02-13, (b) YS03-13 and (c) YS04-

-
13. Black triangles indicate strong wind events with winds exceeding 15 m s^{-1} , and vertical black lines bound the circulation periods. 49
- Figure 3-4: Change in hydrography of the outer Young Sound-Tyrolerfjord from fall to spring: The smoothed time series of (a) salinity and (b) potential temperature at discrete depths (2, 7, 17, 47, 77 and 117 m) at mooring YS03. Dashed lines indicate strong wind events ($>15 \text{ m s}^{-1}$), grey areas mark the different time periods. 50
- Figure 3-5: Time series of (a) depth-averaged current velocity (3-30 m, m s^{-1}) directed across the sill, positive towards the fjord interior, (b) temperature ($^{\circ}\text{C}$) and (c) salinity profiles above the sill (location: YS05). 55
- Figure 3-6: (a) Salinity and (b) temperature above the sill versus tidal phase, for the period of 1 May until 15 May 2014, as measured over the outer sill at mooring YS05. Colors depict the depth of the measurements. (c) Volume exchange versus tidal phase. Volume exchange measurements are based on M2 and S2 harmonic components of the depth-averaged velocity measured at mooring YS05, positive towards the fjord interior. 56
- Figure 3-7: (a) Along fjord transect of snow and sea ice thickness measured on 16-19 May 2014, (b-e) Black arrows on the left panes give a schematic of the circulation patterns. Light blue circular arrows indicate the outer sill mixing zone. Right panes, show average profiles of measured residual currents (blue: outflow, red: inflow) with indication of standard deviation (dashed lines) of the (b) first, (c) second, (d) third and (e) fourth circulation period. Dashed lines mark depth of circulation cell at mooring YS03. Light blue lines indicate the ice cover, while darker blue lines indicate melt water. 64
- Figure 3-8: (a) Depth-averaged salinity from ITP record over the outer sill (b) Cumulative volume exchange over the sill based on the harmonic (M2, S2) analysis of the depth-averaged velocity (3-30 m) over the outer sill. (c) Accumulated salt flux through the cross-section at the outer sill, positive towards the fjord interior. 67
- Figure 4-1: (a) Map of Young Sound - Tyrolerfjord in Northeast Greenland showing the stations and bathymetry (color contours) (Rysgaard et al., 2003). White areas in (a) depict land, and grey areas denote the shelf and coastal waters. The black square shows the location of the oceanographic mooring mZERO. Yellow crosses depict the location of CTD

stations covering the lower basin and red crosses indicate the stations offshore of the outer sill. (b) Bathymetry of the fjord from the coast to the inner parts of the fjord, with the mZERO mooring, outer sill, inner sill and different fjord layers indicated. 83

Figure 4-2: Time series of salinity (a) and temperature (red) and calculated freezing temperature (grey) (b) at 63 m depth at mZERO from August 2003 to May 2015. 86

Figure 4-3: Deseasonalized monthly averaged (a) salinity and (b) temperature anomalies at 63 m from mooring mZero. Black lines indicate monthly anomalies; grey line shows interpolated monthly anomalies and red lines the 11-term low-pass filter of the interpolated monthly anomalies. Grey zones in (a) mark periods with anomalous freshening. 87

Figure 4-4: TS-diagrams of the seasonal (1 July- 31 June) transformation of hydrography at ~63 m at mooring mZero in the upper basin water of Young Sound-Tyrolerfjord. Thin lines indicate the freezing line at 63 m. Note that all y-axes have the same scale (difference between max. and min. value is constant), but the x-axes may have different ranges. ... 90

Figure 4-5: TS- diagram of (a) the lower basin water (>200 m) of Young Sound-Tyrolerfjord from August measurements from 2004 to 2014 and (b) TS- diagram of the offshore water masses around sill depth (45-60 m) and their means (large dots), including the data from (a) in black. Red box in (b) shows the limits of the TS-diagram in (a). Dashed lines in (a) and (b) indicate the freezing line and isopycnals, Locations of the measurement are specified in Fig. 4-1 94

Figure 5-1: (a) Location of Young Sound-Tyrolerfjord along the coast of Northeast Greenland with minimum and maximum median (1981-2010) ice extent (NSIDC, 2017). (b) Schematic circulation in the Greenland Sea (modified from Håvik et al. (2017)), Fresh Polar surface water in the Polar Surface Water Jet (PSW-Jet) and East Greenland Current (EGC) are indicated in blue. Warm Atlantic Water in the Return Atlantic Current (RAC) in orange, and in the West Spitsbergen Current (WSC) in red. Location of the major outlet glaciers of the Northeast Greenland ice stream; Nioghalvfjærdsfjorden Glacier (NG), Zachariae Isstrøm (ZI), and Storstrømmen Glacier (SG) are marked. Bathymetry is obtained from IABCO (Jakobsson et al., 2012). 112

Figure 5-2: (a) Map of Young Sound - Tyrolerfjord in Northeast Greenland showing the location of mooring mZero (blue), CTD station GH (red) and bathymetry (Søren Rysgaard et al., 2003). White areas in (a) depict the land, and grey areas the shelf and coastal waters. (b-c) Time series of salinity (b) and temperature (b) at 63m depth at mZERO from August 2003 to May 2015. Black symbols show the salinity and temperature at sill depth as measured in station GH during the yearly August transects. 115

Figure 5-3: Deseasonalized monthly averaged salinity anomalies at 63 m from mooring mZero. Vertical grid lines mark 01 August of each year. Grey zones in (a) mark periods with anomalous freshening (from Boone et al., 2018). 119

Figure 5-4: Schematic representation of freshwater input to the coastal domain of Northeast Greenland during summer. Reference to the estimates can be found in the text. Black arrows represent solid sea ice transport, green arrow represents pacific water outflow, dark blue arrows represent runoff from Greenland, light blue arrows represent sea ice meltwater, blue arrow represents freshwater transport in the Polar Surface Water-Jet and red arrow schematizes the path of the Return Atlantic Current and the Outer East Greenland Current along the shelfbreak of the East Greenland Shelf. Black triangle indicates the location of Young Sound-Tyrolerfjord. 123

Figure 5-5: Southward flux of freshwater from sea ice in Fram Strait, based on ice area export data as reported by Smedsrud et al. (2017). Annual export is 01 September to 31-August, winter export covers 01 September – 28 February and spring export covers 01 March – 31 August. Values are marked in the middle of the respective period. 125

Figure 5-6: Spatial distribution of correlations between Atlantic Water core temperature anomalies feeding the West Spitsbergen Current (red box) and sea ice bottom melting simulated with the NorESM model for mean annual values between 1954-2005. The triangle marks the location of the Young Sound-Tyrolerfjord. 128

Figure 5-7: Spatial distribution of p-value of the correlation analysis between Atlantic Water core temperature anomalies feeding the West Spitsbergen Current (red box) and Arctic sea ice bottom melting simulated with the NorESM model for mean annual values between 1954-2005. The triangle marks the location of the Young Sound-Tyrolerfjord. 130

Figure 5-8: Spatial distribution of correlations between Atlantic Water core temperature anomalies feeding the West Spitsbergen Current (red box) and sea ice bottom melting simulated with the NorESM model for mean monthly values between 1954-2005. Black dotted line marks the monthly 1981-2010 median Sea Ice Extent (NSIDC, 2017). The triangle marks the location of the Young Sound-Tyrolerfjord. 132

Figure 5-9: Monthly freshwater flux from sea ice due to melting as simulated for the year 2007 from results of the NorESM. Black dotted line marks the monthly 1981-2010 median Sea Ice Extent (NSIDC, 2017). 133

Use of Copyrighted Material

Figure 2-1, Figure 2-2 and Figure 2-3: Carmack, E. C., Yamamoto-Kawai, M., Haine, T. W. N., Bacon, S., Bluhm, B. A., Lique, C., et al. (2016). Freshwater and its role in the Arctic Marine System: Sources, disposition, storage, export, and physical and biogeochemical consequences in the Arctic and global oceans. *J. Geophys. Res. G Biogeosciences* 121, 675–717. doi:10.1002/2015JG003140. Copyright (2016), Copernicus Publications. Copyrighted under Creative common licence: Attribution - Non Commercial- No Derivatives 4.0 International (CC BY-NC-ND 4.0).

Figure 2-4 and Figure 2-5: Håvik, L., R. S. Pickart, K. Våge, D. Torres, A. M. Thurnherr, A. Beszczynska-Möller, W. Walczowski, and W.-J. von Appen (2017), Evolution of the East Greenland Current from Fram Strait to Denmark Strait: Synoptic measurements from summer 2012, *J. Geophys. Res. Oceans*, 122, doi:10.1002/2016JC012228. Copyright (2017), John Wiley & Sons, with permission.

Figure 2-6: Copyright: Håvik, L., Personal communication, 23 March 2017, use with permission.

Figure 2-7: Satellite image from NASA Worldview, NASA supports an open data policy and encourage publication of imagery from Worldview.

Chapter 3 of this thesis is reproduced with minor modifications from Boone et al. (2017), Circulation and fjord-shelf exchange during the ice-covered period in Young Sound-Tyrolerfjord, Northeast Greenland (74°N). *Estuar. Coast. Shelf Sci.* 194, 205–216. doi:10.1016/j.ecss.2017.06.021, with permission from the publisher.

Chapter 4 of this thesis is reproduced with minor modifications from Boone et al. (2018), Coastal freshening prevents fjord bottom water renewal in a Northeast Greenland fjord – a mooring study from 2003-2015, a paper published in the journal *Geophysical Research Letters*.

Chapter 5 of this thesis is reproduced with minor modifications from Boone et al. (2018), ‘Does sea ice melt impact coastal freshening in Northeast Greenland?’, a draft paper in preparation to submit to *Frontiers in Marine Science*

Chapter 1 Introduction

1.1 Motivation

The Arctic is undergoing rapid changes due to climatic changes, and is therefore set at the forefront of international public and governmental interest. The area is vulnerable to cascading effects, where one change in the physical environment can induce changes on ecosystem-level and impact social, economic and geopolitical processes.

Much of the public's focus has been on climate warming, but recent studies show that the Arctic is also freshening (Haine et al., 2015; McPhee et al., 2009; Proshutinsky et al., 2009; Rabe et al., 2011) and losing sea ice (Cavalieri and Parkinson, 2012; Comiso et al., 2008; Kwok et al., 2009; Stroeve et al., 2012a, 2012b). Furthermore, freshwater fluxes from the Greenland Ice Sheet are increasing (Bamber et al., 2012; Khan et al., 2014). These changes may induce alterations in the distribution and spreading pathways of freshwater in the Arctic Marine system (McPhee et al., 2009), which can induce changes of heat, salt and biogeochemical properties of the Arctic Ocean and the bordering (sub)-Arctic seas and oceans, such as the Greenland Sea (Arrigo and Van Dijken, 2011; Beszczynska-Möller et al., 2011; Carmack and McLaughlin, 2011; Pabi et al., 2008; Woodgate et al., 2012). The impact assessment of these changes is hampered by our limited knowledge of the circulation, water mass conversion, and (local) freshwater sources and features of the Arctic Ocean and its bordering seas (Carmack et al., 2016).

The Arctic freshwater cycle should receive much attention, as it is a prominent element of the Earth's climate system. A key area in the freshwater cycle of the Arctic Ocean, and possibly vulnerable to the effects of climate change, is the coast of Northeast Greenland, the coastal area bounded by Fram Strait in the North and Denmark Strait in the South. It plays a prominent role in the freshwater cycle of the Arctic Ocean as it lies along the primary outflow shelf of the Arctic Ocean, where large amounts of sea ice and freshwater exported through Fram Strait are transported southwards via the East Greenland Current. The coastal water also receives vast amounts of glacial meltwater from numerous drainage basins of the Greenland Ice Sheet. Especially the contribution from the Northeast Greenland Ice Stream is an important freshwater input, as it covers 16% of the Greenland Ice Sheet (Khan et al., 2014).

Efforts to understand the effects of freshening on ocean circulation and marine ecosystems rely heavily on numerical ocean models and suffer a lack of long-term measurements. Research in Northeast Greenland was, until recently, mainly based on data from summertime only, which further emphasizes the need for continuous long-term measurements that cover both seasonal and interannual changes in the oceanographic conditions in the area.

1.2 Thesis Objectives

The goal of this thesis is to investigate the vulnerability of Greenland's fjords and coastal zones to impacts of freshening due to climate change. Thereto, we aim to increase the knowledge on the seasonal and interannual variability of oceanographic conditions in the Young Sound-Tyrolerfjord a high Arctic fjord along the coast of Northeast Greenland.

The overall goal of this thesis is subdivided in three objectives:

- (1) Describe seasonal variations in circulation, thermohaline structure and cross-sill exchange of a Northeast Greenland Fjord.
- (2) Quantify the impact of recent regional climate changes to decadal changes in the hydrography of the fjord.
- (3) Investigate drivers of the changing oceanographic conditions along the coast of Northeast Greenland.

1.3 Thesis Outline

The thesis consists of six chapters. After the first introductory Chapter, Chapter Two will present the thesis topic by describing the hydrography and circulation in the Arctic Marine System, with a focus on the coast of Northeast Greenland. This chapter also summarizes the large-scale hydrography, water masses and circulation of the Greenland Sea. The chapter is largely based on recent work on the subject by Haine et

al. (2015) and Carmack et al. (2016), and on the results from a recent cruise along the coast of Northeast Greenland described by Håvik et al. (2017).

Chapter Three addresses thesis objective (1) by describing the analysis of seasonal observations of circulation, hydrography and cross-sill exchange of the Young Sound-Tyrolerfjord system (74° N) in Northeast Greenland. This work has been peer-reviewed and published in the journal *Estuarine, Coastal and Shelf Science*:

Boone, W., Rysgaard, S., Kirillov, S., Dmitrenko, I., Bendtsen, J., Mortensen, J., et al. (2017). Circulation and fjord-shelf exchange during the ice-covered period in Young Sound-Tyrolerfjord, Northeast Greenland (74°N). *Estuar. Coast. Shelf Sci.* 194, 205–216. doi:10.1016/j.ecss.2017.06.021.

Chapter Four addresses thesis objective (2) as it investigates data from 13-year (2003-2015) continuous moored observations of temperature and salinity in Young Sound-Tyrolerfjord (74° N) in Northeast Greenland. This work published in the journal *Geophysical Research Letters*:

Boone, W., Rysgaard, S., Carlson, D. F., Meire, L., Kirillov, S., Mortensen, J., et al. (2018). Coastal freshening prevents fjord bottom water renewal in Northeast Greenland: A mooring study from 2003 to 2015. *Geophysical Research Letters*, 45. <https://doi.org/10.1002/2017GL076591>

Chapter Five addresses thesis objective (3) as it studies the dominant processes which impact freshwater availability along the coast of Northeast Greenland. We plan to

submit this manuscript to the journal *Frontiers of Marine Science*, but this paper is currently in preparation:

Boone, W., Rysgaard, S., Carlson, D., Kirillov, S., Dmitrenko, I., Mortensen, J., Meire, L. (2017). Does sea ice melt impact coastal freshening in Northeast Greenland?.. *Frontiers of Marine Science* (in prep).

Finally, Chapter Six contains the general summary of this research, with suggestions for future research.

Chapter 2 Background

2.1 Hydrography of the Arctic Marine System

2.1.1 Regions, domains and general circulations

The description of the hydrography of the Arctic Marine System starts with a definition of the regions under consideration. Carmack et al. (2016) define the Arctic Marine System as the Pan-Arctic domain north of Bering Strait in the Pacific and north of the Greenland-Scotland Ridge in the Atlantic. They further subdivided this area in the Nordic Seas, which are the Norwegian, the Iceland and the Greenland Seas south of Fram Strait and west of the Barents Sea Opening, and the Arctic Ocean, as the area bounded by the gateways Fram Strait, the Barents Sea Opening, Bering Strait and Davis Strait. We define the coast of Northeast Greenland as the coastal area of Greenland between Fram Strait in the north and Denmark Strait in the south, while the coast of Southeast Greenland lies between Denmark Strait and Cape Farewell at the southern tip of Greenland.

The hydrography and climate of the world's oceans is largely determined by their stratification. Carmack (2007) describes how the stratification of the world's oceans is mainly driven by two aspects of the climate system. First, moisture from the subtropical and tropical Atlantic Ocean is transported via trade winds across Central America

towards the Pacific Ocean, which drives the salinity difference between the North Atlantic and the North Pacific. Second, the difference in warming and evaporation between lower latitudes in comparison to higher latitudes and the poleward transport of latent heat and moisture via the atmosphere make that the upper layers of high-latitude seas are stratified by salinity and the upper layers of subtropical seas are stratified by temperature (Fig. 2-2a) (Carmack et al., 2016). This thermohaline distribution of the world's oceans sets the scene for the circulation in the Arctic Ocean (Fig. 2-2), which can be summarized as follows (after Carmack et al., 2016): Warm and salty waters from Atlantic origin enter the Arctic Ocean via Fram Strait and through the Barents Sea Opening. These waters circulate in the Arctic Ocean's basins as subsurface, cyclonic and topographically steered boundary currents that follow a path along the continental margins and ridge systems, and are modified within the Arctic Ocean before they exit through Fram Strait along the East Greenland Coast. Pacific origin waters, which are cooler and fresher than the Atlantic Waters, enter the Arctic Ocean through the Bering Strait and exit the Arctic Ocean through the Canadian Archipelago and through Fram Strait. In addition, moisture from the Pacific and Atlantic Oceans is delivered to the Arctic catchment areas via storm tracks of the midlatitude Westerlies. They supply the Riverine Coastal Domain, an area where river plumes extend outward across the shelves or form surface-trapped buoyancy boundary currents (Carmack et al., 2015a), with nutrient-rich freshwater.

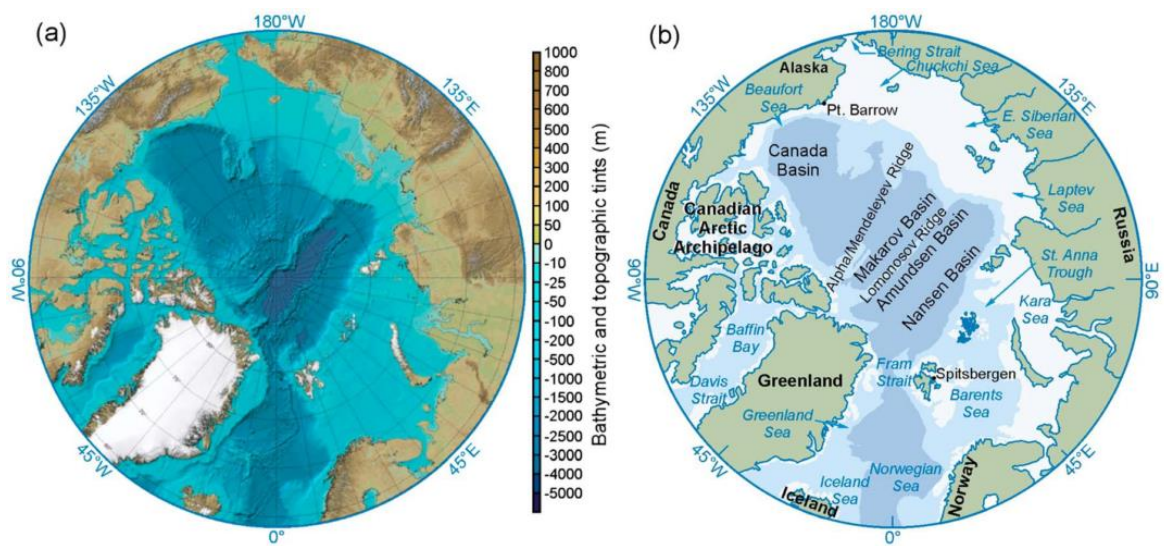


Figure 2-1: 'Maps showing (a) bathymetry of the Arctic Ocean from the International Bathymetric Chart of the Arctic Ocean (Jakobsson et al., 2012) and (b) place names of the major basins, ridges, shelf seas, and gateway straits' (from Carmack et al., 2016).

Based on these circulation patterns, the Arctic Marine System can be subdivided in diverse regions with a variety of physical, morphometric and biological properties (Fig. 2-2b). Following Carmack and Wassmann (2006), we can identify the following hydromorphological domains: inflow shelves (the Barents and Chukchi shelves), outflow shelves (e.g., the Canadian Arctic Archipelago (CAA) and East Greenland shelves), interior shelves (the Kara, Laptev, East Siberian, and Beaufort shelves), basins (two main: Eurasian and Amerasian), the riverine coastal domain (Carmack et al., 2015a) and the ridge and borderland features (reference to place names: Fig. 2-1).

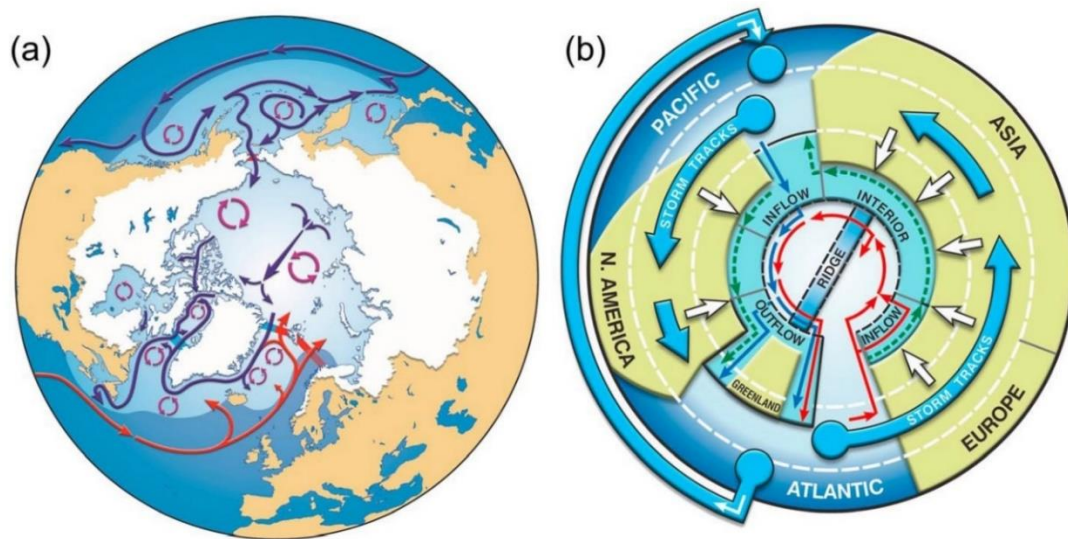


Figure 2-2: 'Schematic maps of (a) the major ocean currents (long arrows), the four Arctic Ocean gateways in Fram Strait, the Barents Sea Opening, Davis Strait, and Bering Strait (thick bars with red denoting inflow and blue denoting outflow), the gyral circulation patterns (circular arrows), the salt-stratified ocean domains are shown in light blue, and the All Arctic Regions definition of the terrestrial contributing areas shown in white, and (b) summary of components of the high-latitude freshwater system as introduced in Prowse et al. (2015a, 2015b).' (Carmack et al. (2016))

2.1.2 Primary freshwater sources of the Arctic Ocean

The three primary sources of freshwater for the Arctic Ocean are discharge from land, Pacific Water inflow through Bering Strait, and precipitation. To describe these sources, we employ the term freshwater anomaly, which can be quantified by 'the amount of zero-salinity water required to attain the observed salinity of a seawater sample (S) starting from a given reference salinity (S_{ref})' (Carmack et al., 2016), in literature mostly chosen as the average mean salinity of the Arctic Ocean (34.8) after Aagaard and

Carmack (1989). The freshwater volume flux (F) of a certain sea water volume flux (V_0) is then calculated as follows (Carmack et al., 2016):

$$F = \frac{(S - S_{ref})}{S_{ref}} V_0$$

The largest influx of freshwater to the Arctic Ocean comes from discharge from land and is estimated to amount to $4200 \pm 420 \text{ km}^3 \text{ yr}^{-1}$ (Haine et al., 2015), although substantial uncertainty in the total flux estimates has to be taken into account, as about a third of the drainage area is not covered by measurements (Carmack et al., 2016). Second largest is the Pacific water inflow through Bering Strait, which supplies water with a freshwater anomaly of $2640 \pm 100 \text{ km}^3 \text{ yr}^{-1}$ (average for 2000-2010) (Haine et al., 2015; Woodgate et al., 2006). The inflow contains roughly 95% liquid freshwater, the rest is sea ice from the Bering Sea (Carmack et al., 2016). The third largest source of freshwater to the Arctic Ocean is precipitation-evaporation, which delivers about $2200 \pm 220 \text{ km}^3 \text{ yr}^{-1}$ (average for 2000-2010) (Haine et al., 2015). This amount is about 60 % of the total precipitation from the Arctic Ocean, the remainder (40 %) is being recycled within the Arctic Ocean. Other freshwater sources are the Arctic Glaciers and the Greenland Ice Sheet, which are especially important as a local source of freshwater to the shelf regions and marginal seas of the Arctic Ocean, such as the Greenland Sea and Baffin Bay. The contribution of Arctic Glaciers (Canadian, Icelandic and Russian glaciers) amounts to $226 \text{ km}^3 \text{ yr}^{-1}$ (2003-2009 mean) (Haine et al., 2015) and the contribution of the Greenland Ice sheet (runoff and ice discharge) is approximately $1200 \text{ km}^3 \text{ yr}^{-1}$ (Bamber et al., 2012).

2.1.3 Fate of freshwater in the Arctic Ocean

Freshwater in the Arctic Ocean is mainly stored in the liquid phase in the upper layers of the Ocean and to lesser extent in the solid phase as sea ice (Carmack et al., 2016), however, due to the seasonal freeze and thaw cycle, a major seasonal exchange exists between these phases (seasonal volume difference $\sim 134\,000\text{ km}^3$, average 2000-2010, Haine et al., 2015). The liquid freshwater content attains approximately $101\,000\text{ km}^3$ (2000-2010 annual average) (relative to salinity 34.8) (Haine et al., 2015) and is not distributed evenly. Most freshwater exists in the Beaufort Gyre above the Canada Basin, where the accumulated freshwater anomaly equals about 20 m (relative to salinity 34.8) (Haine et al., 2015). In contrast, in the Eurasian basin, the accumulated freshwater anomaly is only between 5-10 m thick (Haine et al., 2015). The freshwater content of these basins is controlled by the surface circulation in the Arctic Ocean (Fig. 2-3). Winds and moving ice drive a cyclonic circulation in the Nansen basin and an anticyclonic circulation in the Amerasian Basin (Carmack et al., 2016). At the convergence of these gyres forms the Trans-Polar Drift, which is directed towards Fram Strait (Rudels, 2012). The Eurasian Basin surface water is driven by the transpolar drift towards Fram Strait, while the Beaufort Gyre retains much of its freshwater and is only leaking into the transpolar drift, or to the Canadian Archipelago (Carmack et al., 2016).

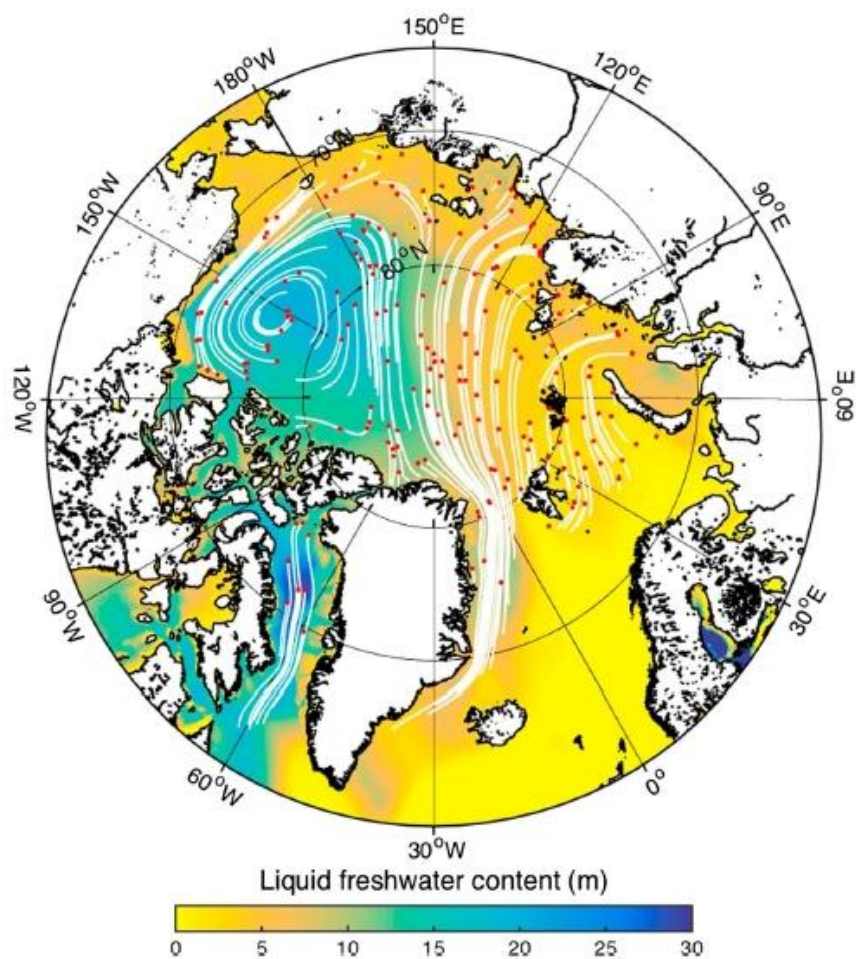


Figure 2-3: Liquid freshwater content (m) from the PHC (Polar Science Center Hydrographic Climatology) 3.0 climatology (Steele et al., 2001) and trajectories of sea ice computed using 2000–2010 satellite ice velocities from the Polar Pathfinder Sea Ice Motion data (Fowler et al., 2013). The small red dots indicate the starting points of the trajectories, which last 2 years' (Carmack et al., 2016).

The solid fraction of the freshwater content contains about $14\,300\text{ km}^3$ of freshwater (2000-2010 average, Haine et al., 2015) and is mainly stored in the areas north of the Canadian Arctic Archipelago and Greenland and across the pole, there the thickest and oldest sea ice is found (Kwok, 2009). Sea ice transport is driven by winds, the surface

ocean currents, and the internal dynamic stresses within the sea ice pack (Carmack et al., 2016). The prevailing currents allow sea ice, formed over the Eurasian shelves, to be transported toward the central Arctic and to the transpolar drift (Fig. 2-3).

Freshwater exits the Arctic ocean mainly through Fram Strait (freshwater flux: $1900 \pm 280 \text{ km}^3 \text{ yr}^{-1}$ as ice; $2800 \pm 420 \text{ km}^3 \text{ yr}^{-1}$ as liquid, including the Fram Strait deep water and West Spitsbergen Current) and Davis Strait (freshwater flux: $2900 \pm 190 \text{ km}^3 \text{ yr}^{-1}$ as liquid freshwater and $320 \pm 45 \text{ km}^3 \text{ yr}^{-1}$ as ice) (Haine et al., 2015). Overall, it can be concluded that about $5700 \pm 460 \text{ km}^3 \text{ yr}^{-1}$ leaves the Arctic Ocean as liquid freshwater, with an equal spread between both Fram and Davis Straits. When it comes to sea ice, approximately $2200 \pm 280 \text{ km}^3 \text{ yr}^{-1}$ of freshwater leaves the Arctic Ocean, with 85% passing through Fram Strait. This emphasizes the importance of Fram Strait for the freshwater balance of the Arctic Ocean (Carmack et al., 2016).

2.2 Hydrography of the Greenland Sea

2.2.1 General circulation and water mass transformation in the Nordic Seas

The coast of Northeast Greenland borders the Greenland Sea, one of the Nordic Seas. The regional scale circulation patterns of the Nordic Seas show warm northward-flowing Atlantic water on the eastern side, and cold Polar Water flowing southward via the East Greenland Current on the western side (Fig. 2-4). Håvik et al. (2017) describe

the circulation in the Nordic seas: warm Atlantic Water penetrate the Nordic Seas via the Faroe-Shetland and the Iceland-Faroe inflows (Hansen et al, 2015). The inflow of Atlantic Water is divided in two distinct branches further north: the Norwegian Atlantic Slope Current (NwASC), and the Norwegian Atlantic Frontal Current (NwAFC). The Norwegian Atlantic Slope Current splits off the coast of Northern Norway into the North Cape Current and the eastern branch of the West Spitsbergen Current (WSC) (Beszczynska-Møller et al., 2012). The Norwegian Atlantic Frontal Current develops into the western branch of the West Spitsbergen Current and recirculates in Fram Strait to feed Atlantic Water to the East Greenland Current and the Greenland Sea.

The water masses undergo significant transformation in the Nordic Seas. The subtropical warm and saline Atlantic Water, transported North via the Norwegian Atlantic Currents, is transformed into two main components (Latarius and Quadfasel, 2016) (Fig. 2-1b). The first is formed by negative buoyancy fluxes, such as heat loss to the atmosphere and brine rejection during sea ice formation, which lead to strong vertical mixing and ultimately creates the dense deep and intermediate depth waters found in the Nordic Seas (Carmack and Aagaard, 1973; Rudels, 1986). The second results from the mixing of Atlantic Water with freshwater from precipitation, run-off from land, and ice-melt, to create Polar Water, a water mass with low salinity and low density that is found in the upper parts of much of the Arctic Ocean and the western Nordic Seas.

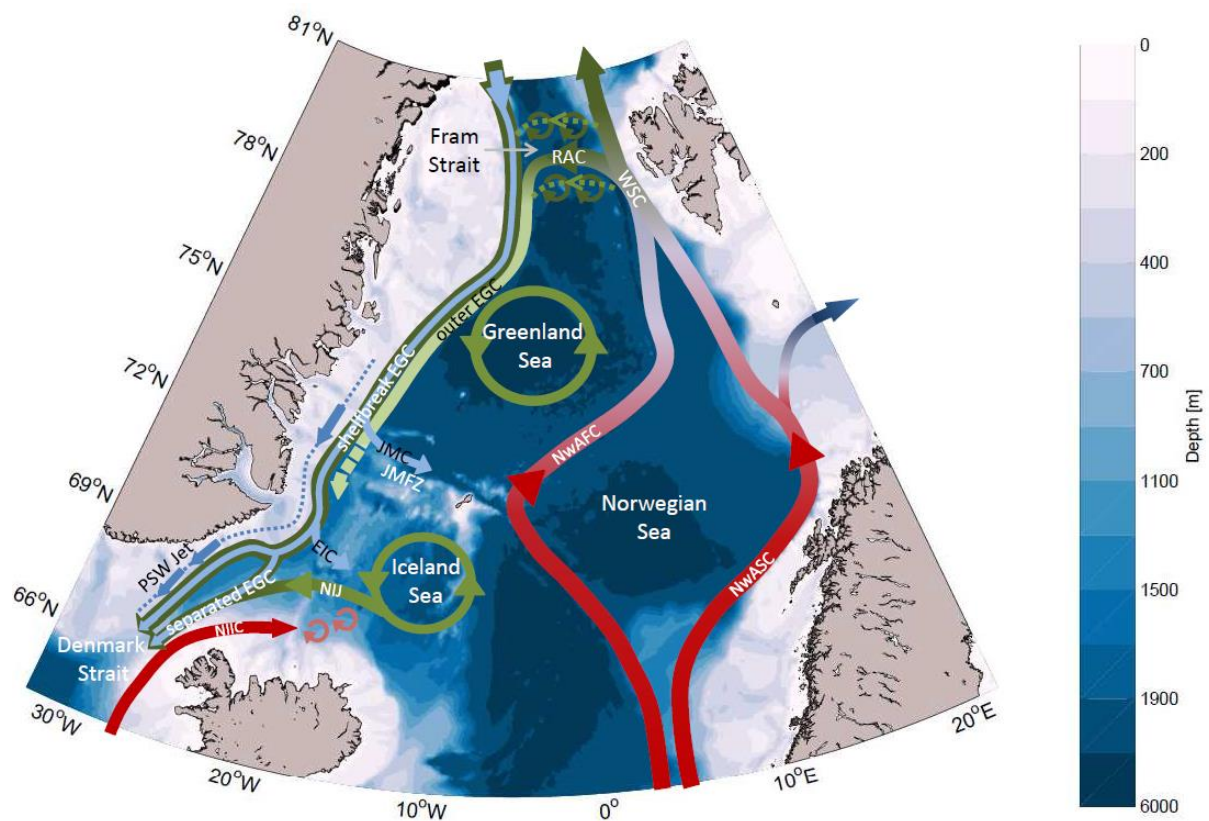


Figure 2-4: 'Schematic circulation in the Nordic Seas. The transformation of warm Atlantic Water to colder, fresher, and denser Atlantic-origin Water in the rim current of the Nordic Seas and Arctic Ocean is illustrated with a transition from red to green colours. The fresh Polar surface water (PSW) in the East Greenland Current is indicated in blue. The green circles in the Greenland and Iceland Seas indicate cyclonic gyres. The acronyms are: NwASC = Norwegian Atlantic Slope Current; NwAFC = Norwegian Atlantic Frontal Current; WSC = West Spitsbergen Current; RAC = Return Atlantic Current; JMC = Jan Mayen Current; JMFZ = Jan Mayen Fracture Zone; NIJ = North Icelandic Jet; EIC = East Icelandic Current; and NIIC = North Icelandic Irminger Current; PSW Jet= Polar Surface Water Jet; EGC= East Greenland Current '(Håvik et al., 2017).

Previously, we identified the East Greenland shelves as the primary outflow shelf of the Arctic Ocean. Along this outflow shelf flows the East Greenland Current, which is an important transport conduit for Polar Water and denser water masses from the Arctic Ocean (Rudels, 2002). The current originates in the Arctic Ocean and runs through the Nordic Seas towards the Subpolar North Atlantic. Its core runs southwards along the slope of the Northeast Greenland shelf. On its way south, two side branches are formed: the Jan Mayen Current and the East Icelandic Current (Fig. 2-4). These side branches feed into a hydrographical transition zone, where gyres (Greenland Sea Gyre, Iceland Sea Gyre) and fronts are formed between the regions, dominated by Polar Water masses in the West, and Atlantic Water Masses in the East. For this transition zone, the term Arctic Surface Water was brought forward to identify the upper layer waters which are colder and less saline than Atlantic Water, but still warmer and more saline than Polar Water (Helland-Hansen and Nansen, 1909).

2.2.2 East Greenland Current

2.2.2.1 Hydrographic structure and water masses

The dominant water masses along the Northeast Greenland coast are associated with the East Greenland Current, which has a three-layered structure (example: Fig. 2-5 and Fig. 2-6). The surface layer consists of fresh Polar Surface Water (PSW) and has a thickness of roughly 150 m to 200 m on the shelf and 50 m further offshore (Håvik et al., 2017; Rudels et al., 2005). The middle layer consists of warmer and saltier Atlantic-origin Water and is typically 500-700 m thick. Finally, below the 0°C isotherm, the

Greenland Sea deep water is found, which consists of different deep water masses, such as Upper Polar Deep Water, Canadian Basin Deep water and Eurasian Deep Water (Buch, 2007). The characteristics of the dominant water masses along the Northeast Greenland coast and in the Greenland Sea are summarized in Table 1.

2.2.2.2 Velocity structure of the East Greenland Current

Håvik et al. (2017) compiled velocity transects along the East Greenland Coast (example: Fig. 2-5; Fig. 2-6). Highest velocities were found near the shelfbreak and upper continental slope. Other strong flows were detected close to the coast and locally offshore from the shelfbreak. From their results, they identified three branches of the East Greenland Current: the shelfbreak East Greenland Current, the Polar Surface Water Jet and the outer East Greenland Current (Fig. 2-4, Fig. 2-5 and Fig. 2-6).

I. Shelfbreak East Greenland Current

Håvik et al. (2017) describe the shelfbreak East Greenland Current as a 'strong surface-intensified flow close to the shelfbreak' and refer to it as the 'most prominent component of the boundary current system' (Fig. 2-5). It flows southward with a velocity that ranges between 0.2 and 0.4 m s⁻¹.

Table 2-1: Dominant Water Masses along the Northeast Greenland coast and in the Greenland Sea (after Buch, 2007; Swift and Aagaard, 1981).

	Salinity	Temperature	Comments
Atlantic Water	>34.9	> 3°C	
Polar (Surface) Water	<34.4	<0°C, surface in summer up to 5°C	
Arctic Surface Water	34.4 – 34.9	> 0°C if S between 34.4 – 34.7; > 2°C if S 34.7 – 34.9	
Upper Arctic Intermediate Water	34.7-34.9	<0°C	winter sea surface
Lower Arctic Intermediate Water	>34.9	0-3°C	
Greenland Sea Deep Water	34.895	-1.24 °C	Densest water of Greenland Sea
Upper Polar Deep Water	34.90<S<34.93	-0.5°C<T< 0°C	Arctic Ocean origin
Canadian Basin Deep Water	S>34.92	-0.8°C<T< 0.5°C	Arctic Ocean origin
Eurasian Deep Water	S>34.92	T< -0.8°C	Arctic Ocean origin

II. Polar Surface Water Jet

Håvik et al. (2017) furthermore measured geostrophic velocities close to the North East Greenland coast and identified the occurrence of a surface intensified jet within the Polar Surface Water layer (Fig. 2-5 and Fig. 2-6). The jet was well observed in sections south of 72°N, and partly sampled on sections at 73°N (Fig. 2-6). Full capture of this feature at higher latitudes was not possible, because the sections did not extend sufficiently far towards the coast (Håvik et al., 2017). As the Jet is found in the fresh Polar Surface Water, it is important for freshwater transport. Håvik et al. (2017) also mention that the current also transports some Atlantic-origin Water that penetrated to the shelf. Velocities peak at 0.2 m s^{-1} and are thus slightly lower than what is observed in the Shelfbreak East Greenland Current (Håvik et al., 2017).

III. Outer East Greenland Current

Finally, Håvik et al. (2017) identify the outer East Greenland Current that flows over the mid to deep continental slope, offshore from the Shelfbreak East Greenland Current. The authors remark that the outer East Greenland Current is a result of the recirculation of the Western Spitsbergen Current in Fram Strait. The current flows south along the Shelfbreak East Greenland Current until it reaches the Jan Mayen Fracture Zone.

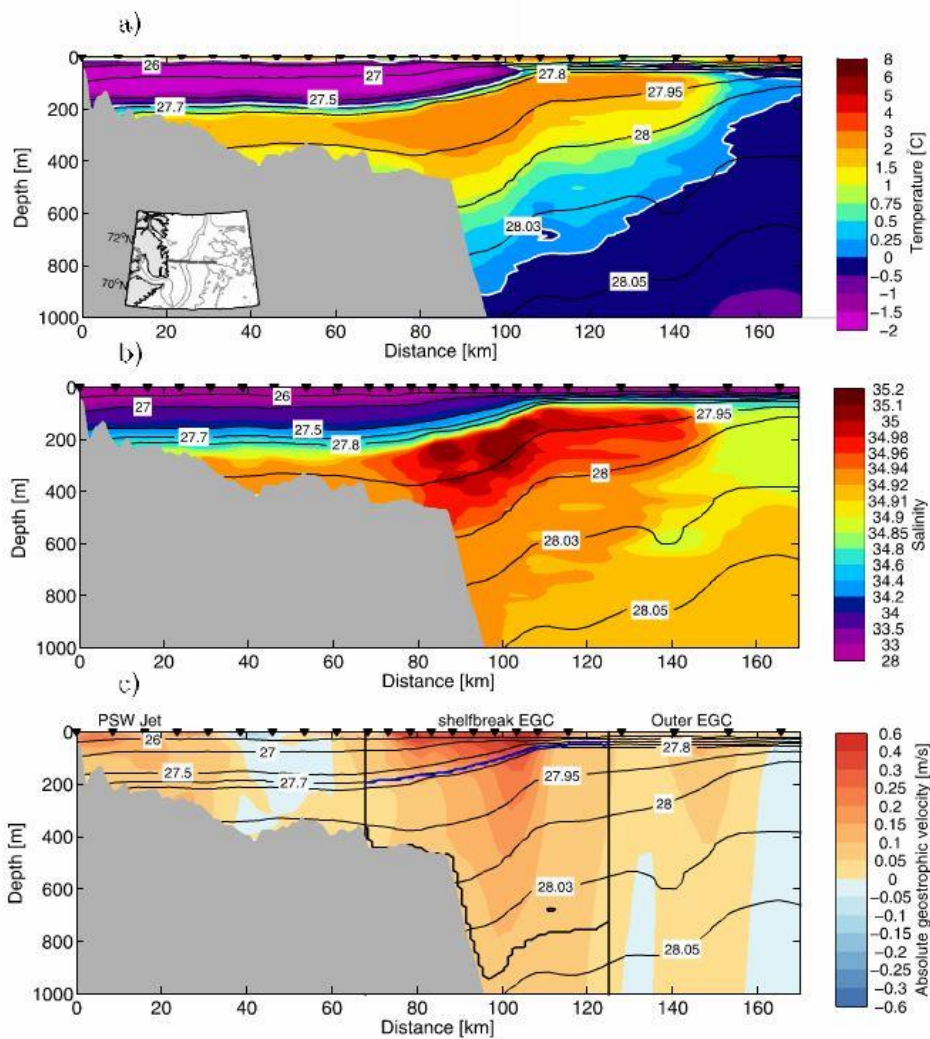


Figure 2-5: ‘Vertical sections of (a) potential temperature, (b) salinity, and (c) absolute geostrophic velocity with contours of potential density (kg/m^3), for a section perpendicular with the coast near the Jan Mayen Fracture Zone. The location of the section is shown in the inset in (a). Positive velocities are towards the south. The black inverted triangles along the top of each panel indicate the station locations. The white contours in (a) represent the $0\text{ }^\circ\text{C}$ isotherm. The black vertical lines in (c) enclose the shelfbreak branch of the East Greenland Current. The blue contour in (c) is the 27.7 kg/m^3 isopycnal which separates the surface layer from the intermediate layer. The lower limit for the Atlantic-origin Water in the shelfbreak EGC is marked by the thick black contour line. The different kinematic features present in the section are identified along the top of panel (c).’ (Håvik et al., 2017).

2.2.3 Sea Ice along the Northeast Greenland coast

Along the East Greenland coast, sea ice from the Arctic Ocean is transported southwards. In a cross section perpendicular to the coast, four different ice types can be found: (a) the landfast ice, (b) a transition zone, (c) the pack ice, and (d) the marginal ice zone (Buch, 2007) (Figure 2-7). (a) Close to the coast, landfast ice is formed during winter. It is attached to the coast and does not move with currents and winds (except vertical displacement by tides). This ice normally breaks up or melts away in spring, but it can occasionally also stay in place and survive the summer melt. (b) The landfast ice is separated from the pack ice by a transition zone, which is not a shear zone with heavy ridging as seen in other places in the Arctic, but a continuous strip of open water or polynyas offshore from the fast ice edge. (c) Offshore from this transition zone the drifting pack ice flows south, containing Paleocrystic ice, North Pole Ice and Siberian Ice (Wadhams, 1981). Paleocrystic ice is a mix of very old ice and heavy deformed ice, while North Pole Ice is ice from both the Beaufort Gyre and distant parts of the Eurasian Basin. Siberian Ice is formed in the near shore of the vast shelves of East Siberia and the Laptev Sea, but contains ice formed in the pack ice where leads and polynyas are responsible for significant sea ice production (Buch, 2007). Finally, the pack ice is divided from the open ocean via the Marginal Ice Zone, where smaller fragments of ice from the pack ice are transported by eddies of different sizes.

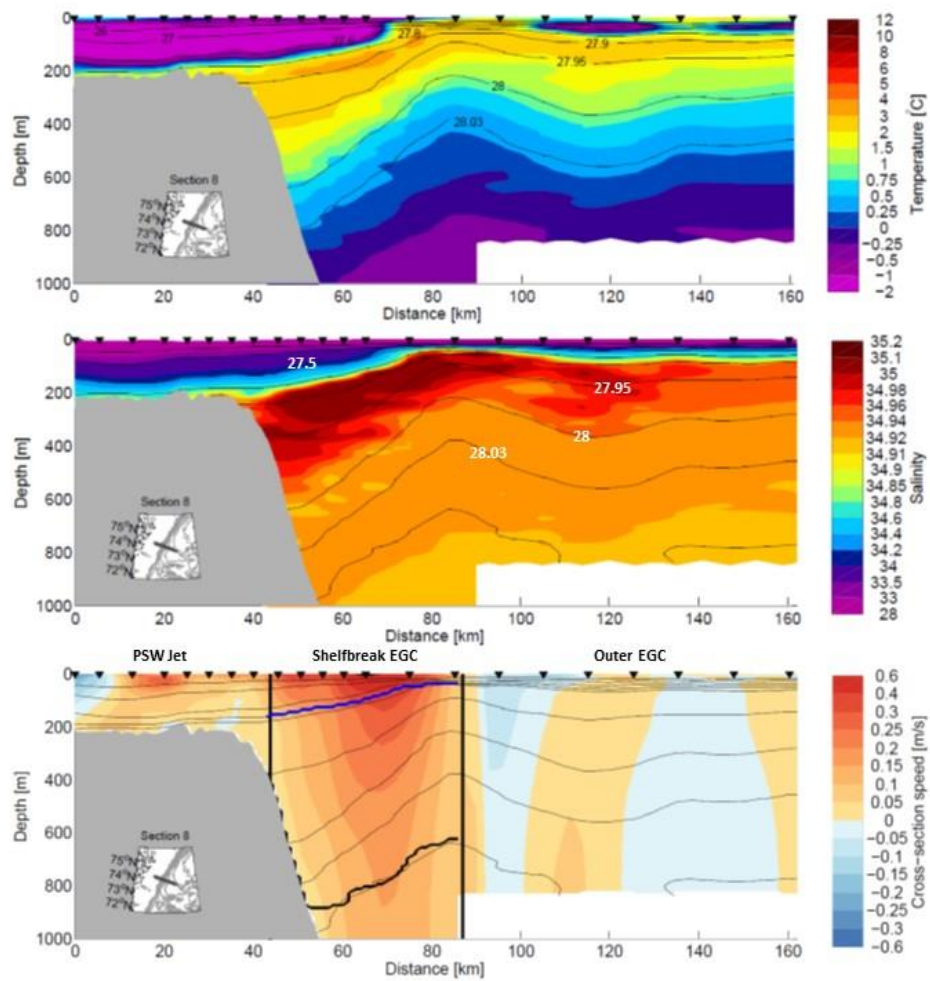


Figure 2-6: Vertical sections of hydrography and velocity for section 8 near Daneborg (~75 km from coast), otherwise as Fig. 2-5 (unpublished data, Håvik, 2017, personal communication).

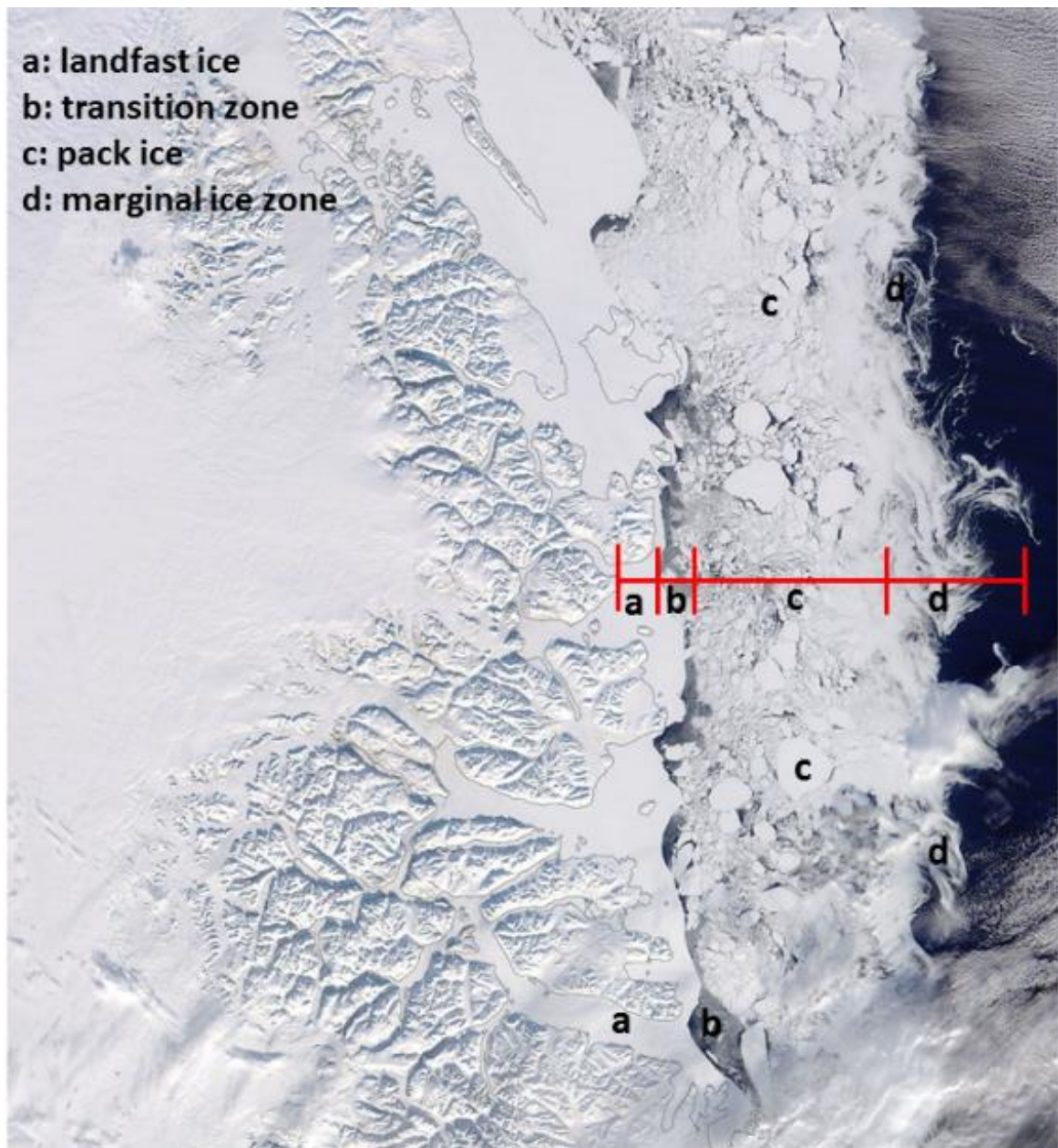


Figure 2-7: Satellite image (NASA Worldview, EOSDIS March 20, 2016) of the Northeast Greenland coast near Daneborg and Young Sound - Tyrolerfjord (74°N) with identification of different sea ice types in a cross-section perpendicular to the coast; (a) landfast ice, (b) transition zone, (c) pack ice, and (d) marginal ice zone.

2.3 Summary

This chapter examines the water masses along the coast of Northeast Greenland and is based on recent literature. It describes the hydrography and circulation of the Arctic Marine System, and places the coast and shelf of East Greenland in an ocean wide perspective.

The Northeast Greenland coast lies along the primary freshwater outflow shelf of the Arctic Ocean and receives approximately 85 % of the total yearly sea ice export out of the Arctic Ocean. A regional analysis of the dominant water masses and circulation in the Greenland Sea emphasizes the importance of the East Greenland Current System for the hydrographic conditions along the coast.

The hydrography of the East Greenland Current shows a three-layer structure, with Polar Surface Water (cold and fresh) at the surface, Atlantic Origin Water in the middle (warmer and saltier), and Greenland Sea deep water at the bottom ($>0^{\circ}\text{C}$, salty). In the velocity structure of the East Greenland Current, three major branches were identified: the outer East Greenland Current, the shelfbreak East Greenland Current, and the Polar Surface Water Jet.

References

- Aagaard, K., & Carmack, E. C. (1989). The role of sea ice and other fresh water in the Arctic circulation. *Journal of Geophysical Research*, *94*(C10), 14485. <https://doi.org/10.1029/JC094iC10p14485>
- Arrigo, K. R., & Van Dijken, G. L. (2011). Secular trends in Arctic Ocean net primary production. *Journal of Geophysical Research: Oceans*, *116*(9), 1–15. <https://doi.org/10.1029/2011JC007151>
- Bamber, J., van den Broeke, M., Ettema, J., Lenaerts, J., & Rignot, E. (2012). Recent large increases in freshwater fluxes from Greenland into the North Atlantic. *Geophysical Research Letters*, *39*(19). <https://doi.org/10.1029/2012GL052552>
- Beszczynska-Møller, A., Fahrbach, E., Schauer, U., & Hansen, E. (2012). Variability in Atlantic water temperature and transport at the entrance to the Arctic Ocean, 1997-2010. *ICES Journal of Marine Science*, *69*(5), 852–863. <https://doi.org/10.1093/icesjms/fss056>
- Beszczynska-Møller, A., Woodgate, R., Lee, C., Melling, H., & Karcher, M. (2011). A Synthesis of Exchanges Through the Main Oceanic Gateways to the Arctic Ocean. *Oceanography*, *24*(3), 82–99. <https://doi.org/10.5670/oceanog.2011.59>
- Buch, E. (2007). Physical oceanography of the Greenland Sea. In S. Rysgaard & R. N. Glud (Eds.), *Carbon cycling in Arctic marine ecosystems: Case study Young Sound* (pp. 14–21). Meddr. Grønland, Bioscience 58.
- Carmack, E., & Aagaard, K. (1973). On the deep water of the Greenland Sea. *Deep Sea Research and Oceanographic Abstracts*, *20*(8), 687–715. [https://doi.org/10.1016/0011-7471\(73\)90086-7](https://doi.org/10.1016/0011-7471(73)90086-7)
- Carmack, E. C. (2007). The alpha/beta ocean distinction: A perspective on freshwater

fluxes, convection, nutrients and productivity in high-latitude seas. *Deep-Sea Research Part II: Topical Studies in Oceanography*, 54(23–26), 2578–2598. <https://doi.org/10.1016/j.dsr2.2007.08.018>

Carmack, E. C., Yamamoto-Kawai, M., Haine, T. W. N., Bacon, S., Bluhm, B. A., Lique, C., ... Williams, W. J. (2016). Freshwater and its role in the Arctic Marine System: Sources, disposition, storage, export, and physical and biogeochemical consequences in the Arctic and global oceans. *Journal of Geophysical Research: Biogeosciences*, 121(3), 675–717. <https://doi.org/10.1002/2015JG003140>

Carmack, E., & McLaughlin, F. (2011). Towards recognition of physical and geochemical change in Subarctic and Arctic Seas. *Progress in Oceanography*, 90(1–4), 90–104. <https://doi.org/10.1016/j.pocean.2011.02.007>

Carmack, E., & Wassmann, P. (2006). Food webs and physical-biological coupling on pan-Arctic shelves: Unifying concepts and comprehensive perspectives. *Progress in Oceanography*, 71(2–4), 446–477. <https://doi.org/10.1016/j.pocean.2006.10.004>

Carmack, E., Polyakov, I. V., Padman, L., Fer, I., Hunke, E. C., Hutchings, J., ... Winsor, P. (2015). Toward Quantifying the Increasing Role of Oceanic Heat in Sea Ice Loss in the New Arctic. *Bulletin of the American Meteorological Society*, 96(12), 2079–2105. <https://doi.org/10.1175/BAMS-D-13-00177.1>

Cavalieri, D. J., & Parkinson, C. L. (2012). Arctic sea ice variability and trends, 1979-2010. *Cryosphere*, 6(4), 881–889. <https://doi.org/10.5194/tc-6-881-2012>

Comiso, J. C., Parkinson, C. L., Gersten, R., & Stock, L. (2008). Accelerated decline in the Arctic sea ice cover. *Geophysical Research Letters*, 35(1), L01703. <https://doi.org/10.1029/2007GL031972>

Haine, T. W. N., Curry, B., Gerdes, R., Hansen, E., Karcher, M., Lee, C., ... Woodgate, R. (2015). Arctic freshwater export: Status, mechanisms, and prospects. *Global and*

Planetary Change, 125, 13–35. <https://doi.org/10.1016/j.gloplacha.2014.11.013>

Håvik, L., Pickart, R. S., Våge, K., Torres, D., Thurnherr, A. M., Beszczynska-Møller, A., ... von Appen, W.-J. (2017). Evolution of the East Greenland Current from Fram Strait to Denmark Strait: Synoptic measurements from summer 2012. *Journal of Geophysical Research: Oceans*, 122(3), 1974–1994. <https://doi.org/10.1002/2016JC012228>

Helland-Hansen, B., & Nansen, F. (1909). *The Norwegian Sea. Its physical oceanography based upon the Norwegian researches 1900-1904*. Retrieved from <http://hdl.handle.net/11250/114874>

Jakobsson, M., Mayer, L., Coakley, B., Dowdeswell, J. A., Forbes, S., Fridman, B., ... Weatherall, P. (2012). The International Bathymetric Chart of the Arctic Ocean (IBCAO) Version 3.0. *Geophysical Research Letters*, 39(12). <https://doi.org/10.1029/2012GL052219>

Khan, S. A., Kjær, K. H., Bevis, M., Bamber, J. L., Wahr, J., Kjeldsen, K. K., ... Muresan, I. S. (2014). Sustained mass loss of the northeast Greenland ice sheet triggered by regional warming. *Nature Climate Change*, 4(4), 292–299. <https://doi.org/10.1038/nclimate2161>

Kwok, R. (2009). Outflow of Arctic Ocean Sea Ice into the Greenland and Barents Seas: 1979–2007. *Journal of Climate*, 22(9), 2438–2457. <https://doi.org/10.1175/2008JCLI2819.1>

Kwok, R., Cunningham, G. F., Wensnahan, M., Rigor, I., Zwally, H. J., & Yi, D. (2009). Thinning and volume loss of the Arctic Ocean sea ice cover: 2003–2008. *Journal of Geophysical Research*, 114(C7), C07005. <https://doi.org/10.1029/2009JC005312>

Latarius, K., & Quadfasel, D. (2016). Water mass transformation in the deep basins of the Nordic Seas: Analyses of heat and freshwater budgets. *Deep Sea Research Part I: Oceanographic Research Papers*, 114, 23–42.

<https://doi.org/10.1016/j.dsr.2016.04.012>

- McPhee, M. G., Proshutinsky, A., Morison, J. H., Steele, M., & Alkire, M. B. (2009). Rapid change in freshwater content of the Arctic Ocean. *Geophysical Research Letters*, *36*(10), 1–6. <https://doi.org/10.1029/2009GL037525>
- Pabi, S., van Dijken, G. L., & Arrigo, K. R. (2008). Primary production in the Arctic Ocean, 1998–2006. *Journal of Geophysical Research: Oceans*, *113*(8), 1998–2006. <https://doi.org/10.1029/2007JC004578>
- Proshutinsky, A., Krishfield, R., Timmermans, M.-L., Toole, J., Carmack, E., McLaughlin, F., ... Shimada, K. (2009). Beaufort Gyre freshwater reservoir: State and variability from observations. *Journal of Geophysical Research*, *114*, C00A10. <https://doi.org/10.1029/2008JC005104>
- Prowse, T., Bring, A., Mard, J., & Carmack, E. (2015). Arctic Freshwater Synthesis: Introduction. *Journal of Geophysical Research: Biogeosciences*, *120*(11), 2121–2131. <https://doi.org/10.1002/2015JG003127>
- Prowse, T., Bring, A., Mård, J., Carmack, E., Holland, M., Instanes, A., ... Wrona, F. J. (2015). Arctic Freshwater Synthesis: Summary of key emerging issues. *Journal of Geophysical Research: Biogeosciences*, *120*(10), 1887–1893. <https://doi.org/10.1002/2015JG003128>
- Rabe, B., Karcher, M., Schauer, U., Toole, J. M., Krishfield, R. A., Pisarev, S., ... Kikuchi, T. (2011). An assessment of Arctic Ocean freshwater content changes from the 1990s to the 2006–2008 period. *Deep Sea Research Part I: Oceanographic Research Papers*, *58*(2), 173–185. <https://doi.org/10.1016/j.dsr.2010.12.002>
- Rudels, B. (1986). The θ -S relations in the northern seas: Implications for the deep circulation. *Polar Research*, *4*(2), 133–159. <https://doi.org/10.1111/j.1751-8369.1986.tb00527.x>

-
- Rudels, B. (2002). The East Greenland Current and its contribution to the Denmark Strait overflow. *ICES Journal of Marine Science*, *59*(6), 1133–1154. <https://doi.org/10.1006/jmsc.2002.1284>
- Rudels, B. (2009). Arctic Ocean circulation. In J. Steele, K. Turekian, & S. Thorpe (Eds.), *Encyclopedia of ocean sciences 2nd ed.* (Second, pp. 211–225). San Diego. <https://doi.org/10.1016/B978-012374473-9.00601-9>
- Rudels, B. (2012). Arctic Ocean circulation and variability – Advection and external forcing encounter constraints and local processes. *Ocean Science*, *8*(2), 261–286. <https://doi.org/10.5194/os-8-261-2012>
- Rudels, B., Björk, G., Nilsson, J., Winsor, P., Lake, I., & Nohr, C. (2005). The interaction between waters from the Arctic Ocean and the Nordic Seas north of Fram Strait and along the East Greenland Current: results from the Arctic Ocean-02 Oden expedition. *Journal of Marine Systems*, *55*(1–2), 1–30. <https://doi.org/10.1016/j.jmarsys.2004.06.008>
- Stroeve, J. C., Serreze, M. C., Holland, M. M., Kay, J. E., Malanik, J., & Barrett, A. P. (2012). The Arctic’s rapidly shrinking sea ice cover: a research synthesis. *Climatic Change*, *110*(3–4), 1005–1027. <https://doi.org/10.1007/s10584-011-0101-1>
- Stroeve, J. C., Kattsov, V., Barrett, A., Serreze, M., Pavlova, T., Holland, M., & Meier, W. N. (2012). Trends in Arctic sea ice extent from CMIP5, CMIP3 and observations. *Geophysical Research Letters*, *39*(16). <https://doi.org/10.1029/2012GL052676>
- Swift, J. H., & Aagaard, K. (1981). Seasonal transitions and water mass formation in the Iceland and Greenland seas. *Deep Sea Research Part A, Oceanographic Research Papers*, *28*(10), 1107–1129. [https://doi.org/10.1016/0198-0149\(81\)90050-9](https://doi.org/10.1016/0198-0149(81)90050-9)
- Wadhams, P. (1981). The ice cover in the Greenland and Norwegian seas. *Reviews of Geophysics*, *19*(3), 345. <https://doi.org/10.1029/RG019i003p00345>

Woodgate, R. A., Weingartner, T. J., & Lindsay, R. (2012). Observed increases in Bering Strait oceanic fluxes from the Pacific to the Arctic from 2001 to 2011 and their impacts on the Arctic Ocean water column. *Geophysical Research Letters*, *39*(24), 2–7. <https://doi.org/10.1029/2012GL054092>

Woodgate, R. A., Aagaard, K., & Weingartner, T. J. (2006). Interannual changes in the Bering Strait fluxes of volume, heat and freshwater between 1991 and 2004. *Geophysical Research Letters*, *33*(15), L15609. <https://doi.org/10.1029/2006GL026931>

Chapter 3

Circulation and fjord-shelf exchange during the ice-covered period in Young Sound-Tyrolerfjord, Northeast Greenland (74°N)

W. Boone^{*1}, S. Rysgaard^{1,2,3}, S. Kirillov¹, I. Dmitrenko¹, J. Bendtsen^{3,4}, J. Mortensen², L. Meire^{2,3}, V. Petrushevich¹ and D. G. Barber¹

Published in:

Estuarine Coastal Shelf Science 194, 205–216. doi:10.1016/j.ecss.2017.06.021.

¹ Centre for Earth Observation Science, Department of Environment and Geography, University of Manitoba, Winnipeg, Canada

² Greenland Climate Research Centre, Greenland Institute of Natural Resources, Nuuk, Greenland

³ Arctic Research Centre, Aarhus University, Aarhus, Denmark

⁴ ClimateLab, Symbion Science Park, Copenhagen, Denmark

3.1 Introduction

High-Arctic fjords are characterized by large seasonal variations between summer and winter (Nilsen et al., 2008; Bendtsen et al., 2014; Noufal et al., 2016). In summer, the fjord is stratified under influence of a decreasing surface salinity due to runoff and melt from both sea ice and glacier ice, and warm surface temperatures due to summer insolation (Bendtsen et al., 2014). In winter, the upper water masses tend to be relatively homogeneous with near freezing temperatures and a relatively small range of salinities (Cottier et al., 2010). The shift in thermohaline structure from summer to winter is greatly impacted by formation of a sea ice cover, which suppresses local wind forcing, and low freshwater runoff. Other processes related to tides, fjord-shelf exchange and brine release from growing sea ice, therefore, become relatively more important dynamic drivers of circulation during the ice-covered period.

Circulation in ice-covered fjords is important because it can regulate the thickness and extent of the seasonal ice cover through an upward heat flux from warmer deeper layers (Maykut and Untersteiner, 1971; Hannah et al., 2009; Melling et al., 2015; Kirillov et al., 2015). In addition, circulation during winter, e.g. related to sea ice formation and brine rejection, can affect the concentration of CO₂ in surface waters the following summer, and, as a result, affect air-sea CO₂ gas exchange (Rysgaard et al., 2007; Else et al., 2011; Parmentier et al., 2013).

Fjords around Greenland vary greatly with respect to fjord topography, sill depth, and shelf water characteristics (Mortensen et al., 2014). Many fjords are characterized by steep ridges and sills at the entrance (Mortensen et al., 2011). A shallow sill forms a natural topographic barrier, which hampers free flow of seawater between the fjord basin and the adjacent shelf, but also creates a zone of enhanced mixing (Drinkwater and Osborn, 1975; Geyer and Cannon, 1982; Mortensen et al. 2011). Temporal correlation between variations in salinity and velocity can result in net salt transport across the sill if the tide does not act as a purely standing wave, with harmonic tidal fluctuations that are 90° out of phase (Geyer and Nepf, 1996; Seim and Greg, 1997). This exchange, known as tidal pumping, will result in a salt flux into the fjord if water flowing through the section during flood has a higher salinity than water flowing through the section during ebb. Valle-Levinson et al. (2006) emphasize the importance of this mechanism for salt fluxes in a fjord with a very shallow sill (3 m), but the mechanism has the potential to impact many fjords with different topography. The advected water will intrude into the fjord until reaching its depth of neutral buoyancy, potentially renewing the basin water, and driving circulation (Edwards and Edelsten, 1977; Gade and Edwards; 1979; Belzile et al., 2016).

Relatively few studies have been conducted north of Sermilik (66°N) and Kangerdlussuaq (68°N) fjords in East Greenland (Straneo et al., 2011; Sutherland et al., 2014; Jackson and Straneo, 2016). The Young Sound-Tyrolerfjord system, located at latitude 74°N, is the only fjord system in Northeast Greenland where measurements have been carried out on a long-term basis (since 2003) (Rysgaard and Glud, 2007).

Young Sound-Tyrolerfjord is, like other fjords further north towards Fram Strait, in contact with the cold, relatively low salinity, and mostly sea ice-covered water of the East Greenland Current (EGC). The EGC undergoes a pronounced seasonal cycle, following the melt and freeze-up cycles of sea ice on the shelf (Holfort and Hansen, 2005). However, seasonal investigations at Northeast Greenland's coast are few and are usually biased towards the summer period (Rysgaard and Glud, 2007; Bendtsen et al., 2014; Wilson and Straneo, 2015, Håvik et al., 2017). More research is needed to explore possible mechanisms controlling seasonal circulation in Northeast Greenland fjords, in particular during the ice-covered period.

Here we present seasonal observations from Young Sound-Tyrolerfjord and analyze variations in the circulation, thermohaline structure and cross-sill exchange. The observational dataset is based on six oceanographic moorings deployed in the fjord during 2013-2014 and resolves the temporal and vertical distribution of temperature, salinity and velocity. The velocity record is harmonically analyzed and observations are investigated in relation to (i) fjord-shelf exchange, (ii) the impact of polynya activity at the fjord entrance, and (iii) the input of snow, sea ice meltwater and river runoff. Finally, cross-sill salinity transport is estimated from a high-resolution mooring located at the outer sill and its role in the salt balance of the fjord is investigated.

3.2 Physical setting

3.2.1 Young Sound-Tyrolerfjord system

The Young Sound-Tyrolerfjord system (74°N) consists of an outer part, Young Sound, and an inner part, Tyrolerfjord, which is impacted by runoff of land-terminating glaciers from the Greenland Ice Sheet (Fig. 3-1). The fjord has a maximum depth of 360 m and is about 90 km long from the mouth to the inner part of Tyrolerfjord. The basin of the fjord system has two sills: a shallow outer sill of ~45 m depth located at the entrance to the fjord and an inner sill of ~56 m located in Tyrolerfjord, about 70 km from the outer sill. The fjord system receives runoff from the surrounding catchment area, partly covered by the Greenland Ice Sheet and local glaciers. The estimated runoff, which peaks in July, varies between ~0.9 to 1.4 km³ yr⁻¹ and causes surface salinities to decrease from ~33 to ~5 in the innermost part of the fjord system in August (Bendtsen et al., 2014). Tidal amplitude in Young Sound varies between about 0.8 m and 0.3 m from spring to neap tides and the dominating M2 and S2 components contribute with 0.48 m and 0.18 m, respectively (Bendtsen et al., 2007).

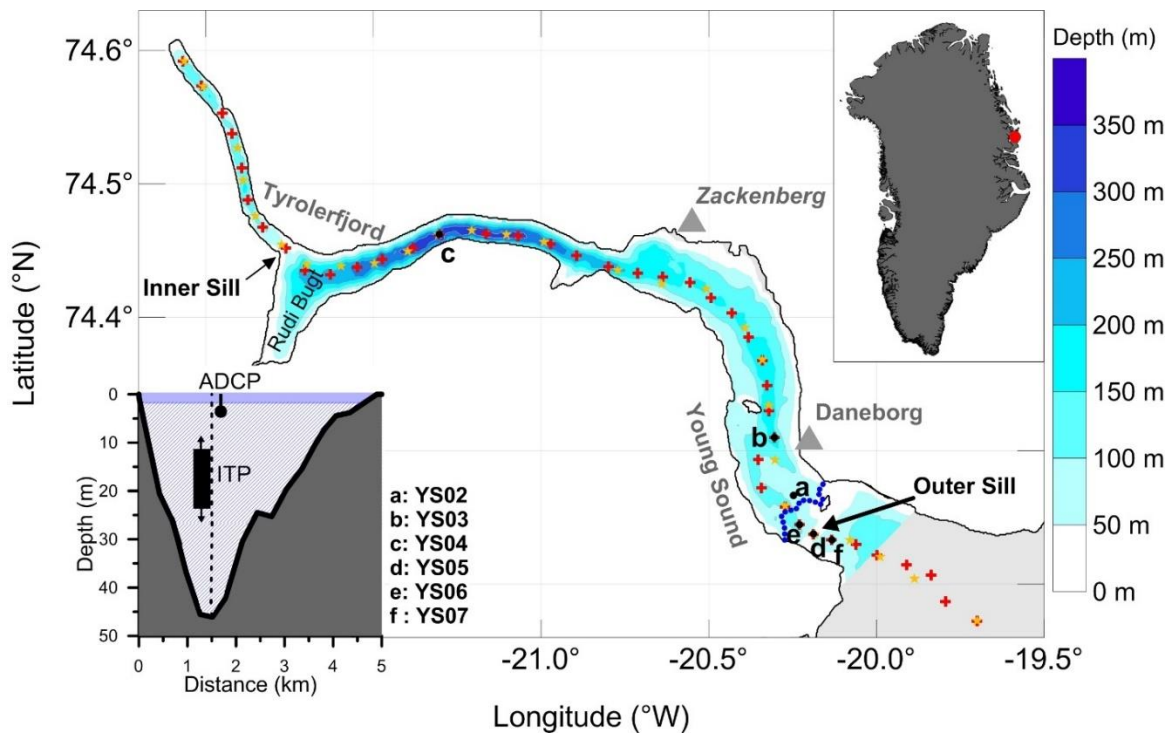


Figure 3-1: Study area, station map with bathymetry (Rysgaard et al., 2003) of the Young Sound - Tyrolerfjord system in Greenland. Red crosses depict the location of the CTD stations of the May transects, yellow stars mark the August transect. Black circles mark the location of the landfast ice-tethered oceanographic moorings (a: YS02, b: YS03, c: YS04, d: YS05, e: YS06, f: YS07). Blue line near the outer sill marks the landfast-ice edge after opening of the coastal polynya in December 2013. Inset shows the cross-section of the outer sill and the placement of the ADCP and ITP (mooring YS05).

3.2.2 Coastal water masses

Coastal water masses outside Young Sound are associated with the East Greenland Current, which transports large amounts of freshwater from the Arctic Ocean via Fram Strait, together with locally generated meltwater from sea ice and glacial ice southward

along the East Greenland continental shelf (Aagaard and Carmack, 1989; Strass et al., 1993). Surface waters consist of Polar Surface Water, characterized by low temperatures ($<0^{\circ}\text{C}$) and relatively low salinities (<34.4). Interannual variability and a pronounced seasonal cycle especially affects the salinity of Polar Surface Water, while temperature undergoes only a weak seasonal cycle (Holfort and Hansen, 2005). For example, a mooring, deployed approximately 70 km offshore of Young Sound (74.000°N , 17.987°W , 18 m depth), recorded a monthly mean potential temperature and salinity in May 2006 of -1.74°C and 32.98 respectively, and the corresponding values evolved to -1.71°C and 31.83 in October 2006 (Holfort and Meincke, 2005; Bendtsen et al. 2014). Below the surface water, the East Greenland Current transports Atlantic Water supplied by the West Spitsbergen Current and the Atlantic layer of the Arctic Ocean (e.g. Aagaard and Coachman, 1968; Håvik et al. 2017). Relatively warm ($0\text{-}2^{\circ}\text{C}$) Atlantic water is found below the Polar Surface Water between 150-800 m depth (Rudels et al., 2002).

3.2.3 Sea ice cover in winter 2013-2014

The fjord is covered by land-fast sea ice during ~ 9 months of the year. A wind-driven shelf polynya is maintained during winter in the transition zone between land-fast ice and pack ice at the outer part of Young Sound (Fig. 3-1, and see also Pedersen et al., 2010). In the winter of 2013-2014, freeze-up of the fjord system started around 15 October and the ice cover was approximately 25 cm thick at the end of October (Kirillov et al., 2015). A northerly storm event from 18 to 25 December forced the formation of

a coastal polynya at the mouth of the fjord on 20 December. The landfast sea ice edge stabilized ~ 3.5 km infjord from the outer sill (Fig. 3-1). Dmitrenko et al. (2015) showed that the opening of the polynya was associated with inflow of cool, saline, oxygenated water to the fjord interior. Several northerly strong wind events maintained a coastal polynya until approximately 4 March after which landfast ice grew within the polynya area and remained stable until breakup (15 July 2014). Thickness of the stable landfast ice within the fjord ranged from ~ 80 cm to 153 cm in May 2014. First open water appeared above the outer sill around 15 June. On 15 July, landfast ice in the coastal area broke up and all remaining ice in the fjord was transported away.

3.3 Data and methods

3.3.1 Ice-tethered mooring data

Three ice-tethered moorings were deployed through the land-fast ice in Young Sound between October 2013 and May 2014 to capture seasonal dynamics and the driving components of fjord hydrodynamics (Fig. 3-1, YS02/86 m, YS03/158 m and YS04/340 m, Table 1). Each mooring carried a 300 kHz downward-looking Teledyne RDI Workhorse Sentinel acoustic Doppler current profiler (ADCP) measuring horizontal and vertical current velocities. The velocity precision and resolution of the ADCPs attained ± 1 % and ± 0.5 cm s⁻¹ respectively, while compass accuracy and resolution were $\pm 2^\circ$ and 0.1° . Furthermore, six conductivity-temperature-depth sensors (CTD, Sea-Bird Electronics, Inc., SBE-37, accuracy temperature ± 0.002 °C and conductivity ± 0.0003 S m⁻¹) at

discrete depths (2, 7, 17, 47, 77 and 117 m) sampling in intervals of 10 min., were measuring the evolution of the thermohaline structure at mooring YS03, approximately 9 km inward from the outer sill. The ADCPs were set to sample 39 bins, with a bin size of 2 m, where each 10 min. sample is made out of ensemble averages of 20 pings. The first/last bins were centered at 6/84 m depth. Velocity directions were corrected by adding magnetic deviation (-18.5°) and samples with insufficient acoustic backscatter in the water column were eliminated by algorithms in the RDI ADCP software.

Dynamics and thermohaline structure at the shallow outer sill in Young Sound were monitored by a McLane ice tethered profiler (ITP) and a downward looking 600 kHz Nortek Aquadopp ADCP, which were installed in May 2014 (Fig. 3-1, YS05). Tidal velocities near the outer sill were measured by two additional Nortek ADCPs, one at each side, moored in sea ice approximately 2 km away from the outer sill (Fig. 3-1, YS06 and YS07). These instruments were operational from 1 May 2014 until 8 June 2014. The ITP was equipped with an SBE 52-MP CTD (accuracy temperature $\pm 0.002^\circ\text{C}$ and conductivity $\pm 0.0003\text{ S m}^{-1}$) and profiled the water column between ~ 1.5 and 35 m every 30 minutes. The ADCPs were set to sample 80 bins, with a bin size of 0.5 m, where each 5 min sample consisted of a 1 minute ensemble average of 60 pings. The first and last bins were centered at 1 m and 41 m depth respectively, and referenced to the ice undersurface as they were ice tethered. Because of a lack of scatters in the water column, vertical resolution, and increasing lateral separation of the sonar beams with distance from the transducer, only bins between 2.5 and 30 m were adequately

measured. The ITP record shows gaps in the deeper layers (>25 m), probably during periods when strong currents hampered the profiler.

Table 3-1: Instrumental details of oceanographic moorings.

Period	Name	Depth	Location	Sampling Interval	Instrument type	Brand
28 Oct 2013 – 15 May 2014	YS02	86 m	74.267°N, 20.248°W	10 min	ADCP	RDI - 300 kHz
	YS03	158 m	74.310°N, 20.304°W	10 min	ADCP,	RDI - 300 kHz
				10 min	CTD string (2, 7, 17, 47, 77 and 117 m)	SBE-37
YS04	340 m	74.462°N, 21.304°W	10 min	ADCP	RDI - 300 kHz	
1 May 2014 to 8 Jun 2014	YS05	45 m	74.238°N, 20.188°W	5 min	ADCP	Nortek - 600 kHz
				30 min	ITP with CTD	McLane ITP with SBE 52-MP
	YS06	93 m	74.245°N, 20.229°W	5 min	ADCP	Nortek - 600 kHz
YS07	73 m	74.233°N, 20.133°W	5 min	ADCP	Nortek - 600 kHz	

For analysis and visualization, the ITP- and ADCP time series from the sill location were aligned. ITP temperature and salinity profiles were averaged over the ADCP bins (average between bin limits) and obtained ADCP data were resampled as half hourly averages on the ITP sampling intervals (i.e. ± 15 min centered around the ITP observation). Residual currents in the along-fjord direction were obtained by removing velocity fluctuation at tidal frequencies with a Pl66 low-pass filter with a half-amplitude period of 33 h (Limeburner, 1985). This filter excludes all major diurnal and semidiurnal tidal constituents. Tidal harmonic analysis of the full available ADCP record was performed using the T-Tide software (Pawlowicz et al., 2002).

3.3.2 Hydrographic and meteorological data

Along-fjord temperature and salinity transects in May 2014 were surveyed on snowmobiles using a SBE-19plus CTD (Seabird Electronics, accuracy temperature: ± 0.005 °C and conductivity: ± 0.0005 S m⁻¹), which was lowered through ice holes drilled in the landfast ice. Survey of the complete transect spanned over three days and consisted of approximately 41 stations. A CTD transect (28 stations) was also conducted by ship between 6 August and 18 August 2013 as part of the Marin Basis Program (Jensen et al., 2014). Summer transect covers the same spatial domain at lower horizontal resolution (Fig. 3-1). Strong wind events (here defined as periods with wind speeds greater than 15 m s⁻¹) were identified from hourly wind velocity and direction measurements from the Daneborg meteorological station (location Fig. 3-1a), which is maintained by the Danish Meteorological Institute.

3.4 Results

3.4.1 Seasonal thermohaline variability

Temperature and salinity of water masses on the shelf and inner part of the fjord system evolved seasonally (Fig. 3-2). In summer, the fjord water mass occupied a large range of temperatures and salinities, but after winter the variability in salinity and temperature was relatively small. On 18 August 2013, temperatures above 4 °C and salinities below 29 were observed in the surface layer, with the highest temperatures (up to 8 °C) and lowest salinities (down to 17) in the inner part of the fjord. Generally, temperatures were negative below 30 m in the fjord basin, with a minimum temperature of ~ -1.6 °C in the depth range of 200-330 m. Below 30 m, salinities increased from ~ 31.0 to 32.2 at 120 m and then increased further with depth, reaching a maximum of 33.1 in the deepest part of Young Sound. Warmer coastal water masses were found on the seaside of the outer sill with temperatures > 0 °C below 180 m and a temperature range of ~ -1.6 °C and 0 °C. Salinities increased with depth from 32.0 at sill depth to 34.5 at 200 m. We note that the summer temperature profiles indicated mixing of warm and fresh surface water in the sill regions down to 100 m.

The CTD transects from 10-12 May 2014 and 16-19 May 2014 showed a weakly stratified water column in the upper 150 m (Fig. 3-2cd). Here, temperatures were just 0.03 – 0.06 °C above the in situ freezing point (~ -1.75 °C) over the range of observed salinities (32.25 - 32.50). Comparison between profiles from August 2013 and from May

2014 showed that salinity and temperature changes since the previous summer below 150 m in Young Sound were very low (Fig. 3-2). Mean temperature and salinity for the combined datasets below 150 m reached $-1.61 \pm 0.02^{\circ}\text{C}$ and 32.8 ± 0.2 , respectively. On the seaside of the outer sill, water masses in May were generally colder than in August but covered a similar salinity range.

Around 16 May, water masses with relatively low salinity and higher temperature appear at the outer sill (Fig. 3-2e-h) and therefore, we define this date as the start of spring. Two transects were measured between 16 May – 28 May and showed a slight decrease in salinity and rise in temperature over the outer sill during this period. We note that the stations at the outer sill on 16 May (Fig. 3-2ef) were occupied during flood (30 min interval between stations), while the stations of the 26 May transect were occupied during ebb tide (Fig. 3-2gh). This difference likely plays a role in the location of water masses above the sill in the two transects.

3.4.2 Seasonal circulation

Circulation in the ice-covered fjord was generally characterized by a two-layer circulation mode with outflow in the upper layer and inflow below. However, observations from the moorings also showed large short-term spatial and temporal variability (Fig. 3-3). Between October 2013 and 20 December, mooring YS02, which was located about 2 km from the outer sill (Fig. 3-3a), recorded a weak ($<5 \text{ cm s}^{-1}$) outflow in the upper 10 m and strong inflow with velocities as high as 12 cm s^{-1} between 15-45 m. Around 20 December 2013, a change in the circulation regime occurred at this

location and deep inflow was observed to take place at increasing depths in the water column (Fig. 3-3a). At that time, inflow with current velocities less than 5 cm s^{-1} was observed below 45 m, with, at times, a relatively strong outflowing current above 45 m (maximum of 10 cm s^{-1}). Furthermore, in early February large inflow events occurred with inflowing currents over the complete water column and current velocities up to 7.5 cm s^{-1} . The regime shift and large inflow events were linked to openings of the polynya in the mouth of the Young Sound fjord (Dmitrenko et al., 2015).

The renewal depth of intruding waters, which equals its depth of neutral buoyancy, varied significantly over the ice-covered season (see YS03, Fig. 3-3b). From October 2013 to January 2014 the renewal depth increased gradually from 10 m to 50 m. This period was followed by large inflow events in the beginning of February, of which some covered the complete water column. Finally, a relative calm period occurred from mid-February to April 2014, when the lower current was evolved and deepened to $\sim 60 \text{ m}$ (Fig. 3-3b). A similar evolution of the circulation was recorded at mooring YS04 in the inner part of the fjord (Fig. 3-3c). This change in renewal depth coincided with a cooling and an increase in salinity with increasing depths (Fig. 3-4). The CTD-mooring at YS03, about 9 km from the outer sill, recorded that the largest salinity and temperature changes before 20 December mainly occurred in the upper 47 m. After 20 December, the deeper layers (i.e. at 47 m, 77 m and 117 m) showed an increase in salinity (the salinity at 47 m increased from 31.8 to 32.3) and some decrease in temperature (from -1.54 to $-1.75 \text{ }^\circ\text{C}$ at 117 m).

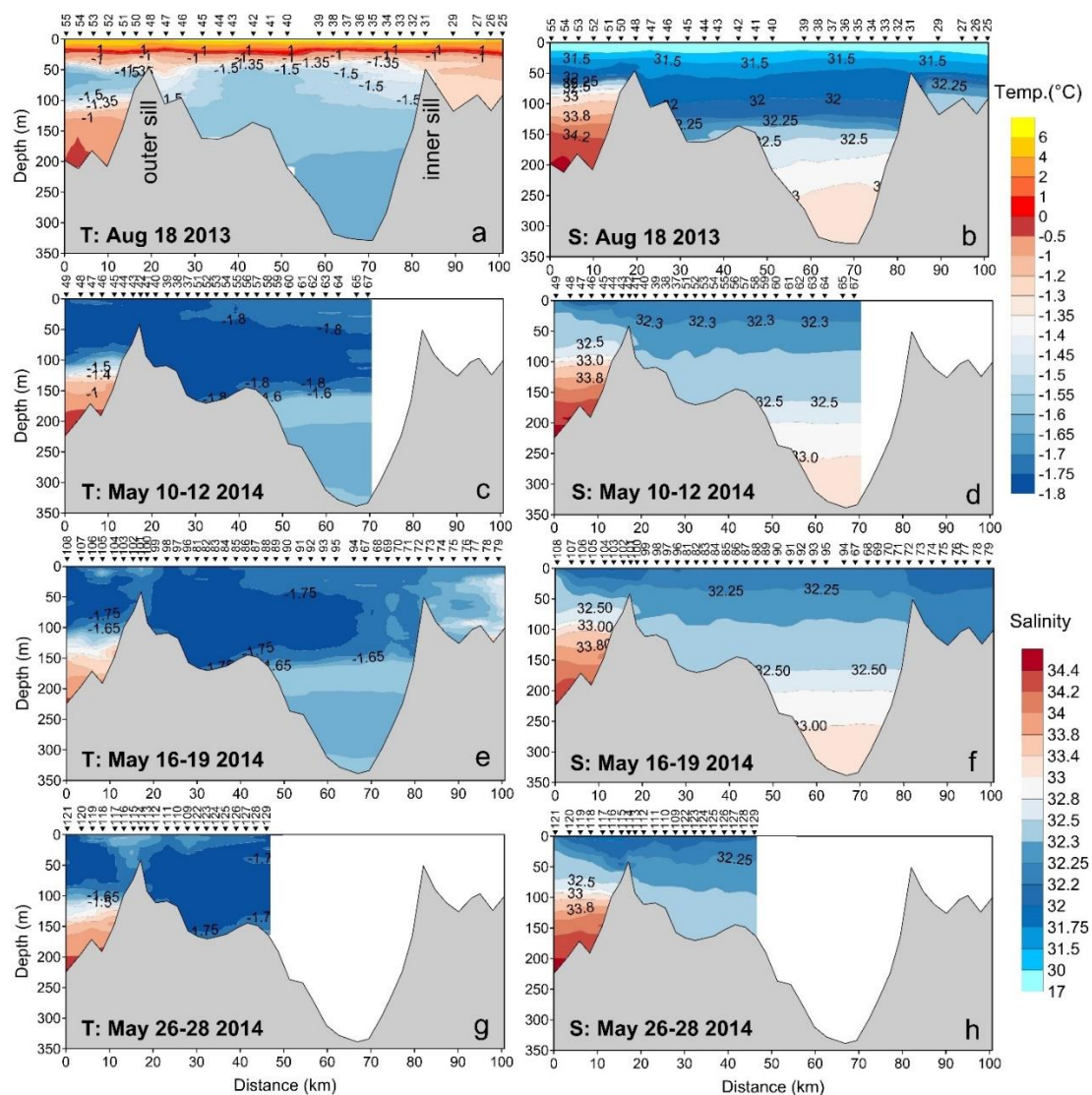


Figure 3-2: Along-fjord transect of temperature (left column) and salinity (right column) taken on (a-b) 18 August 2013, (c-d) 10-12 May, (e-f) 16-19 May and (g-h) 26-28 May 2014. Black triangles on the top identify positions of the CTD stations, distance marked from outermost offshore station.

During the period between 20 December and 4 March, when the polynya was observed offshore of Young Sound, circulation in the fjord was able to lift summer-heated water to surface layers in the inner part of Young Sound, observed as an increase in surface

temperature at the YS03 mooring (Fig. 3-4) (this event has been further analyzed in Kirillov et al., 2015). Between 21 November and 20 December, all temperatures were below $-1.5\text{ }^{\circ}\text{C}$ and after 20 December, temperatures at 2 m and 7 m increased to a maximum $\sim -1.1\text{ }^{\circ}\text{C}$. Furthermore, observations by the ADCP mooring showed that polynya openings slightly preceded events with intensified outflow (maximum current magnitudes of 15 cm s^{-1}) and a temporary deepening of the circulation cell in the fjord (Fig. 3-3).

The along-fjord transects recorded the appearance of fresher and relatively warmer water at the sill around 16 May (Fig. 3-2e-h). Around that period, mooring YS02 measured inward directed currents in the upper 20-30 m and outflow below (Fig. 3-3); only about 10 days later a similar pattern was measured at YS03 (Fig. 3-3b). After 16 May, residual current magnitudes attained up to 10 cm s^{-1} at YS02 and were $<5\text{ cm s}^{-1}$ at YS03. At mooring YS04, residual current magnitudes were close to zero.

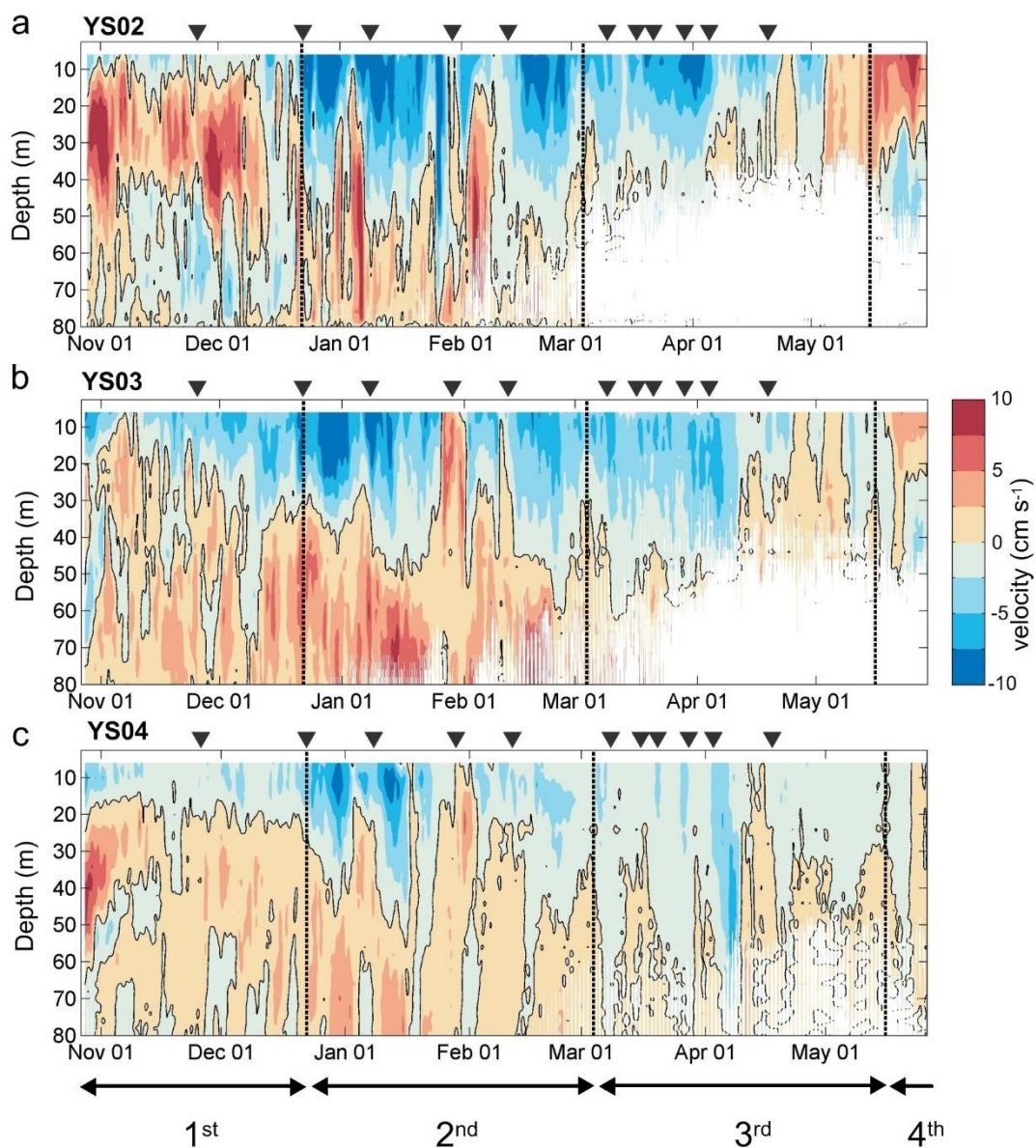


Figure 3-3: Depth time plot and zero contour line of the residual current (m s^{-1}) along the fjord axis and positive toward the inner fjord as calculated with low-pass filter pl66 (Limeburner et al., 1985) from ADCP data at mooring (a) YS02-13, (b) YS03-13 and (c) YS04-13. Black triangles indicate strong wind events with winds exceeding 15 m s^{-1} , and vertical black lines bound the circulation periods.

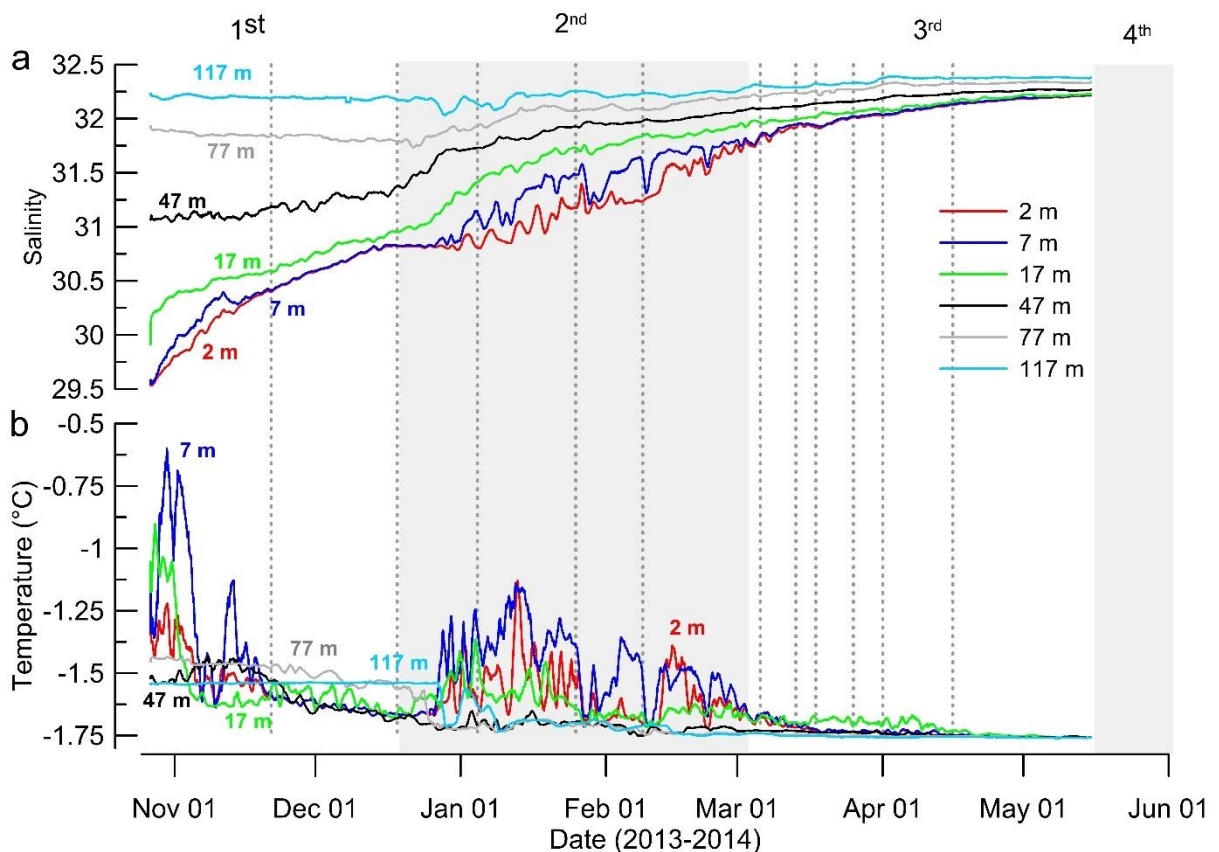


Figure 3-4: Change in hydrography of the outer Young Sound-Tyrolerfjord from fall to spring: The smoothed time series of (a) salinity and (b) potential temperature at discrete depths (2, 7, 17, 47, 77 and 117 m) at mooring YS03. Dashed lines indicate strong wind events ($>15 \text{ m s}^{-1}$), grey areas mark the different time periods.

3.4.3 Tidal analysis

In general, the velocity data showed relatively high tidal velocities over the sill and a decrease of velocities with distance from the outer sill into the fjord basin. The tidal signal of currents was determined for each location from the ADCP record at 20 m depth. Over the outer sill, predicted variability (35 constituents, 37.64 days) accounted for 82.1% of the variability of the original dataset. The signal was dominated by the M2

lunar semidiurnal constituent. At the offshore mooring (YS07), positioned 2 km offshore from the outer sill, the M2 component measured 12 cm s^{-1} . At the outer sill, the M2 velocity component attained $\sim 26 \text{ cm s}^{-1}$ (Table 2), while the maximum measured velocity reached $\sim 50 \text{ cm s}^{-1}$. From the outer sill towards the inner fjord the M2-value decreased from 9.6 cm s^{-1} at the fjord side of the sill (YS06) to 5.7 cm s^{-1} at YS02, 3.3 cm s^{-1} at YS03 and 1.0 cm s^{-1} at YS04. The semidiurnal S2 was the second largest constituent corresponding to about a third of the M2 magnitude at each site.

The M2 tidal currents at the moorings around the outer sill (YS05, YS06 and YS07) showed that the minor axes of the current ellipses were small and that inclinations for all constituents were similar (Table 2). The ADCP located above the outer sill recorded that tidal velocities did not change considerably with depth: the average M2 amplitude reached 25.8 cm s^{-1} with a standard deviation of 1.8 cm s^{-1} for depth bins between 2 and 25 m depth. In May 2014, calculated residual currents over the outer sill were relatively small ($< 2 \text{ cm s}^{-1}$) compared to tidal velocities in the area, and were mostly directed infjord, which suggests that the cross-sectional residual currents were not uniform. Tidal excursion at the sill varies between $\sim 5.0 \text{ km}$ and $\sim 2.6 \text{ km}$ during spring- and neap-tides respectively.

Table 3-2: Primary diurnal and semidiurnal components based on the measured tidal currents at 20 m depth at the three locations close to the outer sill (YS05, YS06, and YS07) and long-term mooring locations (YS02, YS03, YS04).

Tidal constituent	Major Axis, cm s⁻¹ (err)	Minor Axis, cm s⁻¹ (err)	Inclination Major axis, deg. N (err)	Phase, deg (err)
YS07	Sea side sill; Depth: 73 m; Distance sill: 2 km			
M2	12.4 (0.5)	-1.8 (0.4)	282.6 (1.6)	270.1 (2.6)
S2	4.2 (0.5)	0.3 (0.4)	291.3 (5.6)	305.7 (7.8)
YS05	Sill; Depth: 45 m			
M2	26.6 (0.5)	-5.6 (0.6)	290.4 (1.4)	271.0 (1.2)
S2	9.0 (0.5)	-1.8 (0.6)	288.2 (4.1)	312.4 (3.2)
YS06	Fjord side sill; Depth: 93 m; Distance sill: 2 km			
M2	9.6 (0.7)	-1.5 (0.7)	309.5 (3.9)	274.7 (4.2)
S2	2.6 (0.6)	-0.3 (0.6)	301.0 (15.9)	325.4 (14.9)
YS02	Depth: 86 m; Distance sill: ~3 km			
M2	5.7 (0.5)	-0.8 (0.4)	342.0 (4.5)	271.4 (5.2)
S2	2.5 (0.5)	-0.5 (0.5)	347.5 (10.5)	317.3 (13.2)

YS03	Depth: 158 m; Distance sill: ~9 km			
M2	3.3 (0.2)	-0.1 (0.2)	352.6 (4.3)	268.6 (3.1)
S2	1.4 (0.2)	-0.1 (0.3)	348.1 (8.5)	315.8 (7.7)
YS04	Depth: 340 m; Distance sill: ~47 km			
M2	1.0 (0.2)	0.0 (0.1)	75.9 (5.2)	264.5 (10.0)
S2	0.4 (0.2)	0.0 (0.1)	79.5 (12.6)	304.4 (24.0)

3.4.4 Cross sill exchange

Exchange over the outer sill at the entrance of Young Sound was monitored from 1 May 2014 until 8 June 2014 by the ice tethered ADCP and CTD profiler (Fig. 3-1, YS05). During this period, maximum depth-averaged (3-30 m) semidiurnal tidal currents over the sill attained more than 40 cm s^{-1} during spring tide and approximately 10 cm s^{-1} during neap tides (Fig. 3-5a).

The ice-tethered CTD profile data showed a distinct change in temperature and salinity characteristics of the upper 36 m of the water column at the outer sill on 16 May. The first period of the record (prior to 16 May) was characterized by small temperature differences and salinities ranging between 32.20 and 32.51 in the 3-36 m depth interval (Fig. 3-5). During the second period (after 16 May), low-salinity and warmer water was recorded over the outer sill (salinities between 30.63 and 32.56, maximum temperature

of $-1.40\text{ }^{\circ}\text{C}$, 3-36 m). The CTD data showed a tidal (semidiurnal) periodicity of salinity, with higher salinities during flood than during ebb tides (Fig. 3-5bc). In addition, the data showed that spring tides were associated with higher salinities and lower temperatures compared to neap tides (Fig. 3-5bc). A plot of the measured salinities versus tidal phase confirmed that on average, higher salinities were observed during flood compared to ebb tides (Fig. 3-6). For the first period, between 1 May and 16 May (total of 28 salinity profiles), difference in salinity between ebb and flood was higher for the deeper bins (20-30 m and 30-40 m) than for the bins at the surface (1-10 m and 10-20 m). Highest salinities were measured in the hours before maximal flood, when acceleration of the flood flow was maximal. The corresponding temperature differences were negligible, i.e. temperatures were around $-1.76\text{ }^{\circ}\text{C}$ during both ebb and flood phases, which indicated the near freezing state of the water column.

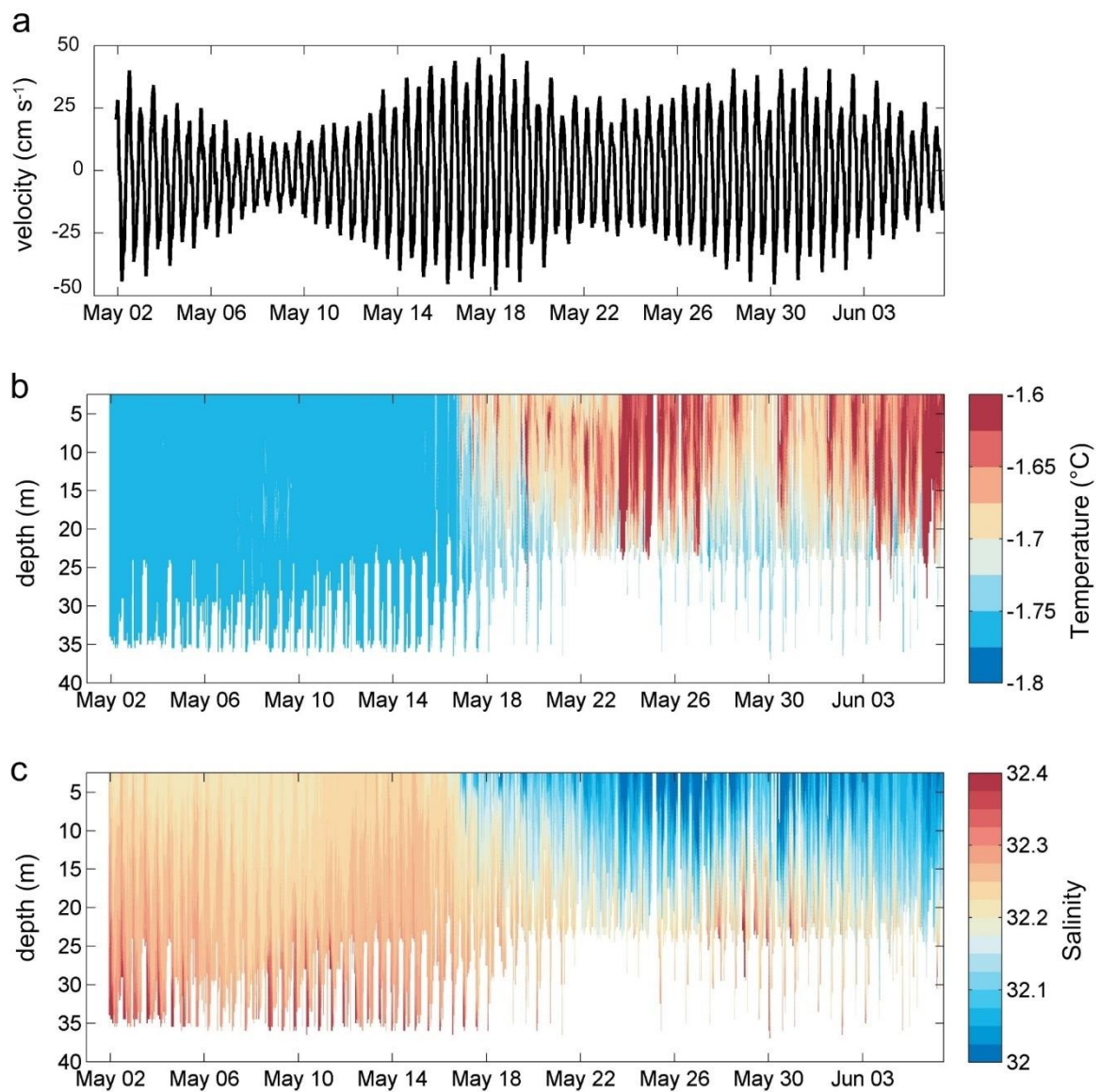


Figure 3-5: Time series of (a) depth-averaged current velocity (3-30 m, m s⁻¹) directed across the sill, positive towards the fjord interior , (b) temperature (°C) and (c) salinity profiles above the sill (location: YS05).

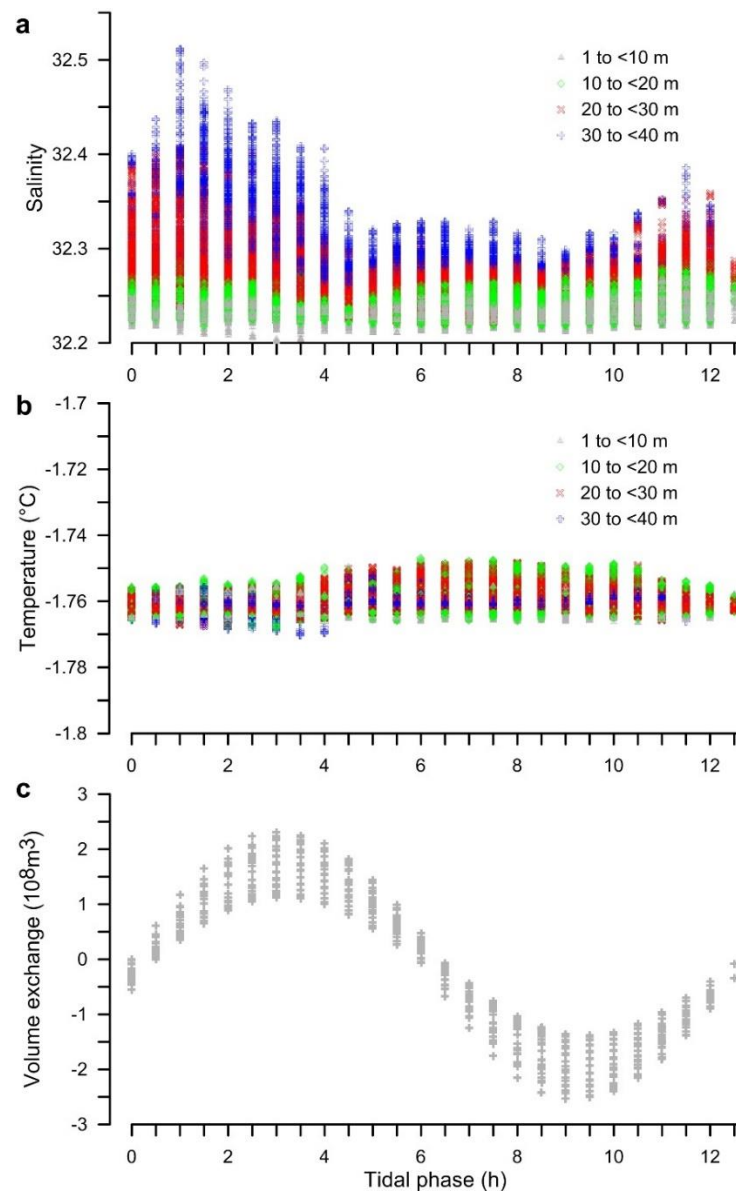


Figure 3-6: (a) Salinity and (b) temperature above the sill versus tidal phase, for the period of 1 May until 15 May 2014, as measured over the outer sill at mooring YS05. Colors depict the depth of the measurements. (c) Volume exchange versus tidal phase. Volume exchange measurements are based on M2 and S2 harmonic components of the depth-averaged velocity measured at mooring YS05, positive towards the fjord interior.

3.5 Discussion

3.5.1 Circulation dynamics and environmental factors

The CTD-transect from August 2013 (Fig. 3-2ab) showed that fjord water masses had a relatively large range of salinities (17.0 to 34.4) and temperatures (-1.6 to 8.0 °C) in the summer period (Fig. 3-2ab). The relatively strong stratification persisted until freeze-up of the fjord in the end of October (Fig. 3-4). Between October 2013 and May 2014, there were no indications of deep-reaching convection. A mixed layer with uniform salinity and temperature was measured throughout this period at 2 m and 7 m depth (Fig. 3-4). This limited surface mixed layer suggests that brine release from local land-fast sea ice formation had a minor impact on the change of the thermohaline structure of the fjord's basin water.

At the outer sill, local surface water was mixed with water masses from the coast, which were advected over the sill and into the fjord. Right after freeze-up, the freshwater content of the fjord was relatively high and the mixture of coastal water and local surface water only caused renewal at intermediate depths close to the outer sill. This changed abruptly around 20 December and occurred slightly after the opening of the polynya at the entrance of Young Sound (Dmitrenko et al., 2015). At this time, a mixture of coastal water and local surface water renewed the upper basin water close to the outer sill (Fig. 3-3a). The opening of the polynya led to intense sea ice formation, and the associated brine release was able to increase the cross-sill salinity gradient and

impact fjord circulation (Dmitrenko et al., 2015). At times, the inflow that followed the opening of the polynya occupied the complete water column, as seen during the large inflow events in early February. Similar circulation shifts in fjords have been linked to salinity increases in the offshore water due to seasonal density variations in coastal water masses (e.g. Belzile et al., 2016).

The time series of residual currents showed that during the ice-covered period, the depth of the circulation cell increased with time (Fig. 3-3b). From 27 October 2013 to 16 May 2014, the depth of zero residual currents, indicated by the iso-lines in Fig. 3-3a-c, increased from about 20 m to 47 m (Fig. 3-3a-c). This shows that partial basin renewal of the fjord was a relatively slow process that modified the fjord water masses on a seasonal timescale. This slow renewal of basin waters in Young Sound-Tyrolerfjord is in contrast to some other fjords in Greenland, e.g. the Sermilik Fjord (Jackson et al., 2014), a fjord without a shallow sill, where fast renewal events, within a timescale of three to ten days, have been observed.

The appearance of warmer and low-salinity water at the sill during onset of spring (Fig. 3-2ef, Fig. 3-5) marks another shift in the circulation regime. The freshwater source may have been sea ice and snow meltwater from inside the fjord itself or meltwater from offshore, because no significant river discharge from major rivers was recorded during this period (Zackenberg Basis monitoring program). Tidally generated turbulence on the lee side (fjord side) of the sill is potentially able to mix water with low salinity deeper into the water column close to the sill. In other areas of the fjord, where the ice cover prevented wind mixing, the water column remained stratified with meltwater in a

shallow surface layer on top of the cold saline winter water. Downward mixing of low-saline surface water at the sill, thereby, impacted fjord stratification and circulation.

3.5.2 Temporal changes in fjord circulation pattern

Based on the described variations in cross sill salinity gradient, polynya activity at the fjord mouth, and input of fresh water, four distinct circulation patterns and periods can be identified. The general circulation patterns, based on the averaged residual currents, are shown in Fig. 3-7.

The first period (27 October to 20 December 2013), covers the dates between the installation of the moorings and the opening of the coastal polynya. This period coincides with the freeze-up of the fjord, when ice thickness increased from about 15 cm to 70 cm near mooring YS04, above the deepest part of the fjord (Kirillov et al., 2015). During this period, freshwater input to the fjord was negligible. However, both the freshwater content of the upper part of the water column in the fjord and the cross-sill salinity gradient were relatively large. Inflow of cold and saline coastal water drove the renewal of water at intermediate depths (i.e. between the surface layer (10 m) and the sill (45 m)) close to the sill (YS02) with maximum average residual velocities of $4.1 \pm 3.2 \text{ cm s}^{-1}$ (Fig. 3-7b), while farther inward (mooring YS03 and YS04) the inflow induced renewal in the upper part of the water column (below 20 m) with maximum average residual velocities of $1.8 \pm 1.4 \text{ cm s}^{-1}$.

The transition to the second period (21 December 2013 to 4 March 2014) was linked to the opening of the polynya at the entrance of Young Sound. The polynya was

maintained by strong wind events throughout this period (Dmitrenko et al., 2015). Renewal of the upper basin water occurred closer to the sill (Fig. 3-7b, Fig. 3-7c). Recurring polynya events intensified circulation with average residual outflow velocities of up to $6.8 \pm 3.1 \text{ cm s}^{-1}$ above 37 m and average residual inflow velocities up to $3.8 \pm 2.1 \text{ cm s}^{-1}$ below this depth (Fig. 3-7c).

The third period (5 March to 16 May 2014) marked a time when the salinity content of the fjord increased without polynya activity (Fig. 3-4). The two-layer circulation mode was maintained during this period with relatively weak average residual velocities ($\sim 3 \text{ cm s}^{-1}$) both in the outflow above 47 m and in the inflow below (Fig. 3-7d). The cross-sill salinity gradient was relatively low during this period.

The fourth period (starting 16 May) was marked by the appearance of fresher and warmer water over the outer sill (Fig. 3-3, Fig. 3-4). During this period, average residual velocities reversed direction in the outer fjord (YS02-YS03), with inflow above 30 m and outflow below. At YS02, the average residual inflow velocities attained $6.6 \pm 1.8 \text{ cm s}^{-1}$ (Fig. 3-7e). In the inner fjord (YS04), average residual velocities were small ($< 0.5 \text{ cm s}^{-1}$). The cross-sill salinity gradient stayed relatively low at the start of this period, but we speculate they may have increased as more meltwater became available (after the period of record).

3.5.3 Link between sea ice cover and circulation

The general circulation pattern during the ice-covered period in the fjord was characterized by a two-layer circulation (Fig. 3-7). Kirillov et al. (2015) showed that

relatively warm summer heated water from the fjord basin was transported upwards and brought in contact with the sea ice, where it impacted local sea ice growth. Particularly after 20 December, water temperatures at 2 m increased from $-1.7\text{ }^{\circ}\text{C}$ to $-1.1\text{ }^{\circ}\text{C}$ (Fig. 3-4b) and associated heat transport impacted the ice growth near mooring YS04 (Kirillov et al., 2015). Further insight into the circulation pattern of the fjord, obtained in this study, reveals that heat loss due to melting of sea ice cooled the summer heated water transported in the upper layers towards the outer sill (Fig. 3-7), and therefore the summer heated water had less impact on sea ice growth at the mouth of the fjord than in the inner fjord. Consequently, the along fjord transect of sea ice thickness showed thinner ice in the inner fjord ($\sim 30 - 55$ km from the outer sill) compared to the mouth of the fjord ($\sim 0 - 30$ km from the outer sill) (Fig. 3-7a). Melling et al. (2015) reported that this pattern of variation, with ice thicker at the fjord's mouth than at its head, also characterized many sill fjords in the Canadian Arctic. Hence, we can speculate that similar circulation patterns as measured and described during the 2013-2014 winter season for the Young Sound-Tyrolerfjord may occur in other ice-covered fjords with shallow sills distributed around the Arctic.

3.5.4 Cross-sill salt fluxes

Circulation in the ice-covered fjord was driven by intrusions of dense water, transported over the outer sill and into the fjord interior. Observations at the outer sill indicated that dense water input across the sill may be partially explained by tidal pumping. Tidal pumping occurs when co-variation of salinity and velocity during a tidal period results

in a net salt transport (Dyer, 1997) (Fig. 3-6). Tidal pumping over the sill can be driven by both aspiration, a process where acceleration of the flow draws water from beneath the sill depth up and across the sill (Seim and Gregg, 1997), and tidal excursion in presence of a horizontal salinity gradient. The ITP dataset shows that highest salinities tend to occur when acceleration of the flood flow is maximal (between slack and maximum flood velocities) (Fig. 3-6). Furthermore, the density at ~70 m on the sea side of the sill (density= 1026.2 kg m^{-3} , Fig. 3-3a, profile 46) corresponds to the maximal density observed by the ITP over the sill (1026.2 kg m^{-3}). These observations suggest that aspiration of coastal water from below sill depth might be one of the sources of dense water advected to the fjord by tidal pumping.

To quantify the potential contribution of tidal pumping to the salt transport into the fjord over a neap-spring tidal period we evaluated the salt balance of the fjord. We separated the flux through the cross-section into an advective flux and a pumping flux, similar to Geyer et al. (2001), Scully and Friederichs (2007) and Becherer et al. (2016). The advective flux is driven by the residual tidally averaged velocity, while the pumping flux is driven by deviations from the tidally averaged value. The pumping flux can be further decomposed in a tidal pumping term, driven by the harmonic tidal variation and a residual pumping term, driven by, for example, short period variations in velocity and salinity due to turbulence.

During the ice-covered period, freshwater input to the fjord was negligible and measured residual currents at station YS05 were low ($<2 \text{ cm s}^{-1}$), therefore, the advective salinity flux is expected to be small. In addition, we note that although

temporal coverage of our records is quite comprehensive, the spatial coverage of our mooring data across the width of the fjord at the sill is rather limited. The measurements suggest the residual flow is not uniform across the sill, therefore our measurements at the sill, with only one station, do not suffice to reliably estimate the advective flux due to residual flow.

In contrast to residual flow, tidal flow over the sill is assessed to be fairly uniform, as the cross section at the outer sill is relatively deep (45 m) and wide (~5 km). The dataset thus enables us to focus on the cross-sectional averaged tidal pumping. We estimate the salt flux due to tidal pumping by multiplying the cross-sectional area (A) with the cross-sectional averaged salinity (S_{av}) and the tidal component of cross-sectional averaged velocity (U_{av}) for every time step of our record (Equation 1).

$$F_T = \int_0^t A S_{av}(t) U_{av}(t) dt \quad (1)$$

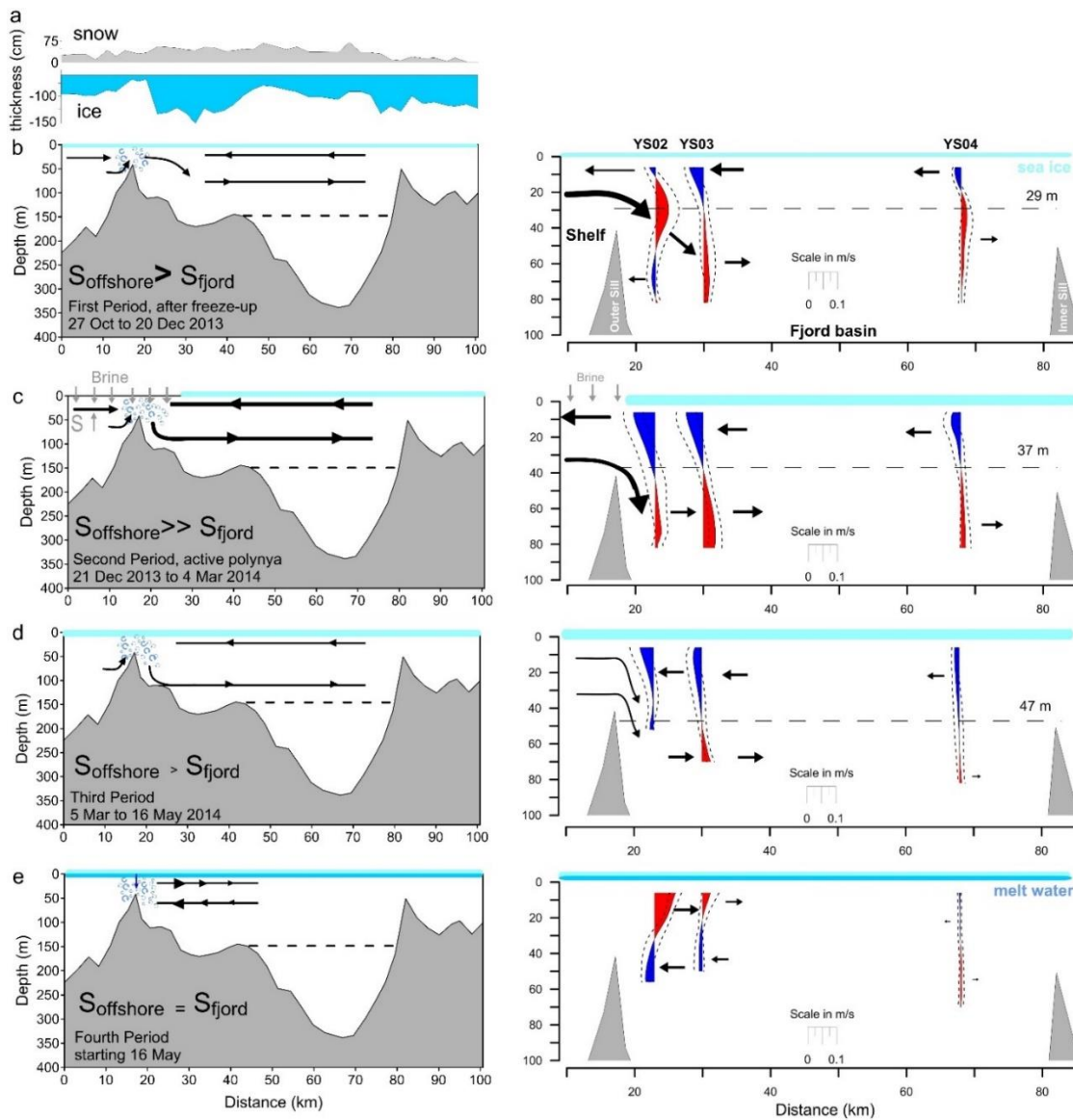


Figure 3-7: (a) Along fjord transect of snow and sea ice thickness measured on 16-19 May 2014, (b-e) Black arrows on the left panes give a schematic of the circulation patterns. Light blue circular arrows indicate the outer sill mixing zone. Right panes, show average profiles of measured residual currents (blue: outflow, red: inflow) with indication of standard deviation (dashed lines) of the (b) first, (c) second, (d) third and (e) fourth circulation period. Dashed lines mark depth of circulation cell at mooring YS03. Light blue lines indicate the ice cover, while darker blue lines indicate melt water.

In our calculations, we assume that lateral and vertical cross-sectional variation of tidal currents and salinity over the sill are small. The tidal component of the depth-averaged velocities is calculated from the ADCP bins covering 3 – 30 m and harmonically reconstructed with the two major components, M2 and S2. The sum of M2 and S2 amplitudes equals 80 % of the total sum of the four major tidal constituents (M2, S2, N2, K1) of the depth-averaged velocity. The cross-sectional averaged salinity is estimated from the depth-averaged salinity from the full ITP record (1 m resolution). When data is missing in deep parts of the profile, the profiles are extrapolated to 40 m with the data of the deepest measured data point. The cross-sectional area over the sill was determined from bathymetric data of Rysgaard et al. (2003) and attains 1.021×10^5 m² (0-45 m). Finally, the total salt transport through the cross-section (F_T) is evaluated after every tidal cycle when the cumulative volume exchange over the cross-section attains zero.

The main source of uncertainty in our calculations is the incomplete coverage of the water column and the cross-section, and the extrapolation of the salinity profiles. These types of errors and uncertainty are inherent to studies of salt balances on a temporal scale, as a compromise has to be made on the allocation of the available resources (Jackson and Straneo, 2016). For the tidal cross-section averaged transport, we did not sample the lowest parts and only record velocities above the deep channel of the cross-section. Measured tidal velocities are thus assumed to be representative for the cross-sectional averaged velocities over the sill. Both shear effects and rotational effects are expected to have minor influence on the final volume exchange estimates. For the

cross-section averaged salinity, we extrapolate the salinity profiles and assume that the depth-averaged salinities are representative for the complete cross-section, thereby neglecting cross-fjord variability. The measurements at the sill show that stratification is very low and that the baroclinic deformation radius (~ 3 km in the end of May) is comparable to the fjord width (~ 5 km). Therefore, we can assume that horizontal gradients across the width of the fjord, due to the Coriolis force, are relatively small. The extrapolation of the salinity profiles from the deepest measured data points results in an underestimate of the difference in depth-averaged salinity between ebb and flood tides. This may be stated because the ITP dataset (Fig. 3-6) shows that higher differences in salinity between ebb and flood tides tend to occur at greater depths. As the gaps in the salinity data mainly occur at depth, the depth-averaged salinities are expected to underestimate the difference in depth-averaged salinity between ebb and flood tides. This will lead to a conservative estimation of the contribution of tidal pumping to the salt flux.

The calculated salinity increase of the Young Sound-Tyrolerfjord by tidal pumping for a neap-spring period (2 May to 14 May 2014) is shown in Fig. 3-8. Salt input to the fjord interior over this period is estimated at approximately 1.6×10^8 kg salt (~ 145 kg s^{-1}) (Fig. 3-8c). Dmitrenko et al. (2015) showed that from fall to spring the volume above 150 m of the fjord basin was ventilated, which corresponds to a volume of approximately 22.2×10^9 m³ (cf. volumetric data of the fjord in Rysgaard et al., 2003). The estimated increase of salinity over a spring neap tidal cycle of this ventilated volume then attains ~ 0.007 .

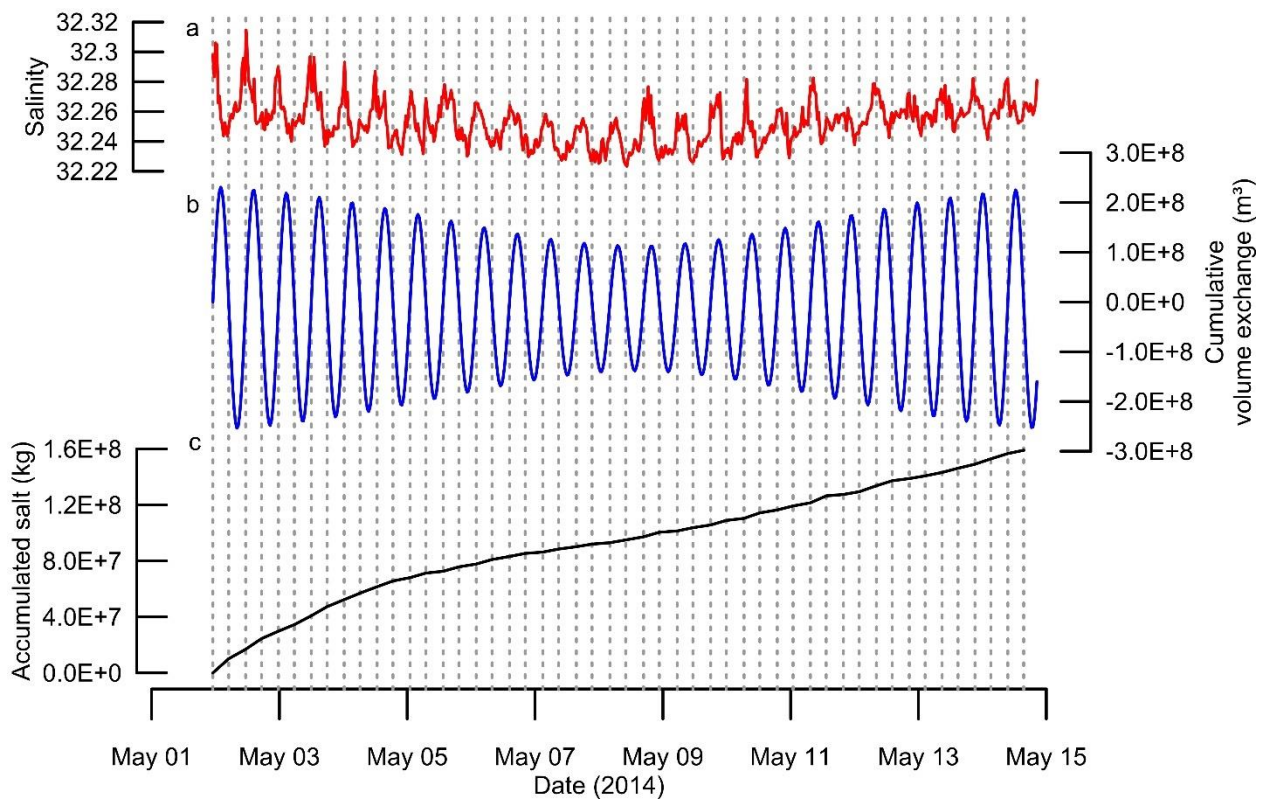


Figure 3-8: (a) Depth-averaged salinity from ITP record over the outer sill (b) Cumulative volume exchange over the sill based on the harmonic (M2, S2) analysis of the depth-averaged velocity (3-30 m) over the outer sill. (c) Accumulated salt flux through the cross-section at the outer sill, positive towards the fjord interior.

In order to estimate the seasonal change of the contribution of tidal pumping to salt flux, we note that changes of the magnitude of the salinity gradient between surface water masses in the fjord and on the shelf, will impact the magnitude of the salt exchange. An increase (decrease) in the horizontal salinity gradient will increase (decrease) the magnitude of tidal pumping. The horizontal salinity gradient is expected to change seasonally with maximal gradients during the ice-free summer and minimal gradients at the end of winter. This is confirmed by our CTD data, as the salinity gradient

(difference in depth average salinity 0-45 m between stations inside and outside the fjord) changes from ~ 0.50 in August 2013 (station 54 and 45, Fig. 3-2b) to ~ 0.12 in May 2014 (station 108 and 96, Fig. 3-2f). Furthermore, calculation of the volume averaged salinity, based on CTD profiles from 18 August 2013 (station 45) and 10 May 2014 (station 51) near mooring YS03 and fjord bathymetry data from Rysgaard et al. (2003), show that the volume averaged salinity of the fjord (0-150 m) changes from 31.18 in August to 32.28 in May. The seasonal change (August-May) of volume averaged salinity of the fjord is thus estimated at ~ 1.10 over ~ 9 months, which equals to $\sim 1032 \text{ kg s}^{-1}$.

The contribution of tidal pumping to the salinity change of the fjord will depend on the evolution of the fjord-shelf salinity gradient over the ice-covered period. No record of the fjord-shelf salinity gradient is available, but if it is assumed that salinity increase due to tidal pumping is linearly proportional to the fjord-shelf salinity gradient, and that the salinity gradient varies seasonally between ~ 0.12 and ~ 0.50 , then salt flux due to tidal pumping is estimated to range between $\sim 145 \text{ kg s}^{-1}$ and $\sim 603 \text{ kg s}^{-1}$. These bounds imply that tidal pumping can contribute between 14% and 58% of the total seasonal salinity change of the fjord (August –May). Tidal pumping may thus be regarded as a major contributor to the salt balance of the fjord.

3.6 Conclusions

The seasonally complex and spatially variable hydrodynamics of a high Arctic fjord are analyzed based on hydrographic transects and ice tethered moorings in the period 2013 - 2014. In summer, the fjord water masses were characterized by a relatively large range of salinities (17 – 33.4) and temperatures (-1.6 °C - 8 °C), while in winter, the water column was weakly stratified with near freezing temperatures (\sim -1.75 °C) and a small range of salinity (32.25 - 32.50). Initial ice formation during freeze-up only affected the surface layers and no deep convection was observed in the fjord. The velocity data indicated relatively high tidal velocities over the sill (up to 40 cm s⁻¹), and gradually decreasing tidal velocities from the outer sill into the fjord basin (\sim 2 cm s⁻¹). The fjord circulation was characterized by a two-layer circulation that deepened and renewed water up to \sim 150 m depth during winter. Observations showed that renewal depth, circulation intensity and direction of the flow were impacted by changes in the coastal water masses and driven by input of meltwater and polynya activity near the fjord's mouth. The fjord circulation brings relatively warm water in contact with sea ice (Kirillov et al., 2015), a process that might explain ice thickness patterns in many fjords with shallow sills around the Arctic, where similar circulation patterns occur. The evaluation of the cross-sill salt flux shows that salt flux due to tidal pumping attains 145 kg s⁻¹ in May. This value represents a salinity increase of 0.007 of the fjord basin (0-150 m) over a spring-neap tidal cycle. Increase of the cross-sill salinity gradient to the observed summer value may increase this salt flux to \sim 603 kg s⁻¹. Extrapolation of these values

over the ice-covered period suggests that tidal pumping is a major contributor to the salt balance of the fjord.

Acknowledgments

This study was funded by the Canada Excellence Research Chair (CERC) program, the Canada Research Chair (CRC) program, the Canada Foundation of Innovation (CFI), the Natural Sciences and Engineering Research Council of Canada (NSERC, grant RGPIN-2014-03606), Research Manitoba, Research Foundation Flanders (FWO aspirant grant to L.M.) and the University of Manitoba, Aarhus University and the Greenland Institute of Natural Resources. We acknowledge the Marine Basis program under the Zackenberg Ecological Research Operations for use of the monitoring data. We thank Emmelia Wiley, Ivali Lennert, Kunuk Lennert and Egon Frandsen for outstanding technical assistance, Dr. Daniel Carlson and Dr. Zou Zou Kuzyk for insightful comments and suggestions. This work is a contribution to the Arctic Science Partnership (ASP) and the ArcticNet Networks of Centres of Excellence programs. CTD data from August 2013 are available from Zackenberg Ecological Research Operations (zackenberg.dk). Data from the ice-covered period (CTD, ITP and ADCP data) is archived at the Centre of Earth observation Science, 535 Wallace Building, University of Manitoba, Winnipeg, MB R3T 2N2 Canada, <http://umanitoba.ca/ceos/>.

References

- Aagaard, K., Coachman, L.K., 1968. The east Greenland current north of Denmark Strait, part I. *Arctic* 21, 181-200.
- Aagaard, K., Carmack, E., 1989. The role of sea ice and other fresh water in the Arctic circulation. *Journal of Geophysical Research: Oceans* 94, 14485–14498. doi:10.1029/JC094iC10p14485.
- Becherer, J., Flöser, G., Umlauf, L., Burchard, H., 2016. Estuarine circulation versus tidal pumping: Sediment transport in a well-mixed tidal inlet. *Journal of Geophysical Research: Oceans* 121. 6251–6270. doi:10.1002/2016JC011640.
- Belzile, M., Galbraith, P., Bourgault, D., 2016. Water renewals in the Saguenay Fjord. *Journal of Geophysical Research: Oceans*, 121: 638–657. doi:10.1002/2015JC011085.
- Bendtsen, J., Gustafsson, K. E., Rysgaard, S., Vang, T., 2007. Physical conditions, dynamics and model simulations during the ice-free period of the Young Sound/Tyrolerfjord system. In: Rysgaard, S., Glud, R. N. (Eds.), *Carbon cycling in Arctic marine ecosystems: Case study Young Sound*. Meddr. Grønland, Bioscience 58, 46-59.
- Bendtsen, J., Mortensen, J., Rysgaard, S., 2014. Seasonal surface layer dynamics and sensitivity to runoff in a high Arctic fjord (Young Sound/Tyrolerfjord, 74°N). *Journal of Geophysical Research: Oceans* 119, 6461–6478. doi:10.1002/2014JC010077.

Cottier, F., Nilsen, F., Skogseth, R., Tverberg, V., Skarðhamar, J., Svendsen, H., 2010. Arctic fjords: a review of the oceanographic environment and dominant physical processes. *Geological Society, London, Special Publications* 344(1), 35-50. doi:10.1144/SP344.4.

Dmitrenko, I., Kirillov, S., Rysgaard, S., Barber, D., Babb, D., Pedersen, L., Koldunov, N., Boone, W., Crabeck, O., Mortensen, J., 2015. Polynya impacts on water properties in a Northeast Greenland fjord. *Estuarine, Coastal and Shelf Science* 153, 10-17. doi:10.1016/j.ecss.2014.11.027.

Drinkwater, K., Osborn, T., 1975. The role of tidal mixing in Rupert and Holberg Inlets, Vancouver Island. *Limnology Oceanography* 20(4), 518–529. doi:10.4319/lo.1975.20.4.0518.

Dyer, K.R., 1997. *Estuaries : a physical introduction*. J. Wiley, Chichester, England ; Toronto, 195p.

Edwards, A., Edelsten, D.J., 1977. Deep water renewal of Loch Etive: A three basin Scottish fjord. *Estuarine and Coastal Marine Science* 5(5), 575–595. doi:10.1016/0302-3524(77)90085-8.

Else, B., Papakyriakou, T., Galley, R., Drennan, W., Miller, L., Thomas, H., 2011. Wintertime CO₂ fluxes in an Arctic polynya using eddy covariance: Evidence for enhanced air-sea gas transfer during ice formation. *Journal of Geophysical Research: Oceans* 116(C9). doi:10.1029/2010JC006760.

Gade, H. G., Edwards, A., 1980. Deep water renewal in fjords. In: Freeland, H. J., Farmer, D. M., Levings, C. D. (Eds.), *Fjord oceanography*. NATO Conference Series vol. 4. Springer US. p. 453-489. doi: 10.1007/978-1-4613-3105-6_43.

Geyer, W. R., and Cannon, G. A., 1982. Sill processes related to deep water renewal in a fjord, *Journal of Geophysical Research* 87 (C10), 1982, 7985–7996, doi:10.1029/JC087iC10p07985.

Geyer, W. R., Nepf, H., 1996. Tidal Pumping of Salt in a Moderately Stratified Estuary, in: Aubrey, D. G. and Friedrichs, C.T., *Buoyancy Effects on Coastal and Estuarine Dynamics*. American Geophysical Union, Washington, D. C, U.S.A. p. 213. doi:10.1029/CE053p0213

Geyer, W. R., Woodruff, J. D., Traykovski, P., 2001. Sediment transport and trapping in the Hudson River Estuary, *Estuaries*, 24, 670 – 679. <http://www.jstor.org/stable/1352875>

Hannah, C.G., Dupont, F., Dunphy, M., 2009. Polynyas and tidal currents in the Canadian Arctic Archipelago. *Arctic* 62(1), 83–95. doi:10.2307/40513267.

Håvik, L., Pickart, R.S., Våge, K., Torres, D., 2017. Evolution of the East Greenland Current from Fram Strait to Denmark Strait: Synoptic measurements from summer 2012. *Journal of Geophysical Research: Oceans* 122. doi:10.1002/2016JC012228.

Holfort, J., Hansen, E., 2005. Timeseries of polar water properties in Fram Strait. *Geophysical Research Letters* 32(19), 1944-8007. doi:10.1029/2005GL022957.

Holfort, J., Meincke, J., 2005. Time series of freshwater-transport on the East Greenland Shelf at 74° N. *Meteorologische Zeitschrift* 14, 703–710. doi: 10.1127/0941-2948/2005/0079.

Jackson, R., Straneo, F., Sutherland, D., 2014. Externally forced fluctuations in ocean temperature at Greenland glaciers in non-summer months. *Nature Geoscience* 7, 503–508. doi:10.1038/ngeo2186.

Jackson, R., Straneo, F., 2016. Heat, Salt, and Freshwater Budgets for a Glacial Fjord in Greenland. *Journal of Physical Oceanography* 46, 2735–2768. DOI: 10.1175/JPO-D-15-0134.1

Jensen, L.M., Christensen, T.R., Schmidt, N.S., 2014. Zackenberg Ecological Research Operations, 19th Annual Report 2013. DCE - Danish Centre for Environment and Energy, Aarhus University, Denmark, Roskilde.

Kirillov, S., Dmitrenko, I., Babb, D., Rysgaard, S., Barber, D., 2015. The effect of ocean heat flux on seasonal ice growth in Young Sound (Northeast Greenland). *Journal of Geophysical Research: Oceans* 120, 4803–4824. doi:10.1002/2015JC010720.

Limeburner, R., 1985. CODE-2: Moored array and large-scale data report. (No. 85–35). Woods Hole Oceanographic Institution, Woods Hole, MA, United States.

Maykut, G.A., Untersteiner, N., 1971. Some results from a time-dependent thermodynamic model of sea ice. *Journal of Geophysical Research* 76(6), 1550–1575. doi:10.1029/JC076i006p01550.

Melling, H., Haas, C., Brossier, E., 2015. Invisible polynyas: Modulation of fast ice thickness by ocean heat flux on the Canadian polar shelf. *Journal of Geophysical Research: Oceans* 120, 777–795. doi:10.1002/2014JC010404.

Mortensen, J., Lennert, K., Bendtsen, J., Rysgaard, S., 2011. Heat sources for glacial melt in a sub-Arctic fjord (Godthåbsfjord) in contact with the Greenland Ice Sheet. *Journal of Geophysical Research* 116, C01013. doi:10.1029/2010JC006528.

Mortensen, J., Bendtsen, J., Lennert, K., Rysgaard, S., 2014. Seasonal variability of the circulation system in a west Greenland tidewater outlet glacier fjord, Godthåbsfjord (64° N). *Journal of Geophysical Research: Earth Surface* 119, 2591–2603. doi:10.1002/2014JF003267.

Nilsen, F., Cottier, F., Skogseth, R., Mattsson, S., 2008. Fjord–shelf exchanges controlled by ice and brine production: The interannual variation of Atlantic Water in Isfjorden, Svalbard. *Continental Shelf Research* 28, 1838–1853. doi:10.1016/j.csr.2008.04.015.

Noufal K.K., Najeem S., Latha G., Venkatesan R., Seasonal and long term evolution of oceanographic conditions based on year-around observation in Kongsfjorden, Arctic Ocean, *Polar Science* 11, 2017, 1–10, <https://doi.org/10.1016/j.polar.2016.11.001>.

Parmentier, F.-J., Christensen, T., Sørensen, L., Rysgaard, S., McGuire, D., Miller, P., Walker, D., 2013. The impact of lower sea-ice extent on Arctic greenhouse-gas exchange. *Nature Climate Change* 3. doi:10.1038/nclimate1784.

Pawlowicz, R., Beardsley, B., Lentz, S, 2002. Classical tidal harmonic analysis including error estimates in MATLAB using T_TIDE. *Computers & Geosciences* 28(8), 929–937. doi:10.1016/S0098-3004(02)00013-4.

Pedersen, J., Kaufmann, L., Kroon, A., Jakobsen, B., 2010. The Northeast Greenland Sirius Water Polynya dynamics and variability inferred from satellite imagery. *Geografisk Tidsskrift-Danish Journal of Geography* 110, 131-142. doi:10.1080/00167223.2010.10669503.

Rudels, B., Fahrbach, E., Meincke, J., Budeus, G., Eriksson, P., 2002. The East Greenland current and its contribution to the Denmark Strait overflow. *ICES Journal of Marine Science*. 59, 1133-1154. doi:10.1006/jmsc.2002.1284

Rysgaard, S., Vang, T., Stjernholm, M., Rasmussen, B., Windelin, A., Kiilsholm, S., 2003. Physical conditions, carbon transport, and climate change impacts in a Northeast Greenland fjord. *Arctic and Alpine Research* 35(3), 301-312. doi: 10.1657/1523-0430(2003)035[0301:PCCTAC]2.0.CO;2

Rysgaard, S., Glud, R. N., Sejr, M. K., Bendtsen, J., Christensen, P. B., 2007. Inorganic carbon transport during sea ice growth and decay: A carbon pump in polar seas. *Journal of Geophysical Research* 112(C3), 2156-2202. doi:10.1029/2006JC003572

Rysgaard, S., Glud, R.N. (Eds), 2007. Carbon cycling in Arctic marine ecosystems: Case study Young Sound. The Commission for Scientific Research in Greenland, Copenhagen. *Bioscience* 58.

Scully, M., Friedrichs, C., 2007. Sediment pumping by tidal asymmetry in a partially mixed estuary. *Journal of Geophysical Research: Oceans* 112, C07028. doi:10.1029/2006JC003784

Seim, H., Gregg, M., 1997. The importance of aspiration and channel curvature in producing strong vertical mixing over a sill. *Journal of Geophysical Research: Oceans* 102, 3451–3472. doi:10.1029/96JC03415.

Straneo, F., Curry, R., Sutherland, D., Hamilton, G., Cenedese, C., Våge, K., Stearns, L., 2011. Impact of fjord dynamics and glacial runoff on the circulation near Helheim Glacier. *Nature Geoscience* 4(5), 322–327. doi:10.1038/ngeo1109.

Strass, V.H., Fahrbach, E., Schauer, U., 1993. Formation of Denmark Strait overflow water by mixing in the East Greenland Current. *Journal of Geophysical Research: Oceans* 98(C4), 6907–6919. doi:10.1029/92JC02732.

Sutherland, D. A., Straneo, F., Pickart, R. S., 2014. Characteristics and dynamics of two major Greenland glacial fjords. *Journal of Geophysical Research: Oceans* 119, 3767–3791. doi:10.1002/2013JC009786.

Valle-Levinson, A., Blanco, J. L., Frangópulos, M., 2006. Hydrography and frontogenesis in a glacial fjord off the Strait of Magellan. *Ocean Dynamics*. doi:10.1007/s10236-005-0048-8

Wilson, N.J., Straneo, F., 2015. Water exchange between the continental shelf and the cavity beneath Nioghalvfjærdsbræ (79 North Glacier). *Geophysical Research Letters* 42, 7648–7654. doi:10.1002/2015GL064944.

Chapter 4

Coastal freshening prevents fjord bottom water renewal in a Northeast Greenland fjord – a mooring study from 2003-2015

Wieter Boone¹, Søren Rysgaard^{1,2,3}, Daniel F. Carlson^{2,4}, Lorenz Meire^{3,5}, Sergei Kirillov¹, John Mortensen³, Igor Dmitrenko¹, Leendert Vergeynst² and Mikael K. Sejr^{2,6}

1. Centre for Earth Observation Science, 584 Wallace Bldg, University of Manitoba, Winnipeg, MB R3T 2N2, Canada⁶

2. Arctic Research Centre, Ny Munkegade, 8000 Aarhus C, Aarhus University, Denmark

3. Greenland Climate Research Centre, Greenland Institute of Natural Resources, Kivioq 2, 3900 Nuuk, Greenland

4. Department of Earth, Ocean, and Atmospheric Science, Florida State University, Tallahassee, FL, United States

5. Department of Estuarine and Delta Systems, NIOZ Royal Netherlands Institute of Sea Research and Utrecht University, Yerseke, The Netherlands

6. Department of Bioscience, Vejlsøvej 25, 8600 Silkeborg, Aarhus University, Denmark

4.1 Introduction

The freshwater content of the Arctic Ocean has increased in recent years in response to climate change (Haine et al., 2015; McPhee et al., 2009; Proshutinsky et al., 2009; Rabe et al., 2011). Alterations of freshwater export from the Arctic Ocean to the subarctic Nordic Seas have the potential to influence surface salinities and impact the rate of dense water formation (Dukhovskoy et al., 2016), with implications for the strength of the Atlantic meridional overturning circulation (e.g. Jahn & Holland, 2013; Rahmstorf et al., 2015), which is a major regulator of the world's climate (Vellinga & Wood, 2002). Recent increases in freshwater fluxes from Arctic glaciers (e.g. Bamber et al., 2012) and general freshening of the coastal domain may also impact Arctic fjords, where freshening can lead to weakened vertical mixing and, subsequently, slow or stop the renewal of bottom water. In extreme cases this could lead to hypoxic or anoxic conditions (Farmer & Freeland, 1983) and ultimately alter the fjord's ecosystem functioning (Diaz & Rosenberg, 2008; Pakhomova et al., 2014).

A vulnerable location to effects of freshening is the Northeast coast of Greenland, where recent evidence from summertime measurements showed local and regional freshening (Sejr et al., 2017). Northeast Greenland's coastal waters receive freshwater from major outlet glaciers such as the Nioghalvfjærdsbrae (79° N), Zachariae Isstrøm and Storstrømmen glaciers, which connect more than 16 % of the Greenland Ice Sheet to the coastal water (Khan et al., 2014) and discharge large amounts of freshwater into the coastal domain. The freshwater export from the Arctic Ocean via Fram Strait forms

another source of low density water for the region. Liquid and solid freshwater export via Fram Strait attain approximately $4000 \text{ km}^3 \text{ y}^{-1}$ (2000-2010 average, de Steur et al., 2014; Haine et al., 2015) and is transported south via the East Greenland Current along the east coast of Greenland (Håvik et al., 2017; Rudels, 2002).

The timing and duration of freshening events cannot be resolved consistently in summertime campaigns; freshening events really can only be resolved through long-term moored monitoring, which provides the temporal resolution necessary to detect subtle shifts in the regional background salinity and to reveal interannual differences in freshening rates. This information is critical to aid in projections of future conditions, assess impacts on ecosystems and to help identification of the drivers of coastal freshening. Despite their importance, few long-term, continuous hydrographic datasets have been collected along the coast of Greenland, due to the costs and logistical constraints encountered when operating in such a harsh, remote environment (Straneo et al., 2016). This is especially the case in Northeast Greenland where studies have mostly been limited to summer (Håvik et al., 2017; Rysgaard & Glud, 2007; Sejr et al., 2017; Wilson & Straneo, 2015). In this study, we present the first long-term (13-year), continuous moored time series of temperature and salinity of Young Sound-Tyrolerfjord.

4.2 Data and Methods

4.2.1 Study Area

Young Sound-Tyrolerfjord, is a high latitude (74° N) fjord system in Northeast Greenland that is approximately 90 km long, 2 - 7 km wide, up to 360 m deep, and covers an area of 390 km² (Fig. 4-1a; Rysgaard et al., 2003). The fjord hydrography undergoes a significant seasonal transition, from water masses with a relatively large range of salinities (17 - 33.4) and temperatures (-1.6 C to 8 °C) in summer, to a weakly stratified water column with near freezing temperatures (~-1.75 °C) and a small range of salinity (32.25 - 32.50) in winter (Fig. 4-2 in Boone et al., 2017). Tides are dominated by the semidiurnal lunar constituent (M2) and the tidal range varies between 0.8 m and 1.5 m (Rysgaard et al., 2003). Freshwater from the Greenland Ice Sheet and local glaciers enters the fjord through rivers and streams. Total annual river runoff to the fjord system varies between 0.63 and 1.57 km³ y⁻¹ (Mernild et al., 2007). Young Sound-Tyrolerfjord is covered by land-fast sea ice from mid-October to mid-July. A wind-driven shelf polynya has been observed in the adjacent coastal water during the ice-covered period, though it varies in occurrence, location, and size (Pedersen et al., 2010).

A shallow (~45 m depth) outer sill limits exchange between the fjord and the coast to the upper layer which consists mainly of cold (<0 °C, except in the surface during summer) and relatively fresh (<34.4) Polar Surface Water (Rudels, 2002). Following Farmer and Freeland (1983), we divide the fjord water column into a surface layer

(upper 10 m), intermediate layer (from 10 m to sill depth), and the basin water (below sill depth). We further divide the latter into the upper basin water (sill depth - 150 m) and lower basin water (150 m - 360 m; Fig. 4-1b), which holds the bottom water (>200 m).

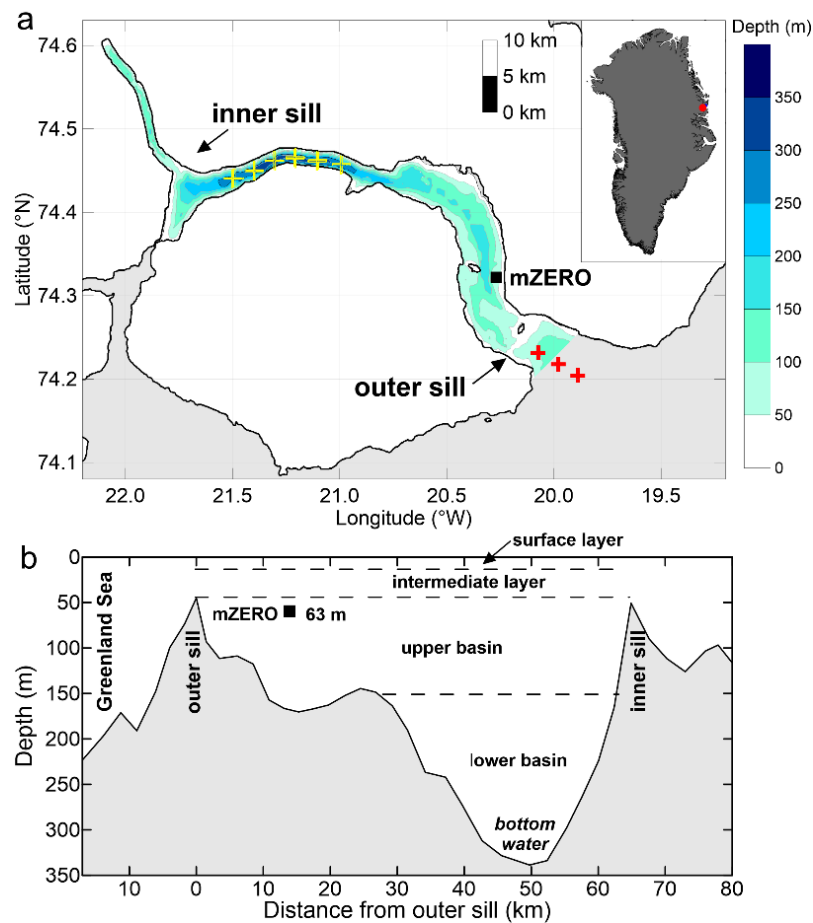


Figure 4-1: (a) Map of Young Sound - Tyrolerfjord in Northeast Greenland showing the stations and bathymetry (color contours) (Rysgaard et al., 2003). White areas in (a) depict land, and grey areas denote the shelf and coastal waters. The black square shows the location of the oceanographic mooring mZERO. Yellow crosses depict the location of CTD stations covering the lower basin and red crosses indicate the stations offshore of the outer sill. (b) Bathymetry of the fjord from the coast to the inner parts of the fjord, with the mZERO mooring, outer sill, inner sill and different fjord layers indicated.

4.2.2 Mooring and CTD data

The Greenland Ecosystem Monitoring Program has maintained a mooring in Young Sound -Tyrolerfjord, approximately 15 km from the outer sill (74.322° N, 20.269° W, Fig. 4-1). This mooring, referred to as mZERO (Fig. 4-1), has been serviced, calibrated and re-deployed every August from 2003 to 2015. mZERO was equipped with a CTD (Sea-Bird SBE37SMP) located in the upper basin layer (Fig. 4-1). The mean sensor depth was ~ 63 m depth (+/- 2.7 m; range: 69 m (2008-2009) - 62 m (2009-2010; 2012-2013)). The CTD sampling interval varied between 15 and 20 min (2003-2009) to 10 min (2009-2015). Data gaps exist due to mooring malfunction, or when redeployment was hampered by ice conditions. Accuracy of the temperature and conductivity sensor is ± 0.002 °C and ± 0.0003 S m⁻¹, respectively. The mooring data resolve the variability of fjord hydrography over a wide range of time scales, from hourly to interannual. In this paper, we focus on interannual variability of the freshening, but note that higher frequency variability is also present, and will be examined in a separate paper.

Additionally, the Greenland Ecosystem Monitoring Program conducted CTD transect surveys in Young Sound-Tyrolerfjord from 2004-2014 during August using a SBE-19plus CTD (Sea-Bird Electronics, accuracy temperature: ± 0.005 °C and conductivity: ± 0.0005 S m⁻¹). Salinity and temperature data from stations sampled in the lower basin water below 200 m and stations offshore from the outer sill were used to investigate the renewal cycle of bottom water (Fig. 4-1).

4.3 Results and Discussion

4.3.1 Temperature and salinity of the upper basin layer in 2003-2015

The CTD transects between 2004 and 2014 demonstrates that salinity changes at mooring mZero, maintained at ~63 m in Young Sound-Tyrolerfjord, are representative for salinity changes in the fjord's complete upper basin water (45-150 m depth range, Text S1). The time series of salinity indicate a freshening trend of the upper basin water (range: 31.2 - 33.2) (Fig. 4-2). The seasonal evolution of salinity, previously described by Boone et al. (2017), shows significant interannual variability. Observed temperatures varied over a narrow range of -1.78 °C to -1.0 °C (Fig. 4-2). Temperatures close to the freezing point mainly occurred from January to June, while maximum temperatures were observed in late September. Both temperature and salinity time series reveal high frequency oscillations, with seasonally varying amplitudes. Amplitudes were largest when stratification of the fjord was strong, which is mainly from July to December (Boone et al., 2017), and might reflect the influence of internal waves in the fjord basin (Cottier et al., 2004).

Deseasonalized monthly anomalies of salinity (Fig. 4-3), processed according to Thomson and Emery (2014)(Text S2), show the occurrence of a freshening trend of -0.11 psu y^{-1} (2003-2015) (Table 1). Trend analysis of August-August segments reveal that the freshening was mainly caused by strong freshening from 2005 to 2007 (-0.92

psu) and from 2009 to 2013 (-0.66 psu). These freshening periods were interrupted by periods when salinity increased as in 2007-2009 (0.16 psu) and 2013-2014 (0.52 psu). Deseasonalized monthly temperature anomalies show only a small warming trend (2003-2015) (<0.01 °C, p-value (5%): <0.001) (Fig. 4-3). We note that a correlation (0.66; p-value (5%): 0.02) exists between trends of August-August segments of salinity and temperature anomalies. Increasing temperatures are therefore correlated with freshening of the basin water.

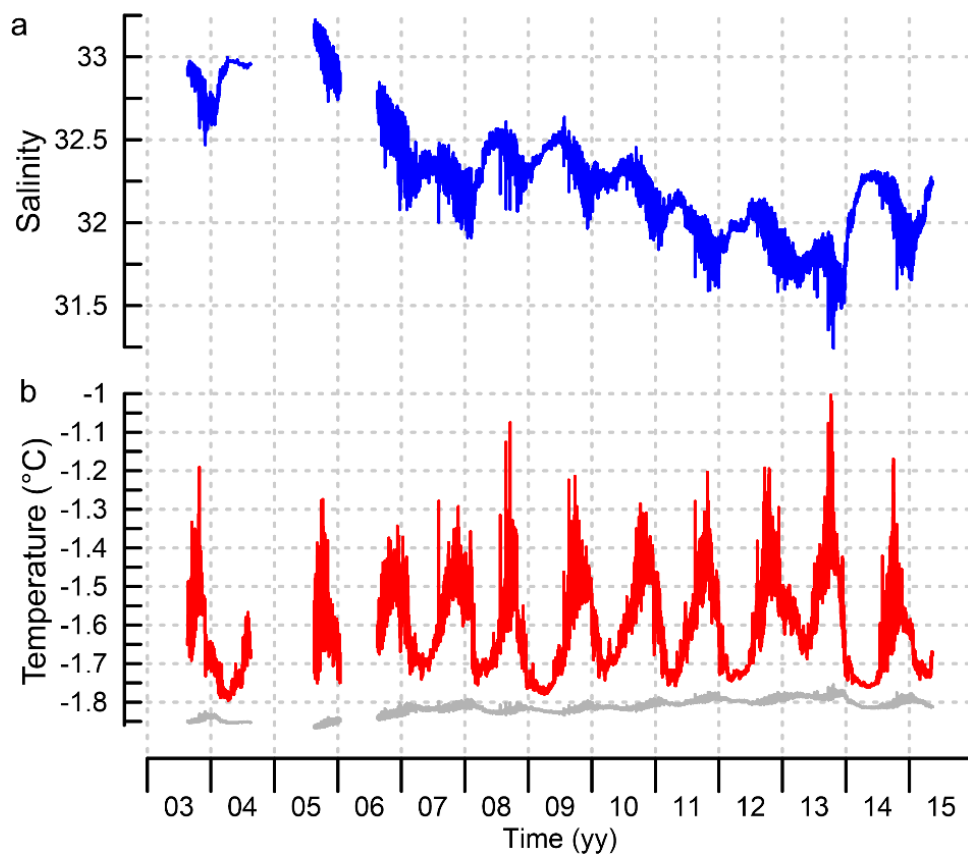


Figure 4-2: Time series of salinity (a) and temperature (red) and calculated freezing temperature (grey) (b) at 63 m depth at mZERO from August 2003 to May 2015.

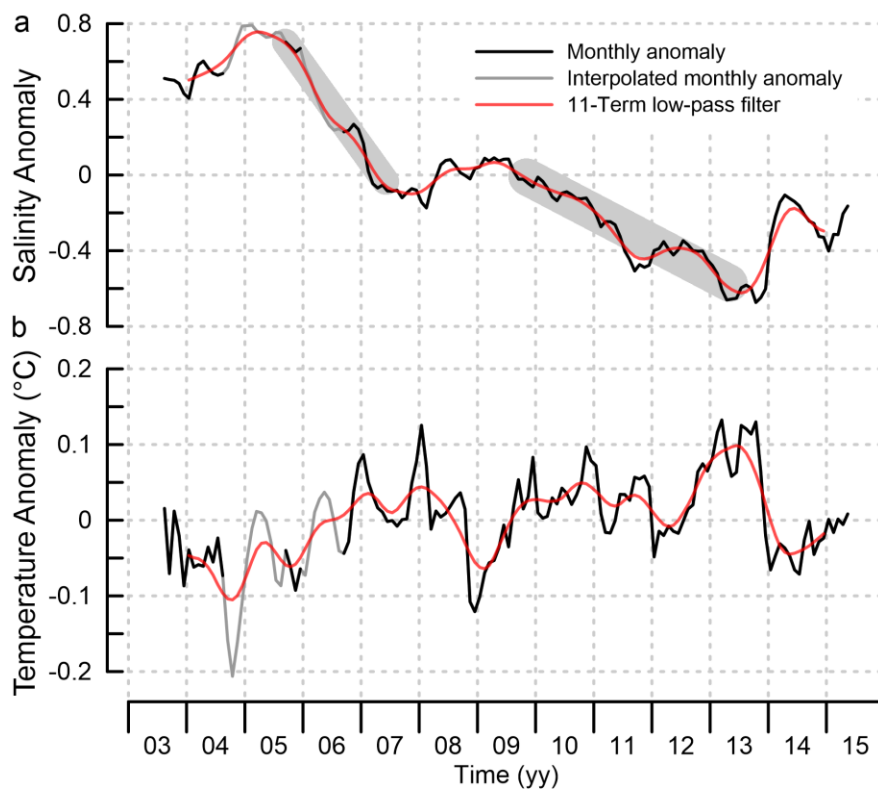


Figure 4-3: Deseasonalized monthly averaged (a) salinity and (b) temperature anomalies at 63 m from mooring mZero. Black lines indicate monthly anomalies; grey line shows interpolated monthly anomalies and red lines the 11-term low-pass filter of the interpolated monthly anomalies. Grey zones in (a) mark periods with anomalous freshening.

Table 4-1: Linear trends of deseasonalized monthly anomalies of salinity at mooring mZERO (Aug-July), with the coefficient of determination (R^2) and root mean squared error (RMSE).

Season	$dS dt^{-1}$ in $psu y^{-1}$	R^2	RMSE
Aug 03- Mar 15	-0.11	0.81	0.17
Aug 04-Jul 05	0.15	0.7	0.03
Aug 05-Jul 06	-0.51	0.99	0.02
Aug 06- Jul 07	-0.41	0.99	0.01
Aug 07-Jul 08	0.14	0.83	0.02
Aug 08- Jul 09	0.03	0.51	0.01
Aug 09-Jul 10	-0.14	0.98	0.01
Aug 10- Jul 11	-0.29	0.98	0.01
Aug 11-Jul 12	0.06	0.6	0.01
Aug 12- Jul 13	-0.29	0.98	0.01
Aug 13-Jul 14	0.56	0.96	0.04

The general freshening trend from August 2003 to March 2015 (-0.11 psu y^{-1}) provides an independent verification of the freshening trend of -0.12 psu y^{-1} , which was based on summer measurements in Young Sound-Tyrolerfjord by Sejr et al., (2017). Other estimates of freshening rates in the Arctic Ocean show freshening rates of -0.04 to -0.2 psu y^{-1} in the mixed layer between 1972 and 2012, though there are strong regional differences (Peralta-Ferriz & Woodgate, 2015). Hamilton & Wu (2013) reported freshening rates attained -0.02 psu y^{-1} in the near-surface layer (50 – 200 m) on the Baffin Island shelf from 1983-2003. While comparing different freshening rates is difficult, as they are measured at different depths, locations and time periods, the aforementioned studies suggest that the freshening rates reported here are at the high end of previously reported values in other Arctic regions.

TS-diagrams of the time series of the upper basin water organized as daily averaged TS-properties from 2003-2015 (Fig. 4-S2) and as seasonal plots from 1 July to 31 June show the seasonal transformation of the hydrography in the fjord from 2006 to 2015 (Figure 4-4). Data collected before 2006 were excluded from Fig.4-4, as they did not resolve a complete seasonal cycle. Based on the shape in TS-space, the seasonal transformations can be grouped in three types. The first type contains years where hydrographic transformations did not lead to a large change in temperature and salinity of the fjord upper basin water. In TS-space, these seasons have a circular shape. Years with such patterns are 2007-2008, 2008-2009, 2011-2012 and 2014-2015 (Figure 4-4). The second type contains years where freshening occurs in the upper basin water leading to a reversed U-shape in TS-space and freshening with time. Freshening was observed in

seasons 2006-2007, 2009-2010, 2010-2011 and 2012-2013 (Figure 4-4). Finally, the third type involves a single year (2013-2014) where renewal in the upper basin occurs, indicated by a cold and salty water mass (Figure 4-4).

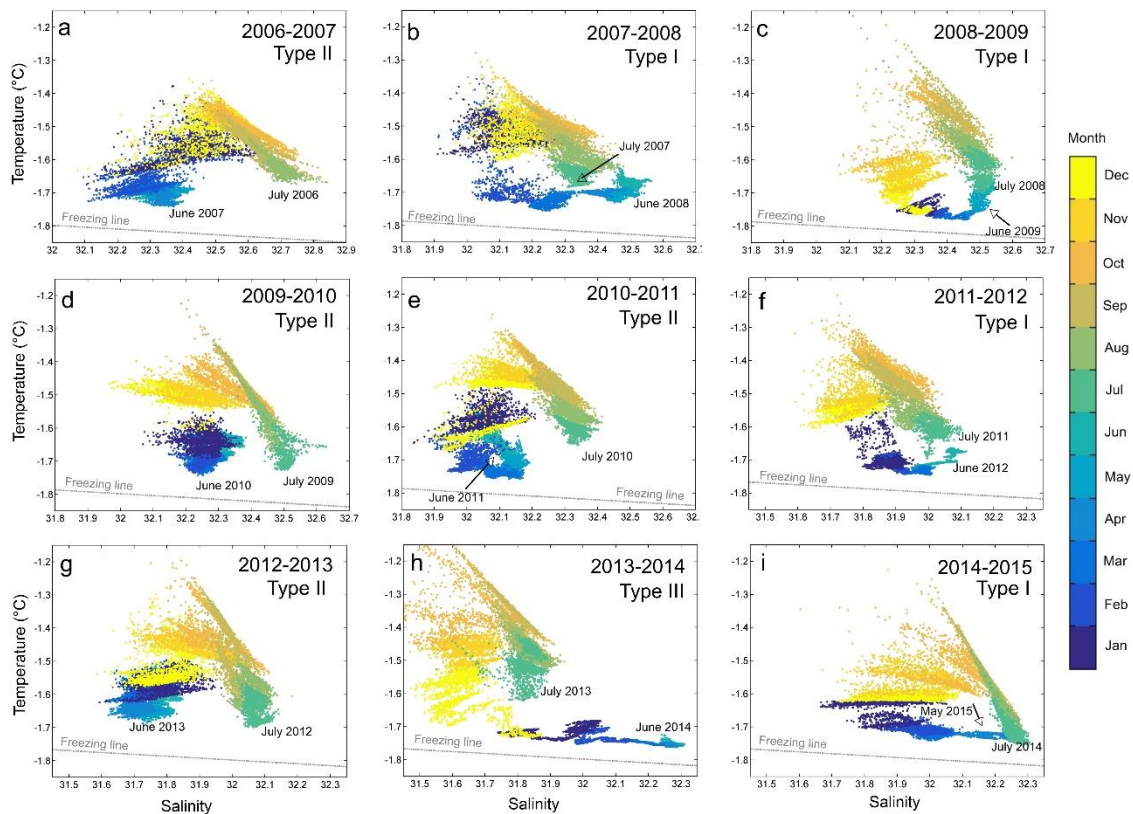


Figure 4-4: TS-diagrams of the seasonal (1 July- 31 June) transformation of hydrography at ~63 m at mooring mZero in the upper basin water of Young Sound-Tyrolerfjord. Thin lines indicate the freezing line at 63 m. Note that all y-axes have the same scale (difference between max. and min. value is constant), but the x-axes may have different ranges.

The events in 2013-2014 were described by Dmitrenko et al. (2015), who illustrated how the opening of a coastal polynya close to the outer sill impacted the ventilation of

the upper basin. As a result, the upper basin was filled with relatively salty (~ 32.3), oxygen rich water around the freezing point (~ -1.75 °C). The associated strong salinity increase (Fig. 4-2, Fig. 4-3.) was unique in the data record, which indicates the unique nature of ventilation by a polynya in Young Sound-Tyrolerfjord.

The TS-analysis further emphasizes that freshening occurred in a stepwise manner, not gradually (Fig. 4-S2). Freshening is not a linear process and is best observed with continuous measurements, as fjord hydrography can be impacted by multiple processes, which can act independently, or in concert. These processes include the evolution of the cross-sill salinity gradient, mixing intensity, polynya activity, sea ice processes and input of low salinity water (Bendtsen et al., 2014; Boone et al., 2017; Dmitrenko et al., 2015). Freshwater input to the coastal waters of East Greenland is comprised mainly of freshwater input from land and input of sea ice meltwater (Bacon et al., 2014). During our study period, the ice mass loss rate from the northeastern sector of the Greenland Ice Sheet has accelerated (Khan et al., 2014) and the amount of sea ice exported through Fram Strait has increased (Smedsrud et al., 2017). The observed variation of the seasonal hydrographic transformation of the fjord might be explained by variability of these regional and local processes as they demonstrate a pronounced seasonal cycle, and significant interannual variability.

4.3.2 Temperature and Salinity of Lower Basin Layer in 2004-2014

August values of temperature and salinity of the lower basin water (>200 m depth) (Fig. 4-1) showed that the bottom water has not been renewed since 2004-2005, when

salinity changed from ~ 33.15 (2004) to ~ 33.25 (2005) (Fig. 4-5a). Instead, stratification in the lower basin increased over time, from nearly uniform salinity in 2004 and 2005 to salinities ranging from 32.75 to 33.05 in 2014. From 2005 to 2014, salinities decreased from ~ 33.25 (2005) to a minimum of 32.75 (2014), equivalent to maximal freshening rate of 0.056 psu y^{-1} . This is well below the salinity in 2004 when the previous bottom renewal took place. Along with decreasing salinities, temperatures increased from $\sim -1.77 \text{ }^\circ\text{C}$ to $\sim -1.60 \text{ }^\circ\text{C}$.

August CTD-measurements of coastal water masses near the sill depth (45-60 m) (see Fig. 4-1a for locations) show that in 2004 and 2005 the density of the lower basin water and water masses at sill depth were comparable (Fig. 4-5b). This changed after 2005, when freshening decreased densities in the coastal water below densities in the lower basin (Fig. 4-5b). The largest change in density of the offshore water masses at sill depth was recorded from 2005 to 2007. During that period, the mean salinity changed from 33.3 to 31.4. Since 2007, mean salinities increased and varied between 32.0 and 32.6, which was still below salinities of the lower basin.

Young Sound-Tyrolerfjord is connected to the Polar Surface Water layer of the coastal water via a shallow outer sill. Major replacements of the basin water will occur whenever the coastal water exchanged over the sill exceeds the density of water within the fjord basin (Farmer & Freeland, 1983). The inflow to the upper basin water recorded in 2013-2014 was not dense enough to renew the lower basin water of the fjord, only partial basin renewal occurred and only impacted the upper basin of the fjord (Dmitrenko et al., 2015). Although our time series contain only one observation of

renewal, the offshore water masses near sill depth clearly show a decrease in density of the coastal water during our observational period. As no significant increasing linear trend in discharge volumes from the main river of the fjord's catchment was observed during the study period (Sejr et al., 2017), our observations suggest that the lack of renewal and freshening of the upper basin water could be caused by freshening of the coastal water. The increasing stratification of lower basin water indicates that downward transport of low density water is dominated by turbulent diffusion or by mixing due to internal waves, which are commonly observed in fjords (Cottier et al., 2010; Mortensen et al., 2011).

3.3 Outlook

Changes in salinity can influence marine ecosystems in several ways. Salinity influences alkalinity (buffer capacity) and calcium ion concentrations, impacting the vulnerability of fjord to ocean acidification (AMAP, 2013), and changes in density-driven circulation can impact nutrient availability for primary production in fjords (Meire et al., 2016, 2017). Furthermore, in Young Sound-Tyrolerfjord, glacial meltwater runoff and input of freshwater from outside the fjord can influence the composition of the bacterial community (Paulsen et al., 2017), as well as the phytoplankton grazer community (Middelbo et al., 2017). A lack of renewal, due to a more stable halocline may over time lead to lower oxygen concentrations or even hypoxic conditions in the bottom water. This may impact biogeochemical cycling and the distribution and composition of the benthic fauna (Rysgaard & Glud, 2007).

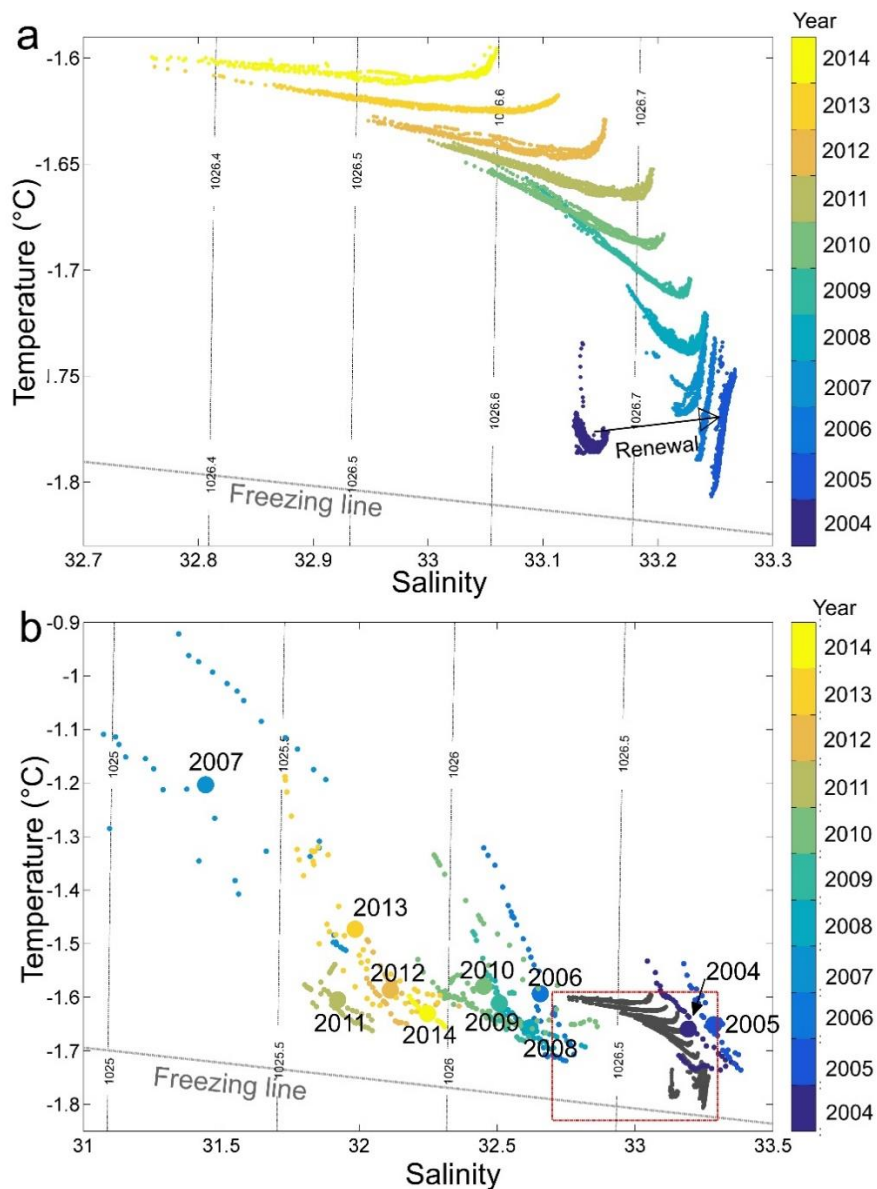


Figure 4-5: TS- diagram of (a) the lower basin water (>200 m) of Young Sound-Tyrolerfjord from August measurements from 2004 to 2014 and (b) TS- diagram of the offshore water masses around sill depth (45-60 m) and their means (large dots), including the data from (a) in black. Red box in (b) shows the limits of the TS-diagram in (a). Dashed lines in (a) and (b) indicate the freezing line and isopycnals, Locations of the measurement are specified in Fig. 4-1

More research is needed to identify the drivers of the coastal freshening. Both regional warming and increased mass loss from the Northeast Greenland Ice Sheet have been reported (Khan et al., 2014). Furthermore, results from Cox et al. (2010) suggest that increasing freshwater from sea ice melt along the coast of East Greenland might be important, as the anomalous strong freshening reported here, coincides with a strong increase in sea ice meltwater input to the East Greenland Current in 2005-2007 (Cox et al., 2010). However, the pathways of freshwater transport and the specific processes involved in the freshening of the coastal water of Northeast Greenland remain unclear, which stresses the importance of dedicated long-term observational studies in this region.

4.4 Conclusions

A 13-year moored timeseries of salinity and temperature near the outer sill of Young Sound-Tyrolerfjord in Northeast Greenland enables us to investigate the interannual evolution of salinity and temperature of the basin water and to quantify the impact of freshening on the fjord's hydrography. Interannual (2003-2015) variability of salinity in the upper basin water indicate a general freshening trend of 0.11 psu y⁻¹. Freshening was anomalous high from August 2005 to August 2007 (-0.92 psu or -0.46 psu y⁻¹) and from August 2009 to August 2013 (-0.66 psu or -0.17 psu y⁻¹). Although the salinities within the fjord have decreased significantly, the reduced density was compensated for by an even stronger freshening of the coastal water. This prevented renewal of the bottom water since 2004-2005. A shift towards fresher coastal water and the

subsequent lack of bottom water renewal in combination with general freshening of the fjord basin water may impact the fjord's ecosystem functioning. The observations in this study provide new insights into the temporal variability of salinity and temperature and thus provides a necessary step towards an impact assessment and identification of underlying processes driving freshening in Northeast Greenland.

Acknowledgments

The Marine Basic program under the Greenland Ecosystem Monitoring Program graciously provided the monitoring data. This study was funded by the Canadian CERC- , CRC- program, CFI, NSERC (grant RGPIN- 2014-03606), Research Manitoba, and University of Manitoba, Aarhus University, Greenland Institute of Natural Resources and the EU H2020 project INTAROS. This work is a contribution to the Arctic Science Partnership. The datasets used in this study are available via the Greenland Ecosystem Monitoring Database at data.g-e-m.dk.

References

Arctic Monitoring and Assessment Program (AMAP), 2013. AMAP Assessment 2013: Arctic Ocean Acidification. Oslo, Norway.

Bacon, S., Marshall, A., Holliday, N.P., Aksenov, Y., Dye, S.R., 2014. Seasonal variability of the East Greenland Coastal Current. *J. Geophys. Res. Ocean.* 119, 3967–3987. doi:10.1002/2013JC009279

Bamber, J., van den Broeke, M., Ettema, J., Lenaerts, J., Rignot, E., 2012. Recent large increases in freshwater fluxes from Greenland into the North Atlantic. *Geophys. Res. Lett.* 39. doi:10.1029/2012GL052552

Bendtsen, J., Mortensen, J., Rysgaard, S., 2014. Seasonal surface layer dynamics and sensitivity to runoff in a high Arctic fjord (Young Sound/Tyrolerfjord, 74°N). *J. Geophys. Res. Ocean.* 119, 6461–6478. doi:10.1002/2014JC010077

Boone, W., Rysgaard, S., Kirillov, S.A., Dmitrenko, I.A., Bendtsen, J., Mortensen, J., Meire, L., Petrusevich, V., Barber, D.G., 2017. Circulation and fjord-shelf exchange during the ice-covered period in Young Sound-Tyrolerfjord, Northeast Greenland (74°N). *Estuar. Coast. Shelf Sci.* 194, 205–216. doi:10.1016/j.ecss.2017.06.021

Cottier, F., Inall, M., Griffiths, C., 2004. Seasonal variations in internal wave energy in a Scottish sea loch. *Ocean Dyn.* 54, 340–347. doi:10.1007/s10236-003-0064-5

Cottier, F.R., Nilsen, F., Skogseth, R., Tverberg, V., Skarðhamar, J., Svendsen, H., 2010. Arctic fjords: a review of the oceanographic environment and dominant physical processes. *Geol. Soc. London, Spec. Publ.* 344, 35–50. doi:10.1144/SP344.4

Cox, K.A., Stanford, J.D., McVicar, A.J., Rohling, E.J., Heywood, K.J., Bacon, S., Bolshaw, M., Dodd, P.A., De La Rosa, S., Wilkinson, D., 2010. Interannual variability of Arctic sea ice export into the East Greenland Current. *J. Geophys. Res. Ocean.* 115, 1–12. doi:10.1029/2010JC006227

De Steur, L., Hansen, E., Mauritzen, C., Beszczynska-Møller, A., Fahrbach, E., 2014. Impact of recirculation on the East Greenland Current in Fram Strait: Results from moored current meter measurements between 1997 and 2009. *Deep Sea Res. Part I Oceanogr. Res. Pap.* 92, 26–40. doi:10.1016/j.dsr.2014.05.018

Diaz, R.J., Rosenberg, R., 2008. Spreading dead zones and consequences for marine ecosystems. *Science* (80-.). 321, 926–929. doi:10.1126/science.1156401

Dmitrenko, I.A., Kirillov, S.A., Rysgaard, S., Barber, D.G., Babb, D.G., Pedersen, L.T., Koldunov, N. V., Boone, W., Crabeck, O., Mortensen, J., 2015. Polynya impacts on water properties in a Northeast Greenland fjord. *Estuar. Coast. Shelf Sci.* 153, 10–17. doi:10.1016/j.ecss.2014.11.027

Dukhovskoy, D.S., Myers, P.G., Platov, G., Timmermans, M., Curry, B., Proshutinsky, A., Bamber, J.L., Chassignet, E., Hu, X., Lee, C.M., Somavilla, R., 2016. Greenland freshwater

pathways in the sub-Arctic Seas from model experiments with passive tracers. *J. Geophys. Res. Ocean.* 121, 877–907. doi:10.1002/2015JC011290

Farmer, D.M., Freeland, H.J., 1983. The physical oceanography of Fjords. *Prog. Oceanogr.* 12, 147–219. doi:10.1016/0079-6611(83)90004-6

Haine, T.W.N., Curry, B., Gerdes, R., Hansen, E., Karcher, M., Lee, C., Rudels, B., Spreen, G., de Steur, L., Stewart, K.D., Woodgate, R., 2015. Arctic freshwater export: Status, mechanisms, and prospects. *Glob. Planet. Change* 125, 13–35. doi:10.1016/j.gloplacha.2014.11.013

Hamilton, J., Wu, Y., 2013. Synopsis and trends in the physical environment of Baffin Bay and Davis Strait. *Can. Tech. Rep. Hydrogr. Ocean Sci.* 282, 1–39.

Håvik, L., Pickart, R.S., Våge, K., Torres, D., Thurnherr, A.M., Beszczynska-Møller, A., Walczowski, W., von Appen, W.-J., 2017. Evolution of the East Greenland Current from Fram Strait to Denmark Strait: Synoptic measurements from summer 2012. *J. Geophys. Res. Ocean.* 122, 1974–1994. doi:10.1002/2016JC012228

Jahn, A., Holland, M.M., 2013. Implications of Arctic sea ice changes for North Atlantic deep convection and the meridional overturning circulation in CCSM4-CMIP5 simulations. *Geophys. Res. Lett.* 40, 1206–1211. doi:10.1002/grl.50183

Khan, S.A., Kjær, K.H., Bevis, M., Bamber, J.L., Wahr, J., Kjeldsen, K.K., Bjørk, A.A., Korsgaard, N.J., Stearns, L.A., van den Broeke, M.R., Liu, L., Larsen, N.K., Muresan, I.S.,

2014. Sustained mass loss of the northeast Greenland ice sheet triggered by regional warming. *Nat. Clim. Chang.* 4, 292–299. doi:10.1038/nclimate2161

McPhee, M.G., Proshutinsky, A., Morison, J.H., Steele, M., Alkire, M.B., 2009. Rapid change in freshwater content of the Arctic Ocean. *Geophys. Res. Lett.* 36, 1–6. doi:10.1029/2009GL037525

Meire, L., Mortensen, J., Meire, P., Juul-Pedersen, T., Sejr, M.K., Rysgaard, S., Nygaard, R., Huybrechts, P., Meysman, F.J.R., 2017. Marine-terminating glaciers sustain high productivity in Greenland fjords. *Glob. Chang. Biol.* doi:10.1111/gcb.13801

Meire, L., Mortensen, J., Rysgaard, S., Bendtsen, J., Boone, W., Meire, P., Meysman, F.J.R., 2016. Spring bloom dynamics in a subarctic fjord influenced by tidewater outlet glaciers (Godthåbsfjord, SW Greenland). *J. Geophys. Res. Biogeosciences* 121, 1581–1592. doi:10.1002/2015JG003240

Mernild, S.H., Sigsgaard, C., Rasch, M., Hasholt, B., Hansen, B.U., Stjernholm, M., Pedersen, D., 2007. Climate, river discharge and suspended sediment transport in the Zackenberg River drainage basin and Young Sound/Tyrolerfjord, Northeast Greenland, in: Rysgaard, S., Glud, R.N. (Eds.), *Carbon Cycling in Arctic Marine Ecosystems: Case Study Young Sound*. *Meddr. Grønland, Bioscience* 58, pp. 24–43.

Middelbo, A.B., Sejr, M.K., Arendt, K.E., Møller, E.F., 2017. Impact of glacial meltwater on spatiotemporal distribution of copepods and their grazing impact in Young Sound NE, Greenland. *Limnol. Oceanogr.* doi:10.1002/lno.10633

Mortensen, J., Lennert, K., Bendtsen, J., Rysgaard, S., 2011. Heat sources for glacial melt in a sub-Arctic fjord (Godthåbsfjord) in contact with the Greenland Ice Sheet. *J. Geophys. Res.* 116, C01013. doi:10.1029/2010JC006528

Pakhomova, S., Braaten, H.F., Yakushev, E., Skei, J., 2014. Biogeochemical consequences of an oxygenated intrusion into an anoxic fjord. *Geochem. Trans.* 15, 5. doi:10.1186/1467-4866-15-5

Paulsen, M.L., Nielsen, S.E.B., Müller, O., Møller, E.F., Stedmon, C.A., Juul-Pedersen, T., Markager, S., Sejr, M.K., Delgado Huertas, A., Larsen, A., Middelboe, M., 2017. Carbon Bioavailability in a High Arctic Fjord Influenced by Glacial Meltwater, NE Greenland. *Front. Mar. Sci.* 4. doi:10.3389/fmars.2017.00176

Pedersen, J.B.T., Kaufmann, L.H., Kroon, A., Jakobsen, B.H., 2010. The Northeast Greenland Sirius Water Polynya dynamics and variability inferred from satellite imagery. *Geogr. Tidsskr.* 110, 131–142. doi:10.1080/00167223.2010.10669503

Peralta-Ferriz, C., Woodgate, R.A., 2015. Seasonal and interannual variability of pan-Arctic surface mixed layer properties from 1979 to 2012 from hydrographic data, and the dominance of stratification for multiyear mixed layer depth shoaling. *Prog. Oceanogr.* 134, 19–53. doi:10.1016/j.pocean.2014.12.005

Proshutinsky, A., Krishfield, R., Timmermans, M.-L., Toole, J., Carmack, E., McLaughlin, F., Williams, W.J., Zimmermann, S., Itoh, M., Shimada, K., 2009. Beaufort Gyre

freshwater reservoir: State and variability from observations. *J. Geophys. Res.* 114, C00A10. doi:10.1029/2008JC005104

Rabe, B., Karcher, M., Schauer, U., Toole, J.M., Krishfield, R.A., Pisarev, S., Kauker, F., Gerdes, R., Kikuchi, T., 2011. An assessment of Arctic Ocean freshwater content changes from the 1990s to the 2006–2008 period. *Deep Sea Res. Part I Oceanogr. Res. Pap.* 58, 173–185. doi:10.1016/j.dsr.2010.12.002

Rahmstorf, S., Box, J.E., Feulner, G., Mann, M.E., Robinson, A., Rutherford, S., Schaaernicht, E.J., 2015. Exceptional twentieth-century slowdown in Atlantic Ocean overturning circulation. doi:10.1038/NCLIMATE2554

Rudels, B., 2002. The East Greenland Current and its contribution to the Denmark Strait overflow. *ICES J. Mar. Sci.* 59, 1133–1154. doi:10.1006/jmsc.2002.1284

Rysgaard, S., Glud, R.N., 2007. Carbon cycling in Arctic marine ecosystems: Case study Young Sound. *Meddelelser om Grønland, Bioscience Vol 58*. Copenhagen, The Commission for Scientific Research in Greenland.

Rysgaard, S., Vang, T., Stjernholm, M., Rasmussen, B., Windelin, A., Kiilsholm, S., 2003. Physical Conditions, Carbon Transport, and Climate Change Impacts in a Northeast Greenland Fjord. *Arctic, Antarct. Alp. Res.* 35, 301–312. doi:10.1657/1523-0430(2003)035[0301:PCCTAC]2.0.CO;2

Sejr, M.K., Stedmon, C.A., Bendtsen, J., Abermann, J., Juul-Pedersen, T., Mortensen, J., Rysgaard, S., 2017. Evidence of local and regional freshening of Northeast Greenland coastal waters. *Sci. Rep.* 7, 13183. doi:10.1038/s41598-017-10610-9

Smedsrud, L.H., Halvorsen, M.H., Stroeve, J.C., Zhang, R., Kloster, K., 2017. Fram Strait sea ice export variability and September Arctic sea ice extent over the last 80 years. *Cryosphere* 11, 65–79. doi:10.5194/tc-11-65-2017

Straneo, F., Hamilton, G., Stearns, L., Sutherland, D., 2016. Connecting the Greenland Ice Sheet and the Ocean: A Case Study of Helheim Glacier and Sermilik Fjord. *Oceanography* 29, 34–45. doi:10.5670/oceanog.2016.97

Thomson, R.E., Emery, W.J., 2014. Spectral Analysis, in: *Data Analysis Methods in Physical Oceanography*. Elsevier, pp. 433–489.

Vellinga, M., Wood, R.A., 2002. Global climatic impacts of a collapse of the atlantic thermohaline circulation. *Clim. Change* 54, 251–267. doi:10.1023/A:1016168827653

Wilson, N.J., Straneo, F., 2015. Water exchange between the continental shelf and the cavity beneath Nioghalvfjærdsbrae (79 North Glacier). *Geophys. Res. Lett.* 42, 7648–7654. doi:10.1002/2015GL064944

Supporting information

Introduction

The supporting information contains methods of the time series analysis and the analysis to investigate if the mooring is representative for changes in the fjord basin water.

Text S1. Salinity at mooring depth and basin salinity

Analysis of 99 CTD casts occupied in August between 2004-2014, along a transects that spanned the entire Young Sound-Tyrolerfjord system, demonstrates that the mooring is representative for changes in the fjord's upper basin water. A scatter plot of mean salinity of the upper basin water (S_{ub}) (45 m – 150 m) versus mean salinity at mooring depth (S_m) (60 m-65 m) (Fig. S1) shows a linear relation. A first-order linear regression model ($S_m=0.88*S_{ub}+3.91$) has R^2 of 0.96 and RMSE 0.08. Following this linear model, 1 psu change in salinity observed at the mooring represents 1.14 psu change in the mean salinity of the upper basin water.

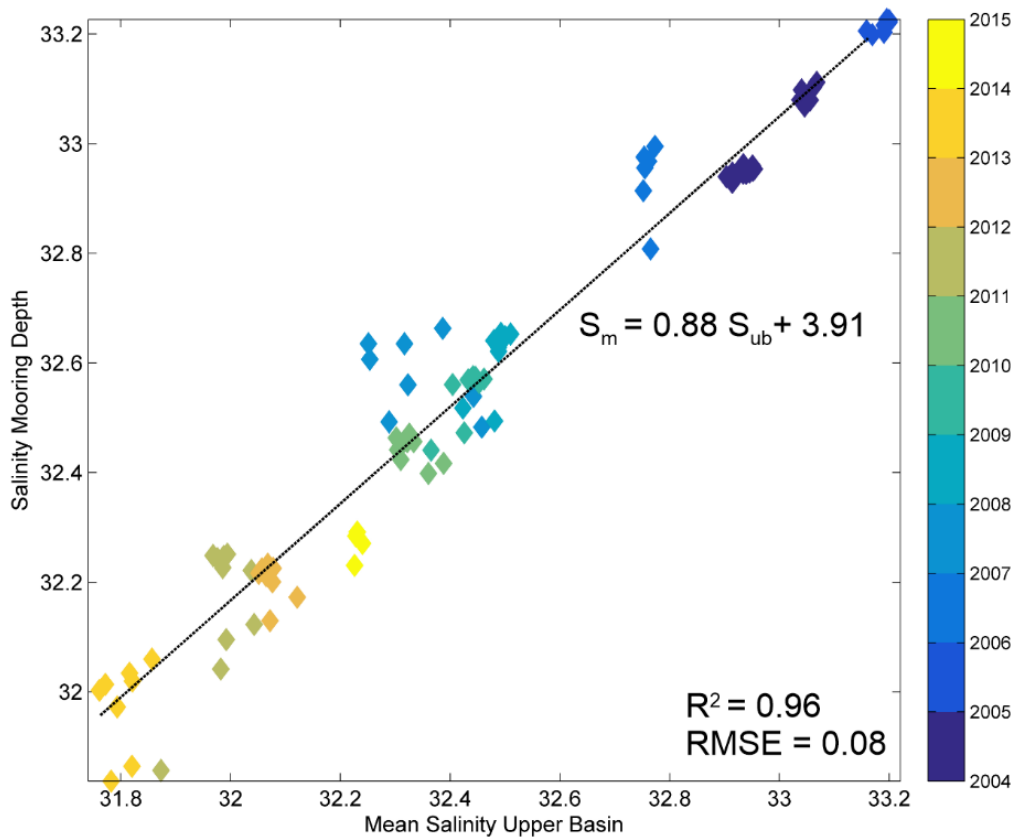


Figure 4-S1. Mean salinity of the upper basin water (S_{ub} ; 45 m-150 m) vs. mean salinity at mooring depth (S_m ; 60 m-65 m) from August transects of the Greenland Ecosystem Monitoring Program between 2004 and 2014.

Text S2. Time Series Analysis

The long-term trends in the 13-year salinity and temperature time series were calculated using least-squares linear regressions from deseasonalized monthly anomalies, calculated following methods described in Thomson and Emery (2014). First, data gaps in the original data were filled by linear interpolation. Mean monthly values were then calculated for each month of the year, noted as $\overline{\eta(t_m)}$ ($m=1,2, \dots,12$). Afterwards these mean monthly values were subtracted from the linearly interpolated monthly averaged data ($\eta(t_m)$) for the appropriate month, to finally obtain monthly anomalies of salinity

and temperature, which can be noted as $\eta'(t_m) = \eta(t_m) - \overline{\eta(t_m)}$. To focus on interannual variability, we then applied a 11-term Trenberth low-pass filter (Trenberth, 1984) to these monthly anomalies, which completely eliminates variance at periods less than 8 months, but retains 80 % of the original amplitude at a period of 24 months. Finally, the deseasonalized monthly anomalies were subjected to least squares regression analysis to quantify interannual and annual trends.

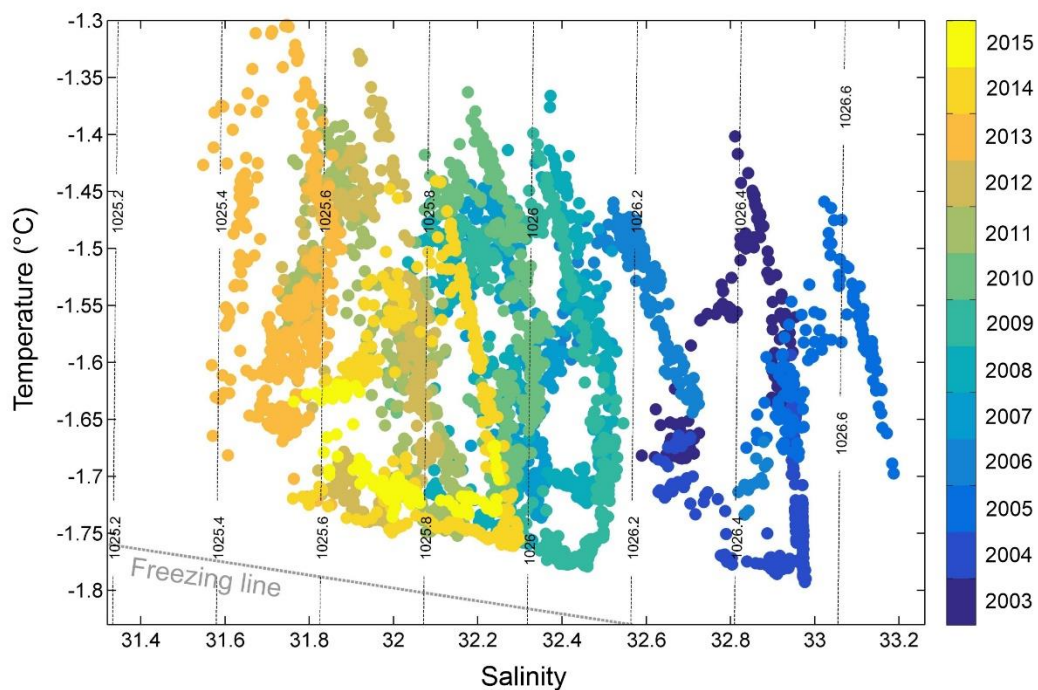


Figure 4-S2. Daily averaged TS-properties of the interannual (2003 - 2015) transformation of hydrography at ~63 m depth at mooring mZero in the upper basin water of the Young Sound-Tyrolerfjord. The thin, nearly vertical lines indicate isopycnals and the dotted line shows the freezing line (63 m).

References

Thomson, R.E., Emery, W.J., 2014. Data Analysis Methods in Physical Oceanography, Data Analysis Methods in Physical Oceanography. doi:10.1016/B978-0-12-387782-6.00006-5

Trenberth, K.E., 1984. Signal Versus Noise in the Southern Oscillation. *Mon. Weather Rev.* 112, 326–332. doi:10.1175/1520-0493(1984)112<0326:SVNITS>2.0.CO;2

Chapter 5

Can sea ice melt impact coastal freshening in Northeast Greenland?

Wieter Boone^{1*}, Søren Rysgaard^{1,2,3}, Morven Muilwijk^{4,5}, Sergei Kirillov¹, Dan Carlson², Igor Dmitrenko¹, John Mortensen³ and Lorenz Meire^{3,6}

Prepared to submit to:

Frontiers of Marine Science

¹ Centre for Earth Observation Science, 584 Wallace Bldg, University of Manitoba, Winnipeg, MB R3T 2N2, Canada

² Arctic Research Centre, Ny Munkegade, 8000 Arhus C, Aarhus University, Denmark

³ Greenland Climate Research Centre, Greenland Institute of Natural Resources, Kivioq 2, 3900 Nuuk, Greenland

⁴ Geophysical Institute, University of Bergen, Bergen, Norway

⁵ Bjerknes Centre for Climate Research, Bergen, Norway

⁶ Department of Estuarine and Delta Systems, NIOZ Royal Netherlands Institute of Sea Research and Utrecht University, Yerseke, The Netherlands

5.1 Introduction

The Arctic freshwater cycle receives much attention as it is a prominent element of the Earth's climate system. The Arctic Ocean is warming (McLaughlin et al., 2009; Polyakov et al., 2005, 2012), freshening (Haine et al., 2015; McPhee et al., 2009; Proshutinsky et al., 2009; Rabe et al., 2011), and freshwater fluxes from the Greenland Ice Sheet are increasing (Bamber et al., 2012; Khan et al., 2014). Climate change has altered the distribution and pathways of freshwater in the Arctic Ocean (McPhee et al., 2009), which resonates in changes of heat, salt and biogeochemical properties of the Arctic Ocean and the bordering (sub)-arctic seas and oceans, such as the Greenland Sea (Arrigo and Van Dijken, 2011; Beszczynska-Möller et al., 2011; Carmack and McLaughlin, 2011; Pabi et al., 2008; Woodgate et al., 2012).

Along the major outflow shelf of the Arctic Ocean lie the coastal waters of Northeast Greenland, bounded by Fram Strait in the North and Denmark Strait in the South. Large amounts of sea ice and freshwater are exported through Fram Strait and transported southwards via the East Greenland Current (Carmack et al., 2016; Rudels et al., 2002). Additionally, these coastal waters receive glacial meltwater from numerous drainage basins, such as the Northeast Greenland Ice Stream, which covers 16 % of the Greenland Ice Sheet and includes important outlet glaciers such as the Nioghalvfjærdsfjorden Glacier, Zachariae Isstrøm, and Storstrømmen Glacier (Khan et al., 2014).

The impact of the changing freshwater cycle on the oceanographic conditions of the many fjords along the Northeast coast of Greenland is not well studied, and observations of the coastal waters in Northeast Greenland are scarce. The area is undersampled in comparison to the coast of Southeast Greenland (Bacon, 2002; Pickart et al., 2005; Sutherland and Pickart, 2008) as coastal navigation is time-consuming due to icebergs and sea ice (Håvik et al., 2017; Rudels et al., 2005). Long-term mooring arrays monitor the gateways of Fram Strait (e.g. (Beszczynska-Møller et al., 2012; de Steur et al., 2014; Rabe et al., 2013) and Denmark Strait (Harden et al., 2016), but the seasonal and interannual variability of the oceanographic conditions along the coast of Northeast Greenland and its impact on fjord hydrography are not well known.

Recent studies by Sejr et al. (2017) and Boone et al. (2018) analyzed a decadal data set (2003-2015) from the fjord and coastal water near Young Sound-Tyrolerfjord, a high arctic fjord system on the Northeast Coast of Greenland (Fig. 5-1a). Their observations presented evidence of strong freshening in the coastal water (Sejr et al., 2017) and quantified the impact of freshening on the renewal of the fjord basin waters (Boone et al., 2018). Sejr et al. (2017) eliminated local climate variability as driver of the freshening as they showed that changes in local climate variables, such as local atmospheric conditions, the presence of sea ice, melting snow and glacial meltwater discharge, could not explain the observed change in the freshwater content. The authors therefore suggested that the coastal water was likely the main source of freshwater for the fjord. However, the processes affecting the freshwater content of the coastal water were not identified.

In this paper, we aim to identify dominant processes that affect the observed freshening in the coastal water of Northeast Greenland. This involves identifying the main freshwater source and study its variability and drivers from 2003 to 2015.

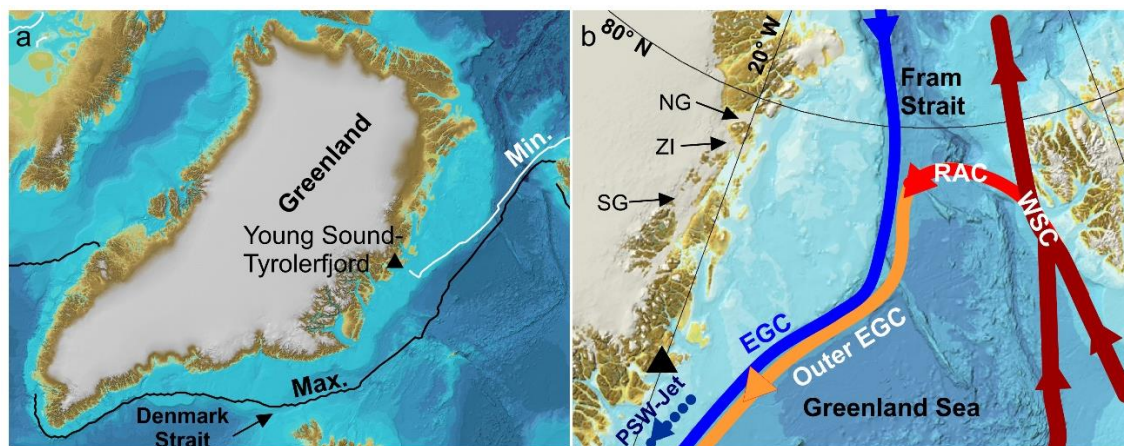


Figure 5-1: (a) Location of Young Sound-Tyrolerfjord along the coast of Northeast Greenland with minimum and maximum median (1981-2010) ice extent (NSIDC, 2017). (b) Schematic circulation in the Greenland Sea (modified from Håvik et al. (2017)), Fresh Polar surface water in the Polar Surface Water Jet (PSW-Jet) and East Greenland Current (EGC) are indicated in blue. Warm Atlantic Water in the Return Atlantic Current (RAC) in orange, and in the West Spitsbergen Current (WSC) in red. Location of the major outlet glaciers of the Northeast Greenland ice stream; Nioghalvfjærdsfjorden Glacier (NG), Zachariae Isstrøm (ZI), and Storstrømmen Glacier (SG) are marked. Bathymetry is obtained from IABCO (Jakobsson et al., 2012).

5.2 Data & Methods

5.2.1 Study Area

We investigate coastal freshening near Young Sound-Tyrolerfjord, a fjord system in Northeast Greenland (Fig. 5-1a). A 45 m deep sill forms a topographic barrier between the fjord basin and the coastal water. The dominant water masses along the coast are associated with the East Greenland Current (Rudels et al., 2002). The surface layer consists of cold (<0 °C) and fresh (<34.4) Polar Surface Water, and has a thickness of roughly 150 m to 200 m on the shelf and 50 m further offshore (Håvik et al., 2017; Rudels et al., 2002). As the sill depth of the fjord is only 45 m, this is the only water mass that is connected to the fjord.

Along the coast of Northeast Greenland an ice wedge is formed. Sea ice transported through Fram Strait is pushed towards the Northeast coast of Greenland (Bacon et al., 2014, 2008). As sea ice melts on its way south, it forms an ice wedge, characterized by a broad and dense ice pack in the north, and a narrow band of fragmented pieces of sea ice in the south. Median monthly ice extent (1981-2010), available through the National Snow and Ice Data Center (NSIDC, 2017), shows the seasonal variability of the ice concentration along East Greenland (Fig. 5-1a). During the maximum seasonal extent (April), the coastal- and shelf area is covered by sea ice from the Fram Strait to Cape Farewell. In summer (August), the sea ice wedge along the coast retreats up to

approximately 74° N, with the southernmost ice-covered area close to Young Sound-Tyrolerfjord.

5.2.2 Mooring data and hydrographic data

Since 2003, the Greenland Ecosystem Monitoring Program have conducted annual hydrographic measurements in Young Sound-Tyrolerfjord. The program monitored the interannual variability of salinity and temperature of the upper basin water, defined as the water mass below sill depth and above 150 m, with a CTD-mooring (Sea-Bird Electronics, Inc., SBE-37). The mooring (mZERO, Fig. 5-1) was replaced every August between 2003 and 2015. The first data point was from 20 August 2003 and the last available data point was from 14 May 2015. The record showed data gaps, when the mooring malfunctioned (2006) or when ice conditions hampered redeployment of the mooring (2004). During the consecutive seasons, the mean mooring depth was 63 m with a standard deviation of 2.7 m. Furthermore, the program measured a hydrographic transect every August that covers Young Sound-Tyrolerfjord and extends approximately 30 km offshore. From this transect we used data from the stations near location GH_{CTD} (Fig. 5-2), to investigate the interannual variation of hydrography in the coastal water and its link to the fjord water masses.

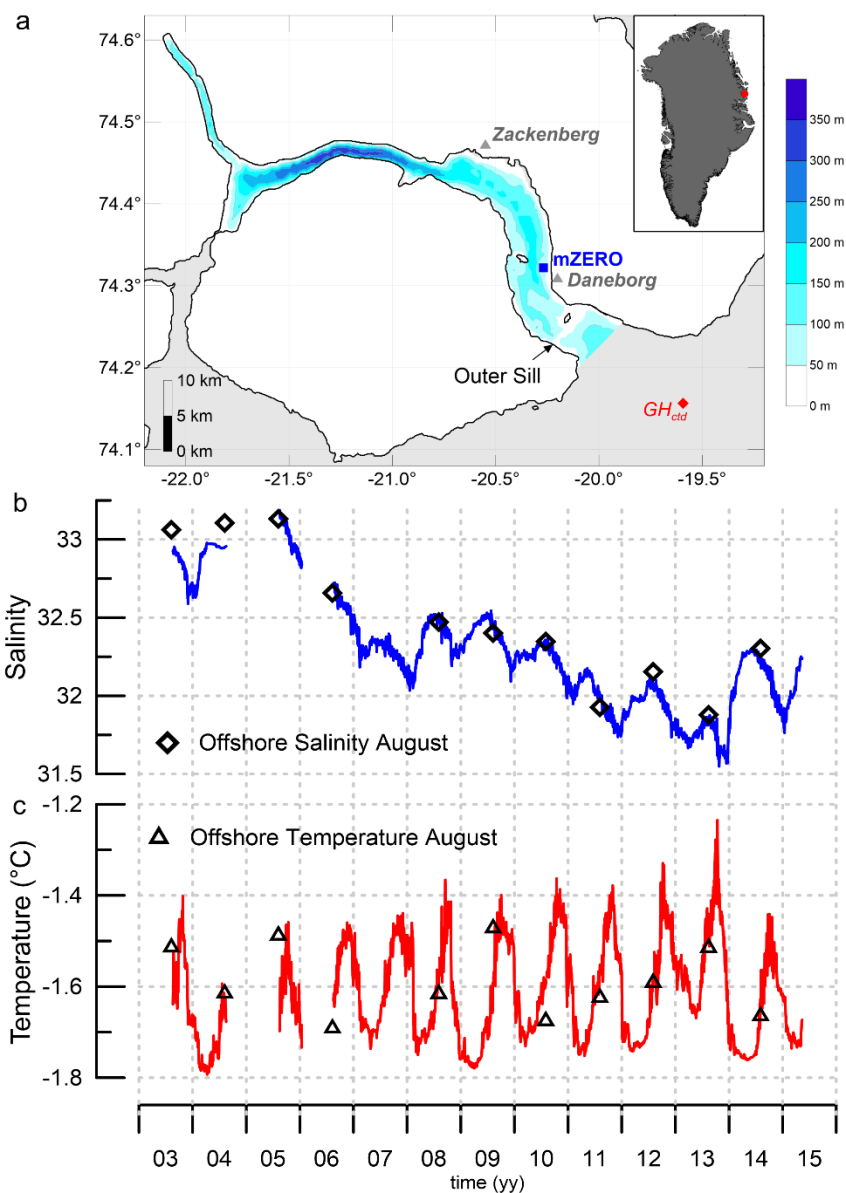


Figure 5-2: (a) Map of Young Sound - Tyrolerfjord in Northeast Greenland showing the location of mooring mZero (blue), CTD station GH (red) and bathymetry (Søren Rysgaard et al., 2003). White areas in (a) depict the land, and grey areas the shelf and coastal waters. (b-c) Time series of salinity (b) and temperature (b) at 63m depth at mZERO from August 2003 to May 2015. Black symbols show the salinity and temperature at sill depth as measured in station GH during the yearly August transects.

5.2.3 Freshwater export variability through Fram Strait

We analyse the interannual variability of freshwater export through Fram Strait from 2003-2015. de Steur et al. (2014, 2009) analyze long-term mooring data in Fram Strait and conclude that the interannual variability of the annual mean liquid freshwater flux (2000-2010 mean: $2100 \text{ km}^3 \text{ yr}^{-1}$ (de Steur et al., 2014, 2009; Haine et al., 2015) is not pronounced. Furthermore, we note that observations in Fram Strait show that the Pacific Water fraction, a possible contributor to short variations in the freshwater content of the Arctic Ocean Outflow, is generally low from 2003-2015, with only a brief appearance in 2011 to 2012 (Dodd et al., 2017, 2012; Falck et al., 2005).

The export of sea ice does show a large interannual variability (de Steur et al., 2009). The volume flux of sea ice is largely controlled by the sea ice drift and not by variability of sea ice thickness (De Steur et al., 2009). Therefore, the interannual variability of freshwater transport via sea ice can be estimated by the areal sea ice export through Fram Strait. We use the time series of sea ice areal export through Fram Strait from Smedsrud et al. (2016). This data set was obtained by using a combination of satellite radar images and station observations of mean sea level pressure differences across Fram Strait (Smedsrud et al., 2017). The dataset contains monthly sea ice area export values from 1935 to 2014, and is available via the Pangaea database (Smedsrud et al., 2016). To obtain the freshwater volume flux from the areal transport values, we use the mean sea ice thickness in Fram Strait (2.2 m; mean: 2008–2011, Hansen et al. (2013)),

a mean sea ice salinity of 4, reference salinity of 34.8 and a sea ice density of 917 kg m^{-3} .

5.2.4 NorESM Climate Model

We use the fully coupled Norwegian Earth System Model (NorESM) to perform a process study on the impact of Atlantic Water temperature on sea ice bottom melt. NorESM is a state of the art global Earth System Model that is part of phase 5 of the Coupled Model Intercomparison Project (CMIP5) (Taylor et al., 2012). The ocean component is an isopycnal coordinate ocean general circulation model with 51 layers, and is based on the Miami Isopycnic Coordinate Model (MICOM) (Bentsen et al., 2012). The sea ice component is described by the CICE4 version used in the Community Climate System Model, version 4 (CCSM4) (Gent et al., 2011). For the experiment presented here, a tri-polar grid is used with approximately 1° zonal resolution along the equator. The Northern hemisphere grid singularities are located in Canada and Siberia, which results in a typical horizontal resolution of 40 km in the Arctic Ocean. A comparison by Langehaug et al. (2013) of historical simulations with satellite observations for Arctic sea ice shows good agreement. The model is well suited for process studies and has previously been used for a similar purpose for a study of the sea ice cover East of Svalbard (Ivanov et al., 2016). In this study, we used monthly data from the CMIP5 historical ensemble for the period 1954 to 2005, which is available through the CMIP5 website (<https://esgf-node.llnl.gov/projects/cmip5/>).

We chose to use temperature of the Atlantic Water temperature in the West Spitsbergen Current in the region southwest of Svalbard, before the Current is impacted by the formation of the Return Atlantic Current (Fig. 5-1b) (Rudels et al., 2005). The latter forms a direct pathway for Atlantic Water from the Western Spitsbergen Current to the Northeast Greenland Shelf, and thus feeds warm Atlantic Water to the outer East Greenland Current and the Greenland Sea (de Steur et al., 2014; Håvik et al., 2017; Rudels et al., 2002). Furthermore, we chose to extract a time series of the core temperature (maximum) of Atlantic Water from below 50 m, as the surface layers might be affected by regional climate variability, which may lead to increased heat loss to the atmosphere and to sea ice melt (Rudels et al., 2005). Finally, the detrended anomalies in core temperature were correlated with spatial fields of sea ice bottom melt. Furthermore, we extracted the monthly freshwater flux from sea ice due to melting from the model to study its temporal and spatial variability.

5.3 Results and discussion

5.3.1 Freshening in Young-Sound

Boone et al. (2018) analyzed a long-term (2003-2015) continuous mooring data timeseries of the basin water in Young Sound-Tyrolerfjord to investigate freshening of the basin water. Deseasonalized time series (Fig. 5-3) showed a long-term freshening trend of $-0.11 \text{ psu } \text{y}^{-1}$ between August 2003- March 2015, and provided an independent verification of the study of summertime data by Sejr et al. (2017). Boone et al. (2018)

showed that anomalously strong freshening occurred in the periods 2005-2007 (-0.92 psu) and 2009-2013 (-0.66 psu). The freshening periods were separated by periods when salinity slightly increased as in 2008 (Aug 2007-Aug 2009: 0.16 psu).

The characteristics of in the fjord basin water were closely linked to surface waters at the coast. This is supported by the observation that temperature and salinity measured at mooring mZERO (65 m) corresponded closely to the salinity and temperature in the coastal water at sill depth (45 m) near GH_{ctd}, a CTD-station occupied every August since 2003 by the Greenland Ecosystem Monitoring Program (location: Fig. 5-1).

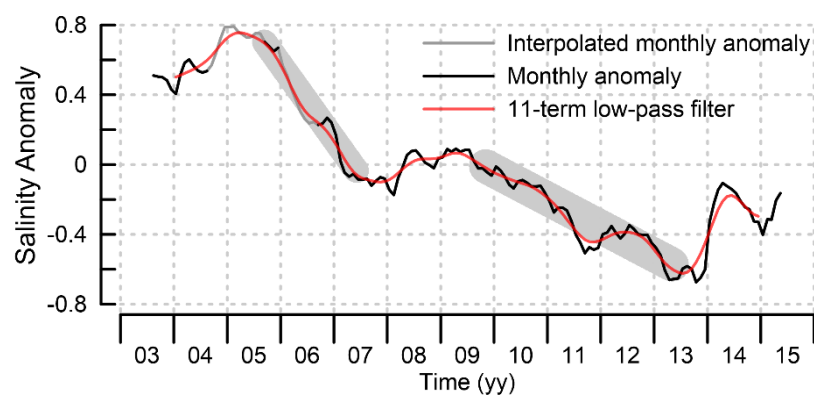


Figure 5-3: Deseasonalized monthly averaged salinity anomalies at 63 m from mooring mZero. Vertical grid lines mark 01 August of each year. Grey zones in (a) mark periods with anomalous freshening (from Boone et al., 2018).

We note that the total yearly runoff to Young-Sound Tyrolerfjord is only a fraction ($\sim 1.1 \text{ km}^3 \text{ yr}^{-1}$, Mernild et al., (2007)) of the mean tidal exchange ($\sim 450 \text{ km}^3/\text{tide}$) and very small in comparison to for example Sermilik Fjord, a fjord with similar length (90 km) and width (5–10 km) (Jackson and Straneo, 2016) as Young Sound-Tyrolerfjord, which has an average yearly freshwater flux of $33.0 \text{ km}^3 \text{ yr}^{-1}$ (Mernild et al., 2012). Young Sound-Tyrolerfjord is therefore highly influenced by the oceanographic conditions in the coastal water. Mixing, associated with sill processes (internal hydraulic jumps, breaking lee waves, shear instabilities, internal waves, etc.) (Boone et al., 2017; Farmer and Freeland, 1983; Geyer and Cannon, 1982; Klymak and Gregg, 2004; Stigebrandt, 1980) are expected to ensure the downward mixing of the coastal water advected to the fjord interior by tidal exchange and make that offshore water masses at sill depth (45 m) compare to the water masses at 65 m in the fjord's upper basin relatively close to the sill ($\sim 7 \text{ km}$). This observation is important as it shows that the mooring is in close connection to the coastal water masses and therefore is representative for variability in the coastal water masses.

5.3.2 Sources of freshwater variability along the coast

The observation of large change in surface salinity and pronounced freshening periods urges for a better understanding of the drivers of the surface layer freshening in the proximity of the Northeast Greenland coast. The main potential contributors to local freshwater variability are sea ice melt and runoff from Greenland. Sea ice is potentially the largest contributor to the freshwater budget of the coastal domain based on a

volumetric balance. Yearly freshwater fluxes of sea ice through the Fram Strait are estimated at $1900 \pm 280 \text{ km}^3 \text{ y}^{-1}$ ($S_{\text{ref}} = 34.8$; mean 2000-2010, (Haine et al., 2015)), while runoff estimates to the coast of Northeast Greenland attain $125 \pm 9 \text{ km}^3 \text{ y}^{-1}$ (mean 1992-2010, Bamber et al., (2012)). Although runoff from the Northeast Greenland sector of the Greenland Ice Sheet are expected to rise (Khan et al., 2014), the volume stays an order of magnitude smaller than that of sea ice export.

Freshwater discharge to the coastal domain may also form coastal boundary currents, which are important features in the coastal domain and largely determine the oceanographic conditions along the coast (Carmack et al., 2015b). Bacon et al. (2014) state that the dominant contributor to the freshwater content of the East Greenland Coastal Current, a freshwater jet along the coast of southeast Greenland, is local melting of sea ice exported through Fram Strait. The authors base their statement on the fact that only the volume of freshwater in sea ice can explain the freshwater volume transported by the East Greenland Coastal Current observed by Wilkinson and Bacon (2005). Furthermore, observations show that there is no evidence of significant growth in transport from Denmark Strait to Cape Farewell, which would be expected if runoff from the Southeast Greenland fjords (mean 1992-2010: $396 \pm 280 \text{ km}^3 \text{ y}^{-1}$, Bamber et al., (2012)) was a dominant driver (Wilkinson and Bacon, 2005). Therefore, freshwater sources, such as terrestrial runoff, precipitation-evaporation and iceberg melt, previously brought forward as drivers by Bacon (2002) and Sutherland and Pickart (2008) are considered contributing factors, but far less dominant than sea ice (Bacon et al., 2008).

Recent observations from 2012 in Northeast Greenland found evidence of a surface-intensified jet within the Polar Surface Water Layer, similar to the East Greenland Coastal Current observed in Southeast Greenland (Håvik et al., 2017). In this so-called “Polar Surface Water Jet” the freshwater flux near 71° N attains ~ 36 mSv or ~ 1140 km³ y⁻¹ (section 6, $S_{ref} = 34.8$). This volume roughly equals the sum of the spring sea ice export through Fram Strait of 2012 (980 km³ y⁻¹, based on data from Smedsrud et al., (2016)) and the runoff estimate from the Northeastern Sector of Greenland (125 ± 9 km³ y⁻¹, mean 1992-2010, Bamber et al., (2012)). The Polar Surface Water Jet was observed up to a latitude of 74° N, which is near Young Sound-Tyrolerfjord. Fig. 5-4 shows a schematic overview of the cited freshwater sources to the coastal domain in Northeast Greenland.

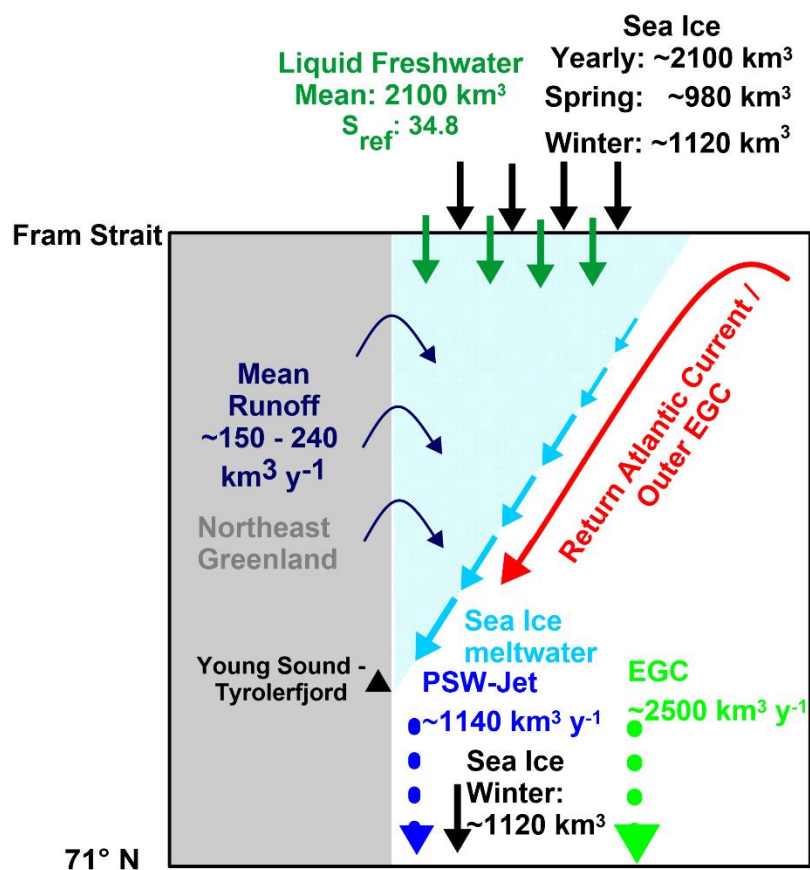


Figure 5-4: Schematic representation of freshwater input to the coastal domain of Northeast Greenland during summer 2011. Reference to the estimates can be found in the text. Black arrows represent solid sea ice transport, dark green arrow represents the liquid water outflow, dark blue arrows represent runoff from Greenland, light blue arrows represent sea ice meltwater, blue arrow represents freshwater transport in the Polar Surface Water- Jet, light green arrows represent freshwater transport in the East Greenland Current and red arrow schematizes the path of the Return Atlantic Current and the Outer East Greenland Current along the shelfbreak of the East Greenland Shelf. Black triangle indicates the location of Young Sound-Tyrolerfjord.

Although this analysis is based on limited data with limited spatial and temporal coverage, it gives insight to the freshwater sources to the coastal domain of Northeast Greenland. Major lack of data is from the freshwater transport and seasonality of the Polar Surface Water Jet. However, even if the Polar Surface Water Jet only occurs during

half of the year, the transport volume cannot be explained by runoff from Greenland. We therefore can assume that sea ice is a dominant driver of freshwater input to the coastal domain, which justifies an investigation of interannual variability of sea ice melt as a driver of freshwater variability along the coast of Northeast Greenland.

5.3.3 Interannual variability of sea Ice export through the Fram Strait

The estimated annual (from September to August) freshwater volume transport of sea ice through Fram Strait shows an increasing trend during the period 2003-2015 (Fig. 5-5). The volume export varied around $\sim 1300 \text{ km}^3$ during 2003–2005, but increased up to $\sim 2100 \text{ km}^3$ in 2012. Study of the seasonal export (Fig. 5-5), shows that volume export mainly occurs during winter (Sep-Feb; range $\sim 820 \text{ km}^3$ (2004) and 1124 km^3 (2007)), but the increase in yearly volume export is mainly caused by variability in the spring-summer volume exports (Mar-Aug; range: 400 km^3 (2005) and 1000 km^3 (2012)). This is emphasized by the fact that relative importance of spring-summer volume export increased with time: total spring-summer export volumes were $\sim 50 \%$ of the winter export volumes in 2005, and $\sim 88\%$ in 2012.

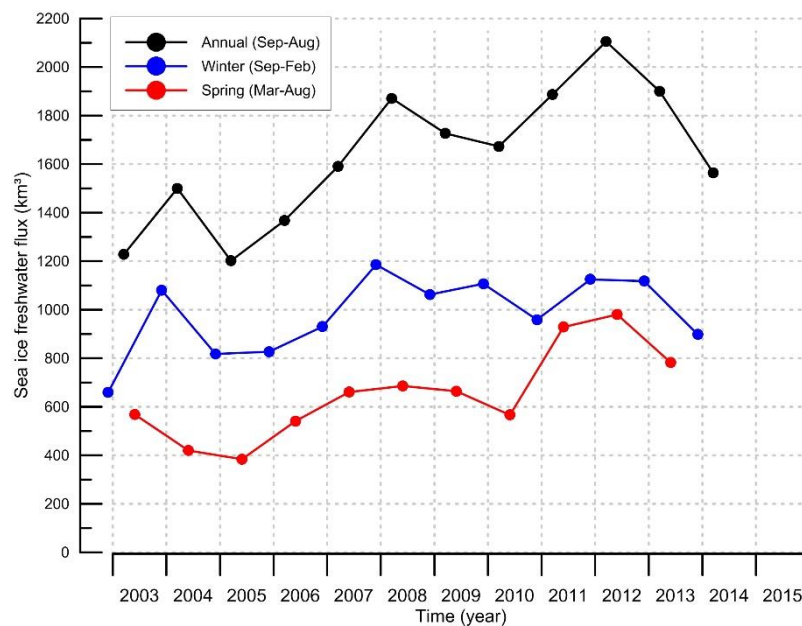


Figure 5-5: Southward flux of freshwater from sea ice in Fram Strait, based on ice area export data as reported by Smedsrud et al. (2017). Annual export is 01 September to 31-August, winter export covers 01 September – 28 February and spring export covers 01 March – 31 August. Values are marked in the middle of the respective period.

We expect that mainly the spring-summer volume export of sea ice exerts a dominant influence on the freshwater variability along the coast of Northeast Greenland. This because sea ice exported during spring-summer is mostly melted along the coast of Northeast Greenland, while the winter sea ice export is mainly transported south along the coast (Koenigk, 2005).

5.3.4 Melt of sea-ice in the coastal domain

As we can assume that sea ice is a major driver of freshwater variability in the coastal domain, we try to link melt dynamics of sea-ice with the freshening trends observed in

Young Sound-Tyrolerfjord. The oceanic heat flux is an important factor that can enhance melt, especially where the halocline, a salinity-stratified layer of water that inhibits upward mixing of the Atlantic Water into the Polar Surface Water and thereby reduces the ocean heat flux to sea ice (Aagaard et al., 1981), is not well developed. Furthermore, it is known that heat loss from the warm Atlantic water plays a key role in shaping the sea-ice cover over the inflow regions of Atlantic Water into the Arctic Ocean (Polyakov et al., 2010).

To investigate the impact of the variability of Atlantic Water Temperature on sea ice melt on the shelf of Northeast Greenland we investigate the correlation between the maximum core temperature of the Atlantic Water in the West-Spitsbergen Current, the source of the Return Atlantic Current, and sea ice melt along the coast of Northeast Greenland from monthly model output between 1954 and 2005 (Fig. 5-6). Positive correlations (red and yellow areas) indicate that positive temperature anomalies in Fram Strait co-vary with increased sea ice melt. Negative correlations indicate that increased heat transport can lead to less sea ice formation in the seasonally sea ice covered areas during winter, which then leaves less sea ice available for melting during the subsequent summer (Sandø et al., 2014).

The analysis reveals complex dynamics with large spatial variability (Fig. 5-6). Correlation was strong ($p\text{-value} > 0.5$) at the inflow branches of the Atlantic Water (West Spitsbergen Current) towards the Arctic Ocean and where Atlantic Water is recirculated in Fram Strait. Correlation was positive over the Northeast Greenland Shelf, from Fram Strait down to a latitude of $\sim 73^\circ$ N. The corresponding p-values (Fig. 5-7) indicate that

the correlation is significant where the correlation is strong. The monthly correlation analysis (Fig. 5-8) shows that correlation is strong along the sea ice edge. The results of this process study therefore suggest that a temperature increase in Atlantic Water in the West-Spitsbergen current results in more melting and a decrease in Atlantic Water temperature results in less melting along the coast of Northeast Greenland.

Although these strong correlations do not directly imply a relation between sea-ice melt and the Atlantic Water temperature variations, it is reasonable that the temperature of the Atlantic Water can affect sea ice melt along the coast of Northeast Greenland. We expect that the Atlantic Water that is recirculated via the Return Atlantic Current is important, as it lies close to the surface, where it can directly impact the ocean–sea-ice–atmosphere interface (Ivanov et al., 2012; Sirevaag and Fer, 2012). Areal plots of monthly freshwater flux from melting from NorESM also show that meltwater input from sea ice in the non-summer months mainly occurs along the sea ice edge (Fig. 5-9). A possible mechanism might be the penetration warm Atlantic Water towards the Northeast Greenland Shelf, as observations show that from Fram Strait towards 75° N, the Return Atlantic Current penetrates towards the Shelf, and induces a temperatures rise in the upper layers (Rudels et al., 2002). This process might be further enhanced by intense mixing along the shelfbreak, which can enhance upward heat transport to the ice undersurface (Carmack et al., 2015a) and cause sea ice melt. The strong correlation over the entire Northeast Greenland shelf during the summer months is more unclear, and the potential link with atmospheric warming should be further studied. We remark that because there is no data available on the heat flux between the Atlantic Water

layer and the Polar Surface Water over the Northeast Greenland Shelf, the aforementioned mechanisms are only speculative.

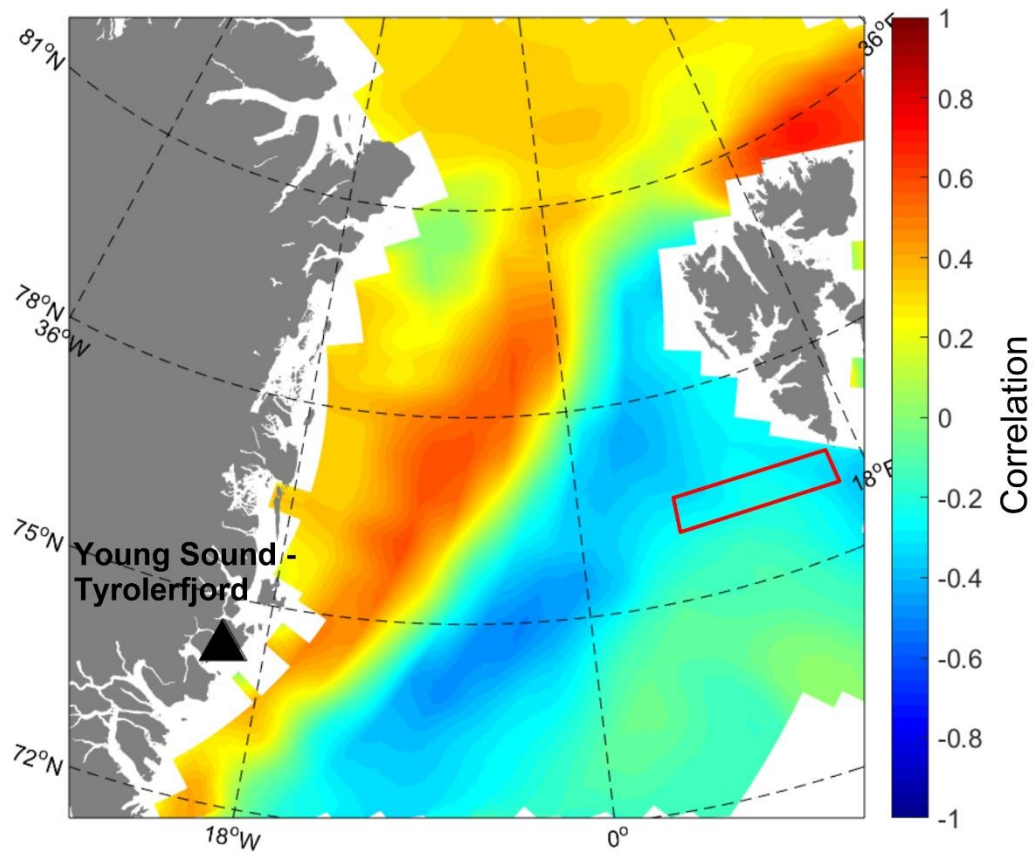


Figure 5-6: Spatial distribution of correlations between Atlantic Water core temperature anomalies feeding the West Spitsbergen Current (red box) and sea ice bottom melting simulated with the NorESM model for mean annual values between 1954-2005. The triangle marks the location of the Young Sound-Tyrolerfjord.

5.3.5 Atlantic Water Temperatures linked with freshwater variability along the coast

To evaluate if the Atlantic Water temperature in Fram Strait impacted freshwater variability along the coast of Northeast Greenland, we compare trends of salinity observations in Young Sound-Tyrolerfjord (Boone et al., 2018), with temperature observations from moored instruments in Fram Strait (Beszczynska-Møller et al., 2012; de Steur et al., 2014; Schauer et al., 2008). Year-round temperature observations from 1997 to 2010 indicated two warming anomalies from the mean seasonal cycle in the Atlantic Water passing through Fram Strait (Beszczynska-Møller et al., 2012). The first, occurred between 1999-2000 and the second between 2005 and 2007. The second was substantially warmer: temperatures anomalies reached >1 °C. The warm anomaly between 2005 and 2007 temporarily doubled the amount of Recirculated Atlantic Water (de Steur et al., 2014), and created an influx of anomalous warm water to the Greenland Sea (Schauer et al., 2008). Furthermore, Beszczynska-Møller et al. (2012) noted that the warming in 2005-2007 was followed by a slightly negative temperature anomaly in 2008, but since summer 2009, a rise in Atlantic Water temperature resulted once more in a weakly positive anomaly (Beszczynska-Møller et al., 2012).

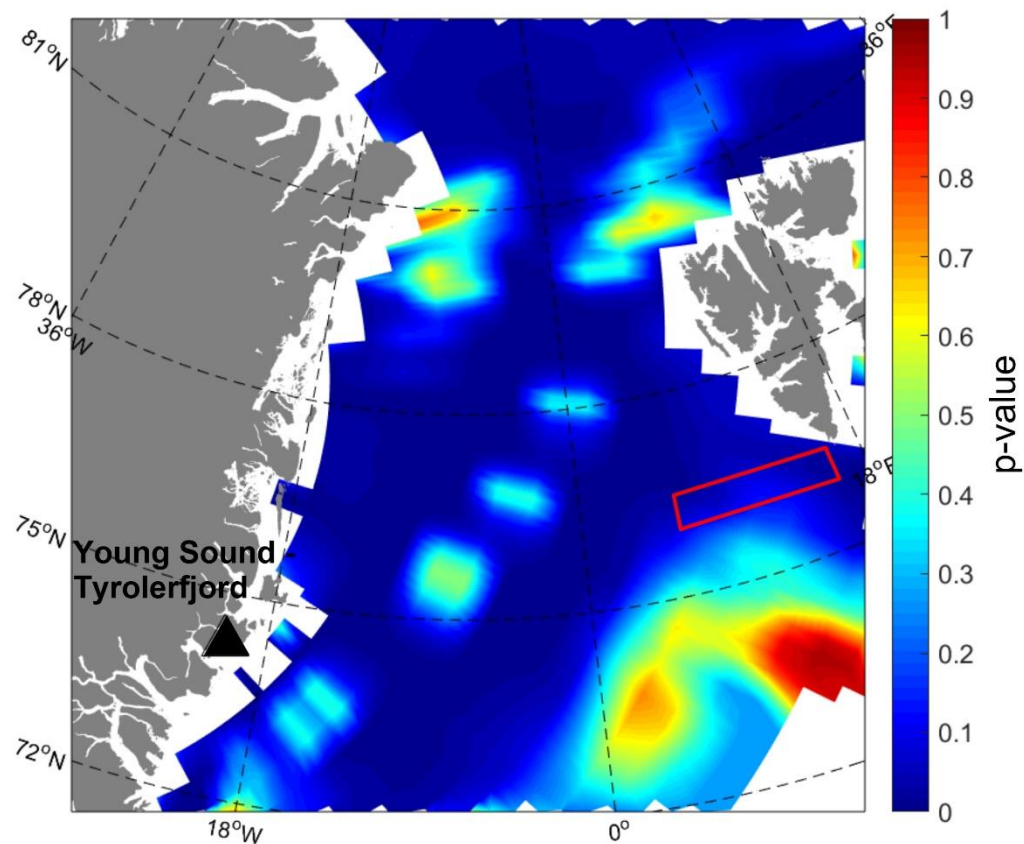


Figure 5-7: Spatial distribution of p-value of the correlation analysis between Atlantic Water core temperature anomalies feeding the West Spitsbergen Current (red box) and Arctic sea ice bottom melting simulated with the NorESM model for mean annual values between 1954-2005. The triangle marks the location of the Young Sound-Tyrolerfjord.

The evolution of the temperature anomaly in Fram Strait can be linked to the freshening trend in Young Sound-Tyrolerfjord (Boone et al., 2017, section 3.1, Fig. 5-3): a strong freshening in the period 2005-2007, followed by a relatively stable period and increase in freshening since 2009-2011. Over the same period oxygen isotope measurements by Cox et al. (2010), show a rise (2005-2007) and fall (2008) of sea ice meltwater addition into the East Greenland Current system, and a tracer study by Dodd et al. (2012)

observed very high sea-ice meltwater inventories in the surface layers of the Fram Strait outflow from 2009-2011. This further suggests a link between Atlantic Water temperatures in Fram Strait, sea ice melt in Fram Strait and along the coast of East Greenland and freshening of the coastal water.

One degree rise in Atlantic Water temperature can significantly increase the heat transported in the Return Atlantic Current. As recent transport volume estimates vary between 1.6 Sv (Håvik et al., 2017) and 2.0 Sv (Marnela et al., 2013), one degree rise in temperature can deliver between 6.7 and 8.4 TJ/s extra heat, which has a sea-ice melt potential of 58-72 km³/month or 691-864 km³/year. If we assume a layer thickness of 50 m, a shelf area of 14000 km² (100 km x 140 km, shelf width near 74° N) and a background salinity of 32.5, 8 km³ of sea ice melt can decrease salinity with 0.3. The latter is roughly the decrease in salinity observed in Young-Sound Tyrolerfjord from August 2010 to August 2011.

This preliminary analysis shows that sea ice melt has the potential to influence salinities in the coastal water of Northeast Greenland. Observations show that Atlantic Water temperatures in the West Spitsbergen have increased in the last decades (Beszczynska-Møller et al., 2012) and temperatures are expected to further increase due to climate warming (IPCC, 2013). In result, our findings suggest that this would lead to an increase of high-latitude sea ice melt, which can potentially further induce freshening along the coast of Northeast Greenland.

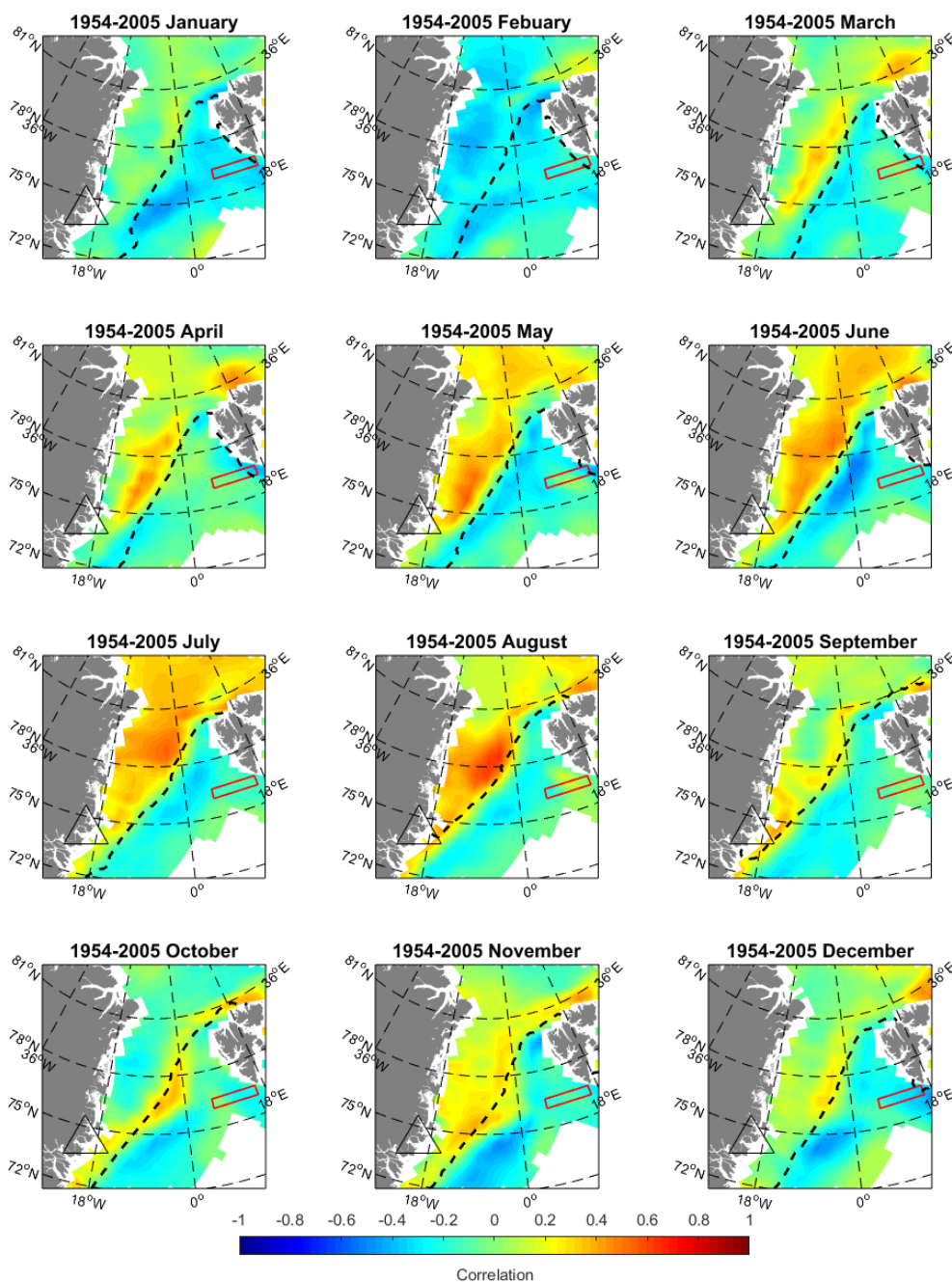


Figure 5-8: Spatial distribution of correlations between Atlantic Water core temperature anomalies feeding the West Spitsbergen Current (red box) and sea ice bottom melting simulated with the NorESM model for mean monthly values between 1954-2005. Black dotted line marks the monthly 1981-2010 median Sea Ice Extent (NSIDC, 2017). The triangle marks the location of the Young Sound-Tyrolerfjord.

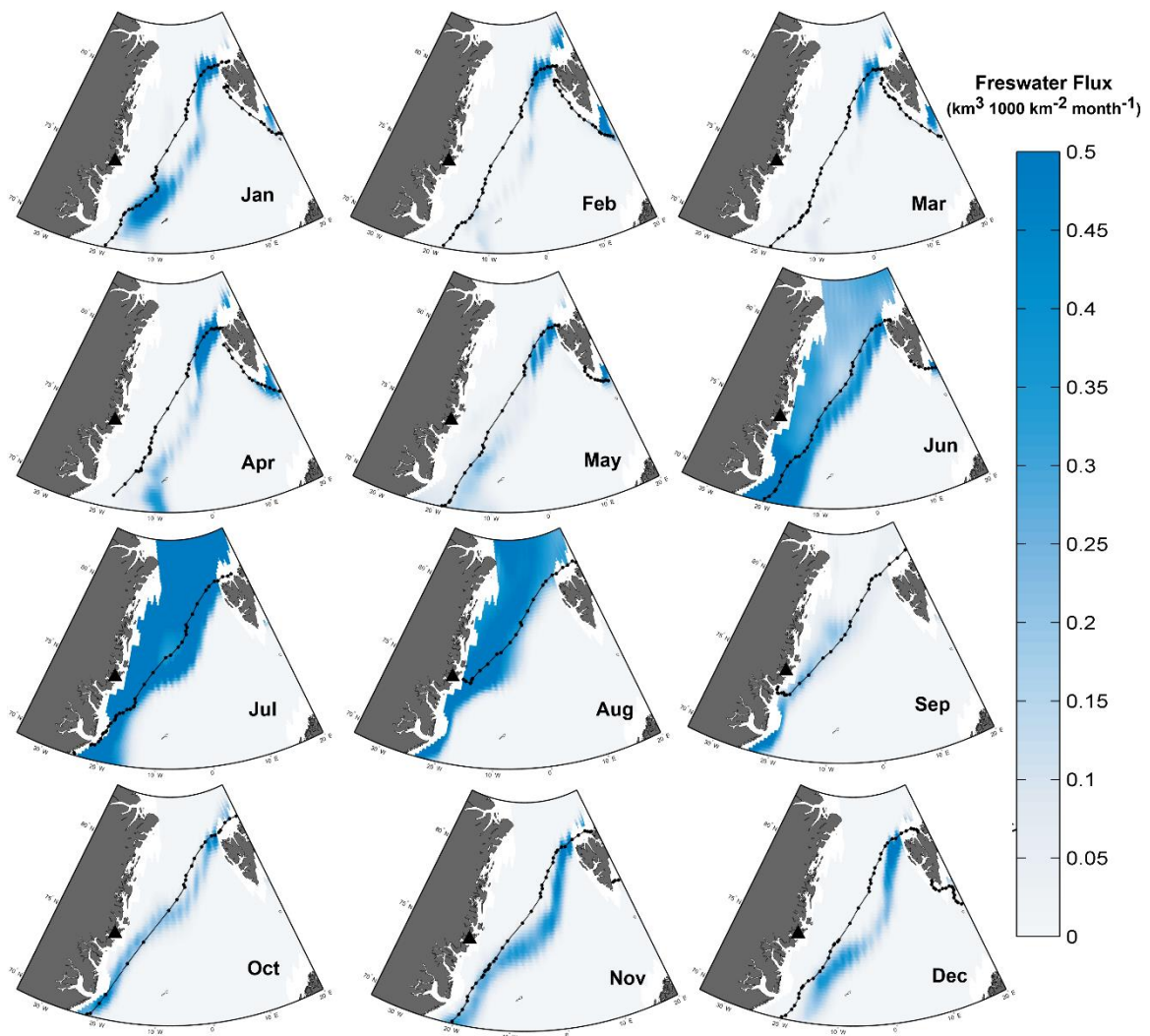


Figure 5-9: Monthly freshwater flux from sea ice due to melting as simulated for the year 2007 from results of the NorESM. Black dotted line marks the monthly 1981-2010 median Sea Ice Extent (NSIDC, 2017).

5.4 Conclusions

This study investigates the role of sea ice melt as driver of the freshwater variability in the coastal domain of Northeast Greenland. Sea ice was identified as a dominant driver of freshwater variability along the coast of Northeast Greenland. A process study with NorESM suggests that sea ice melt along the coast of Northeast Greenland, down to latitude of $\sim 73^\circ$ N, is highly correlated with temperatures of Atlantic Water in the West Spitsbergen Current. We expect that mainly the warm Atlantic Water that is recirculated via the Return Atlantic Current has an important impact. Observations in Young Sound-Tyrolerfjord indicated anomalously strong freshening in the periods 2005-2007 (-0.92 psu) and 2009-2013 (-0.66 psu) (Boone et al., 2017, Fig. 5-3), that can be linked to strong warming anomalies from the mean seasonal cycle in the Atlantic Water passing through Fram Strait as described by Beszczynska-Møller et al. (2012). Our results suggest that further increase of ocean temperatures due to climate warming might lead to further freshening along the coast of Northeast Greenland. This study is only a first step to gain insight in the drivers of the freshwater content along the coast of Northeast Greenland, and would benefit from seasonal data in the coastal areas. More research, including high resolution numerical modelling studies, are needed to map the pathway of sea ice melt along the coast of Northeast Greenland to fully identify its role as driver of freshening and of the coastal boundary currents along the coast of East Greenland.

Acknowledgments

This study was funded by the Canada Excellence Research Chair (CERC) program, the Canada Research Chair (CRC) program, the Canada Foundation of Innovation (CFI), the Natural Sciences and Engineering Research Council of Canada (NSERC, grant RGPIN-2014-03606), Research Manitoba, and the University of Manitoba, Aarhus University and the Greenland Institute of Natural Resources. We acknowledge the Marine Basic program under the Zackenberg Ecological Research Operations for use of the monitoring data. This work is a contribution to the Arctic Science Partnership (ASP-net.org).

References

Aagaard, K., Coachman, L.K., Carmack, E., 1981. On the halocline of the Arctic Ocean. *Deep Sea Res. Part A. Oceanogr. Res. Pap.* 28, 529–545. doi:10.1016/0198-0149(81)90115-1

Arrigo, K.R., Van Dijken, G.L., 2011. Secular trends in Arctic Ocean net primary production. *J. Geophys. Res. Ocean.* 116, 1–15. doi:10.1029/2011JC007151

Bacon, S., 2002. A freshwater jet on the east Greenland shelf. *J. Geophys. Res.* 107, 3068. doi:10.1029/2001JC000935

Bacon, S., Marshall, A., Holliday, N.P., Aksenov, Y., Dye, S.R., 2014. Seasonal variability of the East Greenland Coastal Current. *J. Geophys. Res. Ocean.* 119, 3967–3987. doi:10.1002/2013JC009279

Bacon, S., Myers, P.G., Rudels, B., Sutherland, D. a., 2008. Accessing the Inaccessible: Buoyancy-Driven Coastal Currents on the Shelves of Greenland and Eastern Canada, in: *Arctic–Subarctic Ocean Fluxes*. Springer Netherlands, Dordrecht, pp. 703–722. doi:10.1007/978-1-4020-6774-7_29

Bamber, J., van den Broeke, M., Ettema, J., Lenaerts, J., Rignot, E., 2012. Recent large increases in freshwater fluxes from Greenland into the North Atlantic. *Geophys. Res. Lett.* 39. doi:10.1029/2012GL052552

Bentsen, M., Bethke, I., Debernard, J.B., Iversen, T., Kirkevåg, A., Seland, Ø., Drange, H., Roelandt, C., Seierstad, I.A., Hoose, C., Kristjánsson, J.E., 2012. The Norwegian Earth System Model, NorESM1-M – Part 1: Description and basic evaluation. *Geosci. Model Dev. Discuss.* 5, 2843–2931. doi:10.5194/gmdd-5-2843-2012

Beszczynska-Møller, A., Fahrbach, E., Schauer, U., Hansen, E., 2012. Variability in Atlantic water temperature and transport at the entrance to the Arctic Ocean, 1997-2010. *ICES J. Mar. Sci.* 69, 852–863. doi:10.1093/icesjms/fss056

Beszczynska-Möller, A., Woodgate, R., Lee, C., Melling, H., Karcher, M., 2011. A Synthesis of Exchanges Through the Main Oceanic Gateways to the Arctic Ocean. *Oceanography* 24, 82–99. doi:10.5670/oceanog.2011.59

Boone, W., Rysgaard, S., Carlson, D.F., Meire, L., Kirillov, S.A., Mortensen, J., Dmitrenko, I.A., Vergeynst, L., Sejr, M.K., 2018. Coastal freshening prevents fjord bottom water renewal in Northeast Greenland – a mooring study from 2003-2015. Accepted for *Geophys. Res. Lett.*

Boone, W., Rysgaard, S., Kirillov, S.A., Dmitrenko, I.A., Bendtsen, J., Mortensen, J., Meire, L., Petrusevich, V., Barber, D.G., 2017. Circulation and fjord-shelf exchange during the ice-covered period in Young Sound-Tyrolerfjord, Northeast Greenland (74°N). *Estuar. Coast. Shelf Sci.* 194, 205–216. doi:10.1016/j.ecss.2017.06.021

Carmack, E., McLaughlin, F., 2011. Towards recognition of physical and geochemical change in Subarctic and Arctic Seas. *Prog. Oceanogr.* 90, 90–104. doi:10.1016/j.pocean.2011.02.007

Carmack, E., Polyakov, I. V., Padman, L., Fer, I., Hunke, E.C., Hutchings, J., Jackson, J., Kelley, D., Kwok, R., Layton, C., Melling, H., Perovich, D., Persson, O., Ruddick, B., Timmermans, M.-L., Toole, J., Ross, T., Vavrus, S., Winsor, P., 2015a. Toward Quantifying the Increasing Role of Oceanic Heat in Sea Ice Loss in the New Arctic. *Bull. Am. Meteorol. Soc.* 96, 2079–2105. doi:10.1175/BAMS-D-13-00177.1

Carmack, E., Winsor, P., Williams, W., 2015b. The contiguous panarctic Riverine Coastal Domain: A unifying concept. *Prog. Oceanogr.* 139, 13–23. doi:10.1016/j.pocean.2015.07.014

Carmack, E.C., Yamamoto-Kawai, M., Haine, T.W.N., Bacon, S., Bluhm, B.A., Lique, C., Melling, H., Polyakov, I. V., Straneo, F., Timmermans, M.-L., Williams, W.J., 2016. Freshwater and its role in the Arctic Marine System: Sources, disposition, storage, export, and physical and biogeochemical consequences in the Arctic and global oceans. *J. Geophys. Res. Biogeosciences* 121, 675–717. doi:10.1002/2015JG003140

Cox, K.A., Stanford, J.D., McVicar, A.J., Rohling, E.J., Heywood, K.J., Bacon, S., Bolshaw, M., Dodd, P.A., De La Rosa, S., Wilkinson, D., 2010. Interannual variability of Arctic sea ice export into the East Greenland Current. *J. Geophys. Res. Ocean.* 115, 1–12. doi:10.1029/2010JC006227

de Steur, L., Hansen, E., Gerdes, R., Karcher, M., Fahrbach, E., Holfort, J., 2009. Freshwater fluxes in the East Greenland Current: A decade of observations. *Geophys. Res. Lett.* 36, L23611. doi:10.1029/2009GL041278

de Steur, L., Hansen, E., Mauritzen, C., Beszczynska-Møller, A., Fahrbach, E., 2014. Impact of recirculation on the East Greenland Current in Fram Strait: Results from moored current meter measurements between 1997 and 2009. *Deep Sea Res. Part I Oceanogr. Res. Pap.* 92, 26–40. doi:10.1016/j.dsr.2014.05.018

Dodd, P.A., Rabe, B., Hansen, E., Falck, E., MacKensen, A., Rohling, E., Stedmon, C., Kristiansen, S., 2012. The freshwater composition of the Fram Strait outflow derived from a decade of tracer measurements. *J. Geophys. Res. Ocean.* 117, 1–26. doi:10.1029/2012JC008011

Dodd, P., Blaasterdalen, T., Karcher, M., Stedmon, C., 2017. Pacific Water in the Arctic Ocean and Fram Strait. *Geophys. Res. Abstr.* 19.

Falck, E., Kattner, G., Budéus, G., 2005. Disappearance of Pacific Water in the northwestern Fram Strait. *Geophys. Res. Lett.* 32, 1–4. doi:10.1029/2005GL023400

Farmer, D.M., Freeland, H.J., 1983. The physical oceanography of Fjords. *Prog. Oceanogr.* 12, 147–219. doi:10.1016/0079-6611(83)90004-6

Gent, P.R., Danabasoglu, G., Donner, L.J., Holland, M.M., Hunke, E.C., Jayne, S.R., Lawrence, D.M., Neale, R.B., Rasch, P.J., Vertenstein, M., Worley, P.H., Yang, Z.-L.,

Zhang, M., 2011. The community climate system model version 4. *J. Clim.* 24, 4973–4991. doi:10.1175/2011JCLI4083.1

Geyer, W.R., Cannon, G.A., 1982. Sill processes related to deep water renewal in a fjord. *J. Geophys. Res.* 87, 7985. doi:10.1029/JC087iC10p07985

Haine, T.W.N., Curry, B., Gerdes, R., Hansen, E., Karcher, M., Lee, C., Rudels, B., Spreen, G., de Steur, L., Stewart, K.D., Woodgate, R., 2015. Arctic freshwater export: Status, mechanisms, and prospects. *Glob. Planet. Change* 125, 13–35. doi:10.1016/j.gloplacha.2014.11.013

Hansen, E., Gerland, S., Granskog, M.A., Pavlova, O., Renner, A.H.H., Haapala, J., Løyning, T.B., Tschudi, M., 2013. Thinning of Arctic sea ice observed in Fram Strait: 1990–2011. *J. Geophys. Res. Ocean.* 118, 5202–5221. doi:10.1002/jgrc.20393

Harden, B.E., Pickart, R.S., Valdimarsson, H., Våge, K., de Steur, L., Richards, C., Bahr, F., Torres, D., Børve, E., Jónsson, S., Macrander, A., Østerhus, S., Håvik, L., Hattermann, T., 2016. Upstream sources of the Denmark Strait Overflow: Observations from a high-resolution mooring array. *Deep Sea Res. Part I Oceanogr. Res. Pap.* 112, 94–112. doi:10.1016/j.dsr.2016.02.007

Håvik, L., Pickart, R.S., Våge, K., Torres, D., Thurnherr, A.M., Beszczynska-Møller, A., Walczowski, W., von Appen, W.-J., 2017. Evolution of the East Greenland Current from Fram Strait to Denmark Strait: Synoptic measurements from summer 2012. *J. Geophys. Res. Ocean.* 122, 1974–1994. doi:10.1002/2016JC012228

IPCC, 2013. Fifth Assessment Report Climate Change 2013.

Ivanov, V., Alexeev, V., Koldunov, N. V., Repina, I., Sandø, A.B., Smedsrud, L.H., Smirnov, A., 2016. Arctic Ocean Heat Impact on Regional Ice Decay: A Suggested Positive Feedback. *J. Phys. Oceanogr.* 46, 1437–1456. doi:10.1175/JPO-D-15-0144.1

Ivanov, V. V., Alexeev, V.A., Repina, I., Koldunov, N. V., Smirnov, A., 2012. Tracing Atlantic Water Signature in the Arctic Sea Ice Cover East of Svalbard. *Adv. Meteorol.* 2012, 1–11. doi:10.1155/2012/201818

Jackson, R.H., Straneo, F., 2016. Heat, Salt, and Freshwater Budgets for a Glacial Fjord in Greenland. *J. Phys. Oceanogr.* 46, 2735–2768. doi:10.1175/JPO-D-15-0134.1

Jakobsson, M., Mayer, L., Coakley, B., Dowdeswell, J.A., Forbes, S., Fridman, B., Hodnesdal, H., Noormets, R., Pedersen, R., Rebesco, M., Schenke, H.W., Zarayskaya, Y., Accettella, D., Armstrong, A., Anderson, R.M., Bienhoff, P., Camerlenghi, A., Church, I., Edwards, M., Gardner, J. V., Hall, J.K., Hell, B., Hestvik, O., Kristoffersen, Y., Marcussen, C., Mohammad, R., Mosher, D., Nghiem, S. V., Pedrosa, M.T., Travaglini, P.G., Weatherall, P., 2012. The International Bathymetric Chart of the Arctic Ocean (IBCAO) Version 3.0. *Geophys. Res. Lett.* 39. doi:10.1029/2012GL052219

Khan, S.A., Kjær, K.H., Bevis, M., Bamber, J.L., Wahr, J., Kjeldsen, K.K., Bjørk, A.A., Korsgaard, N.J., Stearns, L.A., van den Broeke, M.R., Liu, L., Larsen, N.K., Muresan, I.S., 2014. Sustained mass loss of the northeast Greenland ice sheet triggered by regional warming. *Nat. Clim. Chang.* 4, 292–299. doi:10.1038/nclimate2161

Klymak, J.M., Gregg, M.C., 2004. Tidally Generated Turbulence over the Knight Inlet Sill. *J. Phys. Oceanogr.* 34, 1135–1151. doi:10.1175/1520-0485(2004)034<1135:TGTOTK>2.0.CO;2

Koenig, T., 2005. Sea Ice Export through Fram Strait : Variability and Interactions with Climate Torben König Berichte zur Erdsystemforschung Reports on Earth System Science. Reports Earth Syst. Sci. Max Planck Institute for Meteorology.

Langehaug, H.R., Geyer, F., Smedsrud, L.H., Gao, Y., 2013. Arctic sea ice decline and ice export in the CMIP5 historical simulations. *Ocean Model.* 71, 114–126. doi:10.1016/j.ocemod.2012.12.006

Marnela, M., Rudels, B., Houssais, M.-N., Beszczynska-Möller, A., Eriksson, P.B., 2013. Recirculation in the Fram Strait and transports of water in and north of the Fram Strait derived from CTD data. *Ocean Sci* 9, 499–519. doi:10.5194/os-9-499-2013

McLaughlin, F.A., Carmack, E.C., Williams, W.J., Zimmermann, S., Shimada, K., Itoh, M., 2009. Joint effects of boundary currents and thermohaline intrusions on the warming of Atlantic water in the Canada Basin, 1993–2007. *J. Geophys. Res.* 114, C00A12. doi:10.1029/2008JC005001

McPhee, M.G., Proshutinsky, A., Morison, J.H., Steele, M., Alkire, M.B., 2009. Rapid change in freshwater content of the Arctic Ocean. *Geophys. Res. Lett.* 36, 1–6. doi:10.1029/2009GL037525

Mernild, S.H., Seidenkrantz, M.S., Chylek, P., Liston, G.E., Hasholt, B., 2012. Climate-driven fluctuations in freshwater flux to Sermilik Fjord, East Greenland, during the last 4000 years. *Holocene*. doi:10.1177/0959683611431215

Mernild, S.H., Sigsgaard, C., Rasch, M., Hasholt, B., Hansen, B.U., Stjernholm, M., Pedersen, D., 2007. Climate, river discharge and suspended sediment transport in the Zackenberg River drainage basin and Young Sound/Tyrolerfjord, Northeast Greenland, in: Rysgaard, S., Glud, R.N. (Eds.), *Carbon Cycling in Arctic Marine Ecosystems: Case Study Young Sound*. *Meddr. Grønland, Bioscience* 58, pp. 24–43.

NSIDC, 2017. Sea Ice Index [WWW Document]. URL https://nsidc.org/data/seaice_index/archives.html (accessed 11.1.17).

Pabi, S., van Dijken, G.L., Arrigo, K.R., 2008. Primary production in the Arctic Ocean, 1998–2006. *J. Geophys. Res. Ocean.* 113, 1998–2006. doi:10.1029/2007JC004578

Pickart, R.S., Torres, D.J., Fratantoni, P.S., 2005. The East Greenland Spill Jet*. *J. Phys. Oceanogr.* 35, 1037–1053. doi:10.1175/JPO2734.1

Polyakov, I. V., Beszczynska, A., Carmack, E.C., Dmitrenko, I.A., Fahrbach, E., Frolov, I.E., Gerdes, R., Hansen, E., Holfort, J., Ivanov, V. V., Johnson, M.A., Karcher, M., Kauker, F., Morison, J., Orvik, K.A., Schauer, U., Simmons, H.L., Skagseth, Ø., Sokolov, V.T., Steele, M., Timokhov, L.A., Walsh, D., Walsh, J.E., 2005. One more step toward a warmer Arctic. *Geophys. Res. Lett.* 32, 1–4. doi:10.1029/2005GL023740

Polyakov, I. V., Pnyushkov, A. V., Timokhov, L.A., 2012. Warming of the Intermediate Atlantic Water of the Arctic Ocean in the 2000s. *J. Clim.* 25, 8362–8370. doi:10.1175/JCLI-D-12-00266.1

Polyakov, I. V., Timokhov, L.A., Alexeev, V.A., Bacon, S., Dmitrenko, I.A., Fortier, L., Frolov, I.E., Gascard, J.-C., Hansen, E., Ivanov, V. V., Laxon, S., Mauritzen, C., Perovich, D., Shimada, K., Simmons, H.L., Sokolov, V.T., Steele, M., Toole, J., 2010. Arctic Ocean Warming Contributes to Reduced Polar Ice Cap. *J. Phys. Oceanogr.* 40, 2743–2756. doi:10.1175/2010JPO4339.1

Proshutinsky, A., Krishfield, R., Timmermans, M.-L., Toole, J., Carmack, E., McLaughlin, F., Williams, W.J., Zimmermann, S., Itoh, M., Shimada, K., 2009. Beaufort Gyre freshwater reservoir: State and variability from observations. *J. Geophys. Res.* 114, C00A10. doi:10.1029/2008JC005104

Rabe, B., Dodd, P.A., Hansen, E., Falck, E., Schauer, U., MacKensen, A., Beszczynska-Möller, A., Kattner, G., Rohling, E.J., Cox, K., 2013. Liquid export of Arctic freshwater components through the Fram Strait 1998–2011. *Ocean Sci.* 9, 91–109. doi:10.5194/os-9-91-2013

Rabe, B., Karcher, M., Schauer, U., Toole, J.M., Krishfield, R.A., Pisarev, S., Kauker, F., Gerdes, R., Kikuchi, T., 2011. An assessment of Arctic Ocean freshwater content changes from the 1990s to the 2006–2008 period. *Deep Sea Res. Part I Oceanogr. Res. Pap.* 58, 173–185. doi:10.1016/j.dsr.2010.12.002

Rudels, B., Björk, G., Nilsson, J., Winsor, P., Lake, I., Nohr, C., 2005. The interaction between waters from the Arctic Ocean and the Nordic Seas north of Fram Strait and along the East Greenland Current: results from the Arctic Ocean-02 Oden expedition. *J. Mar. Syst.* 55, 1–30. doi:10.1016/j.jmarsys.2004.06.008

Rudels, B., Fahrbach, E., Meincke, J., Gereon, B., Eriksson, P.B., 2002. The East Greenland Current and its contribution to the Denmark Strait overflow. *ICES J. Mar. Sci.* 59, 1133–1154. doi:10.1006/jmsc.2002.1284

Rysgaard, S., Vang, T., Stjernholm, M., Rasmussen, B., Windelin, A., Kiilsholm, S., 2003. Physical Conditions, Carbon Transport, and Climate Change Impacts in a Northeast Greenland Fjord. *Arctic, Antarct. Alp. Res.* 35, 301–312. doi:10.1657/1523-0430(2003)035[0301:PCCTAC]2.0.CO;2

Sandø, A.B., Gao, Y., Langehaug, H.R., 2014. Poleward ocean heat transports, sea ice processes, and Arctic sea ice variability in NorESM1-M simulations. *J. Geophys. Res. Ocean.* 119, 2095–2108. doi:10.1002/2013JC009435

Schauer, U., Beszczynska-Möller, A., Walczowski, W., Fahrbach, E., Piechura, J., Hansen, E., 2008. Variation of Measured Heat Flow Through the Fram Strait Between 1997 and 2006, in: *Arctic–Subarctic Ocean Fluxes*. Springer Netherlands, Dordrecht, pp. 65–85. doi:10.1007/978-1-4020-6774-7_4

Sejr, M.K., Stedmon, C.A., Bendtsen, J., Abermann, J., Juul-Pedersen, T., Mortensen, J., Rysgaard, S., 2017. Evidence of local and regional freshening of Northeast Greenland coastal waters. *Sci. Rep.* 7, 13183. doi:10.1038/s41598-017-10610-9

Sirevaag, A., Fer, I., 2012. Vertical heat transfer in the Arctic Ocean: The role of double-diffusive mixing. *J. Geophys. Res. Ocean.* 117, n/a-n/a. doi:10.1029/2012JC007910

Smedsrud, L.H., Halvorsen, M.H., Stroeve, J.C., Zhang, R., Kloster, K., 2017. Fram Strait sea ice export variability and September Arctic sea ice extent over the last 80 years. *Cryosphere* 11, 65–79. doi:10.5194/tc-11-65-2017

Smedsrud, L.H., Halvorsen, M.H., Stroeve, J.C., Zhang, R., Kloster, K., 2016. Fram Strait sea ice export variability over the last 80 years. *Suppl. to Smedsrud, LH al. Fram Strait sea ice Export Var. Sept. Arct. sea ice extent over last 80 years. Cryosphere*, 11(1), 65-79, <https://doi.org/10.5194/tc-11-65-2017>. doi:10.1594/PANGAEA.868944

Stigebrandt, A., 1980. Some aspects of tidal interaction with fjord constrictions. *Estuar. Coast. Mar. Sci.* 11, 151–166. doi:10.1016/S0302-3524(80)80038-7

Sutherland, D.A., Pickart, R.S., 2008. The East Greenland Coastal Current: Structure, variability, and forcing. *Prog. Oceanogr.* 78, 58–77. doi:10.1016/j.pocean.2007.09.006

Taylor, K.E., Stouffer, R.J., Meehl, G.A., 2012. An Overview of CMIP5 and the Experiment Design. *Bull. Am. Meteorol. Soc.* 93, 485–498. doi:10.1175/BAMS-D-11-00094.1

Wilkinson, D., Bacon, S., 2005. The spatial and temporal variability of the East Greenland Coastal Current from historic data. *Geophys. Res. Lett.* 32, L24618. doi:10.1029/2005GL024232

Woodgate, R.A., Weingartner, T.J., Lindsay, R., 2012. Observed increases in Bering Strait oceanic fluxes from the Pacific to the Arctic from 2001 to 2011 and their impacts on the Arctic Ocean water column. *Geophys. Res. Lett.* 39, 2–7. doi:10.1029/2012GL054092

Chapter 6 Summary & Conclusions

6.1 Summary of major findings

Major Finding 1: Analysis and description of seasonal circulation patterns and drivers of circulation in an ice-covered Northeast Greenland Fjord

The first results chapter of this thesis (Chapter 3) focused on circulation in a high-Arctic fjord during winter, when the fjord was covered with sea-ice and freshwater input was low. This chapter is based on a unique dataset with unprecedented spatial and temporal coverage in a high Arctic fjord. The study site is the Young Sound-Tyrolerfjord system (74°N) in Northeast Greenland. The analysis of the seasonal observations of circulation, hydrography and cross-sill exchange revealed a distinct seasonal circulation pattern, that changes in relation to polynya activity, meltwater, and inflow of coastal water masses. Renewal of basin water in the fjord was a relatively slow process which modified the fjord water masses on a seasonal timescale. By the end of winter, there was two-layer circulation, with outflow in the upper 45 m and inflow extending down to approximately 150 m. Tidal analysis showed that tidal currents were dominated by the M2 tidal constituents, and that residual currents were relatively small during the ice-covered period.

Detailed observation of the sill area with an autonomous ice tethered profiler during the transition from winter to spring enabled analysis of the fjord-shelf exchange over the outer sill of the Young Sound-Tyrolerfjord. Analysis indicated that tidal pumping, a tidally driven fjord-shelf exchange mechanism, drove a salt flux that is estimated to range between 145 kg s^{-1} and 603 kg s^{-1} . Preliminary extrapolation of these values over the ice-covered period indicates that tidal pumping likely is a major source of dense water. Therefore, tidal pumping is expected to be one of the drivers of fjord circulation during the ice-covered period.

Major Finding 2: Young Sound- Tyrolerfjord, a fjord along the coast of Northeast Greenland is vulnerable to the effects of freshening

In Chapter 4, we describe interannual variability of salinity and temperature in the basin water of the Young Sound-Tyrolerfjord, based on a long term continuous data series that covers 2003 - 2015. This dataset, together with data from the Marin Basis Monitoring Program, is the first ever decadal continuous dataset of a fjord system in Greenland and enables us to study the variability and the effect on the renewal of the fjord bottom water due to regional freshening.

In this study, we deseasonalized the salinity timeseries and found, besides a general freshening of -0.11 psu y^{-1} , anomalous high freshening in the periods 2005-2007 (-0.46 psu y^{-1}) and 2009-2013 (-0.17 psu y^{-1}). These freshening rates were at the high end in comparison with estimates of freshening around the Arctic reported earlier.

Furthermore, temperature-salinity analysis from 2004 to 2014 shows that freshening of the coastal water (~range at sill depth: 33.3 psu in 2005 to 31.4 psu in 2007) prevented renewal of the fjord's bottom water. These data provide critical observations of interannual freshening rates in a remote fjord in Greenland and in the adjacent coastal waters, and show that coastal freshening impacts the fjord hydrography, which may impact the ecosystem functions on long term.

Major Finding 3: Fjord freshening rates might be impacted by sea ice melt along the Northeast Greenland Coast.

In Chapter 5, we analyzed the driving forces for the freshening discussed in Chapter 4. Previous studies could not attribute the observed change in freshwater variability in Young Sound Tyrolerfjord to local climate variables. Therefore, we analyzed the dominant drivers of freshwater variability along the coast of Northeast Greenland.

Sea ice meltwater was identified as the dominant driver of freshwater variability in the coastal domain. Using a climate model we showed that sea ice bottom melt along the coast and north of 73° N is highly correlated with the temperature of Atlantic Water in the West-Spitsbergen Current. Furthermore, we found that freshening rates observed near Young Sound-Tyrolerfjord (Chapter 4) were highly correlated with positive temperature anomalies observed in the Fram Strait.

These findings are important, as climate predictions forecast further increase of the North Atlantic Ocean temperature. The results from this chapter, if confirmed, indicate

that this would lead to more sea ice melt along the coast of Northeast Greenland, which would induce further freshening and may impact fjord ecosystems in long-term.

6.2 Limitations and future work

Chapter 3 of this thesis presented the circulation and fjord-shelf exchange during the ice-covered period in Young Sound-Tyrolerfjord. Compared to other studies of fjords in Greenland, this research was based on a rather extensive dataset. However, observations remain, in many cases, a limiting factor. For this study, the main limitation were the observations of the fjord-shelf exchange over the sill. The observations with an autonomous ice tethered profiler (ITP) indicated a tidal (semidiurnal) periodicity of salinity, with higher salinities during flood than during ebb tides. These observations suggest that dense water input across the sill, a driver of winter fjord circulation, may be partially explained by tidal pumping. This finding urged for the calculation of a salt balance. However, the ITP dataset and the ADCP did not completely cover the water column and only one point in the cross-section was sampled. In the study, we addressed the related uncertainties, but also cited a remark by Jackson and Straneo (2016) that these types of uncertainty are inherent to studies of salt balances on a temporal scale, as a compromise must be made on the allocation of the available resources. However, to fully understand the fjord-shelf exchange processes at the sill in the Young Sound-Tyrolerfjord and to fully understand its role as driver of circulation in the fjord, more data is needed. Significant progress can be made if observations enable full closure of

the salt balance over the sill and enable quantification of the contribution of aspiration to tidal pumping.

Therefore, a new experiment should aim to:

- Measure the currents and salinity across the sill at high resolution and on multiple points across the sill.
- Measure the hydrographic evolution of the fjord to quantify the effect of cross-sill inflow on the fjord hydrography in the basin water and in the bottom water.
- Measure salinity inside and outside the fjord to measure evolution of cross-sill salinity difference and enable quantification of aspiration depths.

Chapter 4 of this thesis presented the analysis of an interannual dataset from the Marin Basis Monitoring Program. The study shows that Young Sound-Tyrolerfjord is an interesting research site to monitor the effects of coastal freshening. The system is highly influenced by the oceanographic conditions in the coastal water. The presented data already covers an exceptional period, but for future work, I highly recommend the continuation of the Marin Basis mooring program. In our study, we show that the mooring at 65 m deep, is a good representation of the hydrography of the upper basin of the fjord. If funding allows, I would suggest adding a mooring in the bottom water to the monitoring program.

Chapter 5 of this thesis aimed to identify processes that affect the freshening in the coastal water of Northeast Greenland. The main limitation to this study is the lack of data from the coastal domain of Northeast Greenland and on the shelf. The area is

remote, mostly ice covered and hard to navigate. More information on mixing processes on the Northeast Greenland Shelf and along the shelfbreak that may potentially increase upward heat-flux from the Atlantic Water layer to the ice bottom can improve the interpretation of the presented correlation analysis.

Another suggestion for future research is to focus on the pathway of sea ice melt along the coast of East Greenland and aim to identify its role as driver of the coastal boundary currents along Greenland's coast. Håvik et al. (2017) remark that the formation of the (South)East Greenland Coastal Current is unclear, as it was previously attributed to the formation of a coastal boundary current due to runoff and sea ice melt (Bacon et al., 2008, 2014), and to bathymetric steering of the shelfbreak East Greenland near the Kangerdlugssuaq Trough (Sutherland and Pickart, 2008). As Håvik et al. (2017) recently also observed a coastal boundary current in Northeast Greenland, they named the Polar Surface Water Jet, the question was raised if the Polar Surface Water Jet and the East Greenland Current might be one connected feature that is part of a contiguous coastal domain around Greenland.

The region near Young Sound-Tyrolerfjord might be a key location to study the formation of the Polar Surface Water Jet. According to the median sea ice extent, shown in Fig. 5-1, Young Sound lies near the southern tip of the sea ice wedge during the summer months, when sea ice melt reaches its seasonal maximum. This region might be the location where the boundary current is formed, or reaches the coast. Sampling the hydrographic structure and velocity profiles of the East Greenland current system from the coast to the shelfbreak from the southern ice edge of the sea ice wedge and further

southwards might clarify the mechanism driving the formation of the Polar Surface Water Jet and how it develops on its way south.

6.3 Summary & Conclusions

This work examines the seasonal and interannual variability of oceanographic conditions in Young Sound-Tyrolerfjord (74° N), a high Arctic fjord system along the coast of Northeast Greenland. Prior to this work, measurements of fjord hydrography in Northeast Greenland were mainly limited to seasonal measurements in the ice-free summer period. In this study, we extended the temporal scale and research annual and interannual variability in the fjord system and attempt to link the observed change to coastal processes.

Seasonal observations of circulation, hydrography and cross-sill exchange indicate that fjord circulation in Young Sound-Tyrolerfjord may be impacted by polynya activity, meltwater and inflow of coastal water masses. The transition from summer- to winter hydrography was a relatively slow process, that modified the fjord from a relatively strong stratification in summer to almost uniform stratification in winter, this occurs on a seasonal timescale.

Water masses in Young Sound-Tyrolerfjord are largely influenced by the oceanographic conditions in the coastal domain. The analysis of a 13-year continuous time series (2003-2015), together with summer CTD-data, indicate that the fjord basin water is freshening and that bottom water renewal in the fjord is prevented by coastal freshening. Freshening of the fjord system mainly occurred between 2005-2007 and 2009-2013, when anomalous strong freshening rates were recorded. In search of the

drivers of this change, a process study suggests that sea ice melt might be the dominant driver of freshwater variability along the coast of Northeast Greenland and showed that sea ice melt increases with increasing temperatures of Atlantic Water in the West Spitsbergen Current. The first anomaly of freshening (2005-2007) could be linked with strong temperature anomalies observed in the West-Spitsbergen Current. These anomalies were also associated with an increased recirculation of warm Atlantic Water to the East Greenland Current (Beszczynska-Møller et al., 2012), which might have caused an increase in sea ice melt at higher latitude.

The Arctic is undergoing a rapid transformation due to climatic changes. As we expect a further increase of temperatures in the North Atlantic, the results of this study suggest that more sea ice might melt at higher latitude and further freshen the coastal waters of Northeast Greenland. This study is only a first step to gain insight in the drivers of the freshwater content along the coast of Northeast Greenland. More research, including numerical modelling studies, are needed to map the pathway of sea ice melt along the coast of Northeast Greenland and to identify its role as driver of the coastal boundary currents along the coast of East Greenland.

References

- Bacon, S., Marshall, A., Holliday, N. P., Aksenov, Y., & Dye, S. R. (2014). Seasonal variability of the East Greenland Coastal Current. *Journal of Geophysical Research: Oceans*, 119(6), 3967–3987. <https://doi.org/10.1002/2013JC009279>
- Bacon, S., Myers, P. G., Rudels, B., & Sutherland, D. a. (2008). Accessing the Inaccessible: Buoyancy-Driven Coastal Currents on the Shelves of Greenland and Eastern Canada. In *Arctic–Subarctic Ocean Fluxes* (pp. 703–722). Dordrecht: Springer Netherlands. https://doi.org/10.1007/978-1-4020-6774-7_29
- Beszczynska-Møller, A., Fahrbach, E., Schauer, U., & Hansen, E. (2012). Variability in Atlantic water temperature and transport at the entrance to the Arctic Ocean, 1997–2010. *ICES Journal of Marine Science*, 69(5), 852–863. <https://doi.org/10.1093/icesjms/fss056>
- Håvik, L., Pickart, R. S., Våge, K., Torres, D., Thurnherr, A. M., Beszczynska-Møller, A., ... von Appen, W.-J. (2017). Evolution of the East Greenland Current from Fram Strait to Denmark Strait: Synoptic measurements from summer 2012. *Journal of Geophysical Research: Oceans*, 122(3), 1974–1994. <https://doi.org/10.1002/2016JC012228>
- Jackson, R. H., & Straneo, F. (2016). Heat, Salt, and Freshwater Budgets for a Glacial Fjord in Greenland. *Journal of Physical Oceanography*, 46(9), 2735–2768. <https://doi.org/10.1175/JPO-D-15-0134.1>
- Mernild, S. H., Sigsgaard, C., Rasch, M., Hasholt, B., Hansen, B. U., Stjernholm, M., & Pedersen, D. (2007). Climate, river discharge and suspended sediment transport in the Zackenberg River drainage basin and Young Sound/Tyrolerfjord, Northeast Greenland. In S. Rysgaard & R. N. Glud (Eds.), *Carbon cycling in Arctic marine ecosystems: Case study Young Sound* (pp. 24–43). Meddr. Grønland, Bioscience 58.

Rysgaard, S., Vang, T., Stjernholm, M., Rasmussen, B., Windelin, A., & Kiilsholm, S. (2003). Physical Conditions, Carbon Transport, and Climate Change Impacts in a Northeast Greenland Fjord. *Arctic, Antarctic, and Alpine Research*, 35(3), 301–312. [https://doi.org/10.1657/1523-0430\(2003\)035\[0301:PCCTAC\]2.0.CO;2](https://doi.org/10.1657/1523-0430(2003)035[0301:PCCTAC]2.0.CO;2)

Appendix A:

Contribution of Authors to Thesis Chapters.

Chapter 3

For this Chapter, WB was part of the team (WB, SR, SK, ID, VP) that collected the field data, except summer CTD-data, and performed all processing of the presented data. Summer CTD-data were provided by the Greenland Ecosystem Monitoring Program. WB wrote the bulk part of the manuscript and prepared all figures. SR, SK, ID, JB, JM, LM, DGB provided expertise, contributed to the discussion and reviewed the manuscript.

Chapter 4

For this Chapter, WB wrote the bulk part of the manuscript, all co-authors contributed to discussion and data interpretation. MKS and SR conducted the fieldwork. WB, MKS, JM, SR and DC retrieved the data and performed the data analysis. Figures were prepared by WB. Summer CTD-data were provided by the Greenland Ecosystem Monitoring Program.

Chapter 5

For this Chapter, WB wrote the bulk part of the manuscript, all co-authors contributed to discussion and data interpretation. MM performed the correlation analysis based on NorESM, in collaboration with WB.

Appendix B:

Additional Contributions to Peer Reviewed

Literature

In addition to the papers in the body of this thesis, I also co-authored seven other peer-reviewed articles. The articles and my contributions are detailed below.

Dmitrenko, I. A., Kirillov, S. A., Rysgaard, S., Barber, D. G., Babb, D. G., Pedersen, L. T., Koldunov, N. V., Boone, W., Crabeck, O., Mortensen, J. (2015). Polynya impacts on water properties in a Northeast Greenland fjord. *Estuar. Coast. Shelf Sci.* 153, 10–17. doi:10.1016/j.ecss.2014.11.027.

For this paper, I assisted the first author with field sampling, and provided comments and suggestions on the manuscript drafts.

Petrusevich, V., Dmitrenko, I. A., Kirillov, S. A., Rysgaard, S., Falk-Petersen, S., Barber, D. G., Boone, W., Ehn, J. (2016). Wintertime water dynamics and moonlight disruption of the acoustic backscatter diurnal signal in an ice-covered Northeast Greenland fjord. *J. Geophys. Res. Ocean.* 121, 4804–4818. doi:10.1002/2016JC011703.

For this paper, I assisted the first author with field sampling, and provided comments and suggestions on the manuscript drafts.

Meire, L., Mortensen, J., Rysgaard, S., Bendtsen, J., Boone, W., Meire, P., et al. (2016). Spring bloom dynamics in a subarctic fjord influenced by tidewater outlet glaciers (Godthåbsfjord, SW Greenland). J. Geophys. Res. Biogeosciences 121, 1581–1592. doi:10.1002/2015JG00240.

For this paper, I provided the first author with expertise, and comments and suggestions on the manuscript drafts.

Bendtsen, J., Mortensen, J., Lennert, K., K. Ehn, J., Boone, W., Galindo, V., et al. (2017). Sea ice breakup and marine melt of a retreating tidewater outlet glacier in northeast Greenland (81°N). Sci. Rep. 7, 4941. doi:10.1038/s41598-017-05089-3.

For this paper, I assisted the first author with field sampling, and provided comments and suggestions on the manuscript drafts.

Carlson, D. F., Boone, W., Meire, L., Abermann, J., and Rysgaard, S. (2017). Bergy Bit and Melt Water Trajectories in Godthåbsfjord (SW Greenland) Observed by the Expendable Ice Tracker. Front. Mar. Sci. 4, 1–14. doi:10.3389/fmars.2017.00276.

For this paper, I assisted the first author with field sampling, and provided comments and suggestions on the manuscript drafts.

Hu, Y., Wang, F., Boone, W., Barber, D., Rysgaard, S. (2017) Assessment and improvement of the sea ice processing for dissolved inorganic carbon analysis. *Limnology & Oceanography Methods*. 16: 83-91. 10.1002/lom3.10229

For this paper, I assisted the first author with the method development, field sampling, and provided comments, figures and suggestions for the manuscript.

Kirillov, S., Dmitrenko, I., Rysgaard, S., Babb, D., Ehn, J., Bendtsen, J., Boone, W., Barber, D., Geilfus, N. (2017) Meltwater induced formation of a porous layer of platelet ice below the multiyear landfast sea ice in the Wandel Sea (NE Greenland) during the melt season. Accepted for publication to the *Journal of Geophysical Research -Oceans*.

For this paper, I provided the first author with expertise, and comments and suggestions on the manuscript drafts.